EA790-SAR-001

DOCKET NO. 71-9270

UMS®

UNIVERSAL MPC SYSTEM®

SAFETY ANALYSIS REPORT

for the

UMS® Universal Transport Cask

NOVEMBER 2001 UMST-01D

VOLUME 1 OF 2

NAC INTERNATIONAL

List of Effective Pages

Master Table of Contents

Chapter 1

List of Effective Pages (Continued)

List of Effective Pages (Continued)

List of Effective Pages (Continued)

List of Effective Pages (Continued)

List of Effective Pages (Continued)

List of Effective Pages (Continued)

List of Effective Pages (Continued)

List of Effective Pages (Continued)

List of Effective Pages (Continued)

List of Effective Pages (Continued)

List of Effective Pages (Continued)

List of Effective Pages (Continued)

List of Effective Pages (Continued)

List of Effective Pages (Continued)

Chapter 3

List of Effective Pages (Continued)

List of Effective Pages (Continued)

List of Effective Pages (Continued)

Chapter 4

Chapter 5

List of Effective Pages (Continued)

List of Effective Pages (Continued)

5.3-26 .... Revision 0
5.3-27 .... Revision UMST-99A
5.3-28 .... Revision UMST-97A
5.3-29 .... Revision UMST-97A
5.3-30 .... Revision UMST-97A
5.3-31 .... Revision UMST-97A
5.3-32 .... Revision UMST-97A
5.3-33 .... Revision UMST-97A
5.3-34 .... Revision UMST-97A
5.3-35 .... Revision 0
5.4-1 .... Revision 0
5.4-2 .... Revision UMST-00A
5.4-3 .... Revision UMST-00A
5.4-4 .... Revision UMST-00A
5.4-5 .... Revision UMST-01D
5.4-6 .... Revision UMST-00A
5.4-7 .... Revision UMST-01D
5.4-8 .... Revision UMST-00A
5.4-9 .... Revision UMST-00A
5.4-10 .... Revision UMST-00A
5.4-11 .... Revision UMST-00A
5.4-12 .... Revision UMST-00A
5.4-13 .... Revision UMST-00A
5.4-14 .... Revision UMST-00A
5.4-15 .... Revision UMST-00A
5.4-16 .... Revision UMST-00A
5.4-17 .... Revision UMST-00A
5.4-18 .... Revision UMST-00A
5.4-19 .... Revision UMST-00A
5.4-20 .... Revision UMST-00A
5.4-21 .... Revision UMST-00A
5.4-22 .... Revision UMST-00A
5.4-23 .... Revision UMST-00A
5.4-24 .... Revision UMST-00A
5.4-25 .... Revision UMST-00A
5.4-26 .... Revision UMST-00A
5.5-1 .... Revision UMST-00A
5.5.1-1 .... Revision UMST-99A
5.5.1-2 .... Revision UMST-01D
5.5.1-3 .... Revision UMST-00A
5.5.1-4 .... Revision UMST-00A
5.5.1-5 .... Revision UMST-01D
5.5.1-6 .... Revision UMST-00A
5.5.1-7 .... Revision UMST-01D
5.5.1-8 .... Revision UMST-00A
5.5.1-9 .... Revision UMST-00A
5.5.1-10 .... Revision UMST-00A
5.5.1-11 .... Revision UMST-00A
5.5.1-12 .... Revision UMST-00A
5.5.1-13 .... Revision UMST-00A
5.5.1-14 .... Revision UMST-00A
5.5.1-15 .... Revision UMST-00A
5.5.1-16 .... Revision UMST-00A
5.5.1-17 .... Revision UMST-00A
5.5.1-18 .... Revision UMST-00A
5.5.1-19 .... Revision UMST-01D
5.5.1-20 .... Revision UMST-00A
5.5.1-21 .... Revision UMST-00A
5.5.1-22 .... Revision UMST-00A
5.5.1-23 .... Revision UMST-00A
5.5.1-24 .... Revision UMST-00A
5.5.1-25 .... Revision UMST-00A
5.5.1-26 .... Revision UMST-00A
5.5.1-27 .... Revision UMST-00A
5.5.1-28 .... Revision UMST-00A
5.5.1-29 .... Revision UMST-00A

List of Effective Pages (Continued)

Chapter 6

List of Effective Pages (Continued)

List of Effective Pages (Continued)

List of Effective Pages (Continued)

List of Effective Pages (Continued)

Chapter 7

List of Effective Pages (Continued)

Master Table of Contents (Continued)

Master Table of Contents (Continued)

Master Table of Contents (Continued)

Master Table of Contents (Continued)

Master Table of Contents (Continued)

Master Table of Contents (Continued)

Master Table of Contents (Continued)

Master Table of Contents (Continued)

Master Table of Contents (Continued)

Master Table of Contents (Continued)

Master Table of Contents (Continued)

Master Table of Contents (Continued)

Master Table of Contents (Continued)

Master Table of Contents (Continued)

Radioactive material shipments in the Universal Transport Cask shall be subject to the following limits:

1. The maximum contents weight for the Universal Transport Cask shall not exceed 77,500 lb.

2. The design basis fuel characteristics shall be in accordance Tables 1.2-4 and 1.2-5.

3. The total decay heat of the cavity contents shall not exceed 20 kW for PWR fuel and 16 kW for BWR fuel.

4. The total weight of the PWR fuel assemblies, including standard inserts such as burnable poison rods or guide tube thimble plugs, shall not exceed 38,500 lb.

5. The total weight of the BWR fuel assemblies shall not exceed 39,000 lb.

6. Radiation levels shall not exceed the requirements of 10 CFR 71.47, 10 CFR 71.51, and IAEA Safety Series No. 6, paragraph 469.

7. Surface contamination levels shall not exceed the requirements of 10 CFR 71.87(i)(1) and IAEA Safety Series No. 6, paragraph 408.

8. Cask general spent fuel contents shall be in accordance with the limiting values shown below, and must be loaded in accordance with Tables 1.2-6 (PWR) and 1.2-7 (BWR).

PARAMETERS	PWR CASK	BWR CASK
No. of assemblies	24	56
Max. UO_2 weight (MTU)	11.53	11.08
Max initial enrichment (wt % ^{235}U)	4.2	4.0
Min. initial enrichment (wt % ^{235}U)	1.9	1.9
Max. Burnup (MWD/MTU)	45,000	45,000
Min. cooling time (years)	5	6

9. Cask site-specific contents may include Maine Yankee fuel with maximum burnup up to 50,000 MWD/MTU and GTCC waste as described in Section 1.3.1.1 based on the site-specific fuel characteristics and preferential loading pattern.

Figure 1.2-1 Operational Schematic for the Universal Transport Cask

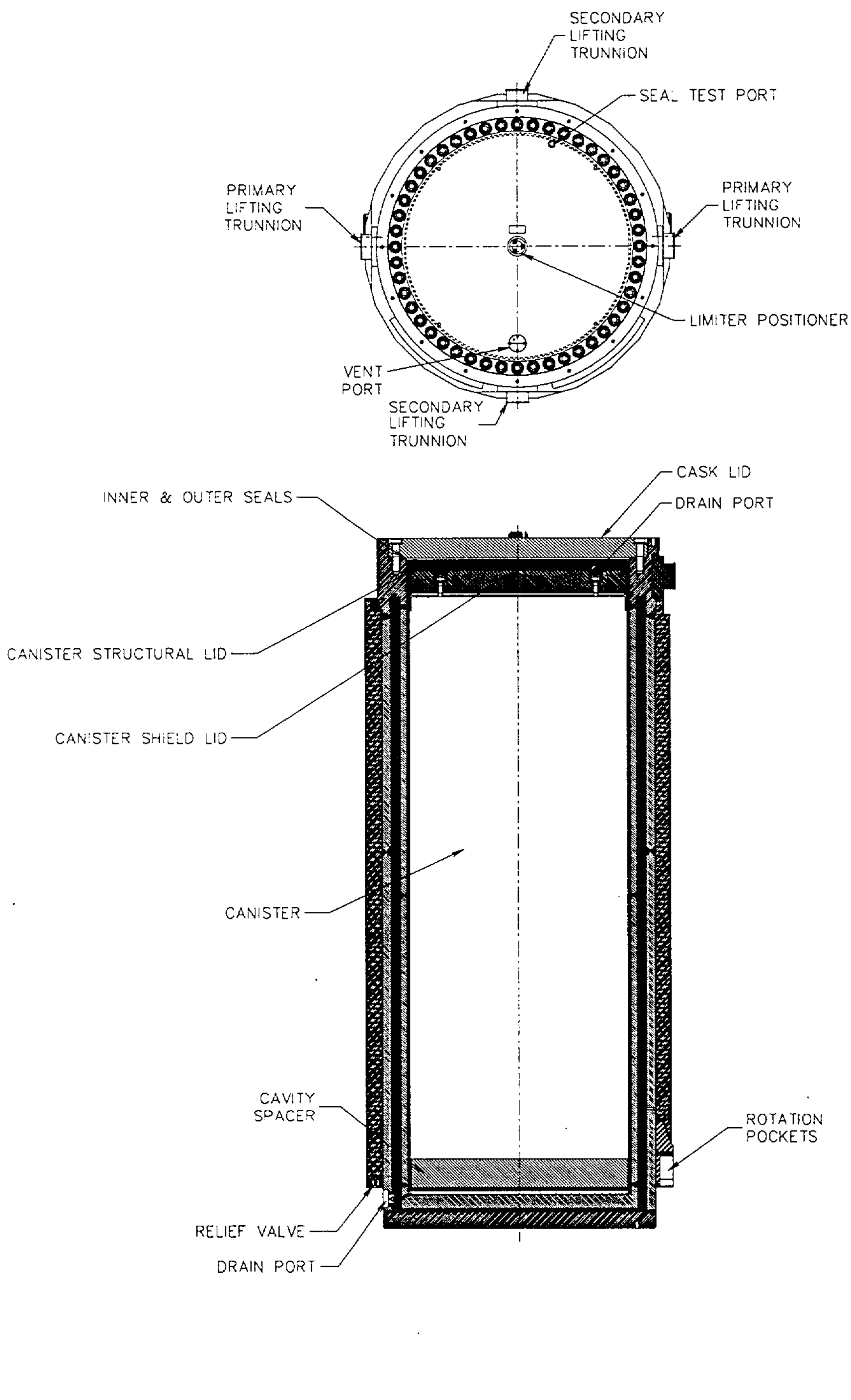

1.3.4 License Drawings

This section contains the License Drawings pertinent to the Universal Transport Cask. The dimensions indicated on the drawings are generally limited to one significant digit past the decimal point. Note that analysis of systems or components may present dimensions with additional significant digits based on more detailed engineering drawings.

Drawing No.	Rev. No.	Title
790-209	1	Impact Limiter Assembly-Upper, Cask, NAC-UMS®
790-210	1	Impact Limiter Assembly-Lower, Cask, NAC-UMS®
790-500	2	Assembly, Universal Transport Cask, Overpack, NAC-UMS®
790-501	3	Canister/Basket Assembly Table, NAC-UMS®
790-502	4	Cask Body, Transport Cask, NAC-UMS®
790-503	1	Lid Assembly, NAC-UMS® Cask
790-504	1	Port Coverplate Assembly, NAC-UMS®
790-505	1	Lifting Trunnion, NAC-UMS®
790-508	1	Misc. Details, Transport Cask, NAC-UMS®
790-509	2	Nameplates- NAC-UMS®
790-516	1	Package Assembly, Universal Transport Cask (UTC), NAC-UMS®
790-519	0	Package Assembly, Transport, Universal Transport Cask (UTC), NAC-UMS®
790-520	2	Spacers, Universal Transport Cask, NAC-UMS®
790-570	3	Fuel Basket Assembly, 56 Element BWR, NAC-UMS®
790-571	2	Bottom Weldment, Fuel Basket, 56 Element BWR, NAC- UMS®

Licensed Drawings (Continued)

Drawing No.	Rev. No.	Title
790-572	4	Top Weldment, Fuel Basket, 56 Element BWR, NAC- UMS®
790-573	7	Support Disk and Misc. Basket Details, 56 Element BWR, NAC- UMS®
790-574	3	Heat Transfer Disk Fuel Basket, 56 Element BWR, NAC- UMS®
790-575	7	BWR Fuel Tube, NAC- UMS®
790-581	5	PWR Fuel Tube, NAC- UMS®
790-582	6	Shell Weldment, Canister, NAC- UMS®
790-583	4	Assembly, Drain Tube, Canister, NAC- UMS®
790-584	9	Details, Canister, NAC- UMS®
790-585	7	Transportable Storage Canister (TSC), NAC-UMS®
790-591	2	Bottom Weldment, Fuel Basket, 24 Element PWR, NAC- UMS®
790-592	4	Top Weldment, Fuel Basket, 24 Element PWR, NAC- UMS®
790-593	4	Support Disk and Misc. Basket Details, 24 Element PWR, NAC- UMS®
790-594	2	Heat Transfer Disk, Fuel Basket, 24 Element PWR, NAC- UMS®
790-595	4	Fuel Basket Assembly, 24 Element PWR, NAC-UMS®
790-605	8	BWR Fuel Tube, Over-Sized Fuel, NAC-UMS®
790-611	0	GTCC Waste Basket, Maine Yankee, NAC-UMS®
790-612	1	GTCC Waste Canister, Maine Yankee, NAC-UMS®

FIGURE WITHHELD UNDER 10 CFR 2.390

DIMENSIONING AND TOLERANCING SHALL BE PER ANSI Y14.5-82
UNSPECIFIED DIMENSIONS AND TOLERANCES SHOWN BELOW.
DIMENSIONS ARE IN INCHES. FRACTIONAL TOLERANCE: ±1/8

SYM	GEOMETRY	.XXX	TOL.	.XX	TOL.
		UNDER 3		UNDER 6	±.04
▱	FLATNESS	3-12		6-18	±.06
—	STRAIGHTNESS	OVER 12		OVER 18	±.09
∠	ANGULARITY	.X	±.1	ANGLES ±.5°	
⊥	PERPENDICULARITY	ALL UNSPECIFIED TOOL RADII: .01 - .03			
//	PARALLELISM	BREAK ALL SHARP CORNERS .01 - .03			
◎	CONCENTRICITY	ALL UNSPECIFIED MACHINED SURFACES SHALL BE 125/OR BETTER			
⊕	TRUE POSITION	NEXT ASSEMBLY: 790-570			
		DRAWING TYPE: LICENSE			

GROUP	NAME	DATE
PREPARER	S. Graham	11-16-01
CHECKER	R. Walker	11-16-01
PROJECT MANAGER	[illegible]	11/16/01
DIRECTOR DESIGN AND ANALYSIS	[illegible]	11-16-01
DIRECTOR, LICENSING	[illegible]	11/16/01
VICE PRESIDENT, QUALITY	[illegible]	11/16/01

BWR FUEL TUBE,
NAC-UMS®

PROJECT 790		DRAWING 575	REV 7
SCALE 1/1	EST. WT.	SH 1 OF 2	2:06PM 11-16-2001

FIGURE WITHHELD UNDER 10 CFR 2.390

NAC INTERNATIONAL

BWR FUEL TUBE,
NAC–UMS®

PROJECT 790		DRAWING 575	REV 7
SCALE 1/1	EST.WT.	SH 2 OF 2	2:05PM 11-16-2001

FIGURE WITHHELD UNDER 10 CFR 2.390

QUANTITY						
DIMENSIONING AND TOLERANCING SHALL BE PER ANSI Y14.5-82 UNSPECIFIED DIMENSIONS AND TOLERANCES SHOWN BELOW. DIMENSIONS ARE IN INCHES. FRACTIONAL TOLERANCE: ±1/8						
SYM.	GEOMETRY	.XXX	TOL.	.XX	TOL.	
	FLATNESS	UNDER 3		UNDER 6	±.04	
		3-12		6-18	±.06	
	STRAIGHTNESS	OVER 12		OVER 18	±.09	
		.X	±.1	ANGLES ±.5°		
∠	ANGULARITY	ALL UNSPECIFIED TOOL RADII: .01 - .03				
⊥	PERPENDICULARITY	BREAK ALL SHARP CORNERS .01 - .03				
//	PARALLELISM	ALL UNSPECIFIED MACHINED SURFACES SHALL BE ∀ OR BETTER				
◎	CONCENTRICITY	NEXT ASSEMBLY: 790-570				
⊕	TRUE POSITION	DRAWING TYPE: LICENSE				

GROUP	NAME	DATE
PREPARER	S. Graham	11-16-01
CHECKER	R. Walke	11-16-01
PROJECT MANAGER	[illegible]	11/16/01
DIRECTOR DESIGN AND ANALYSIS	[illegible]	11-16-01
DIRECTOR, LICENSING	[illegible]	11/16/01
VICE PRESIDENT, QUALITY	[illegible]	11/16/01

INTERNATIONAL

BWR FUEL TUBE, OVER-SIZED FUEL, NAC-UMS®

PROJECT 790		DRAWING 605	REV 8
SCALE 1/1	EST.WT.	SH 1 OF 2	2:15PM 11-16-2001

FIGURE WITHHELD UNDER 10 CFR 2.390

NAC INTERNATIONAL

BWR FUEL TUBE,
OVER-SIZED FUEL,
NAC-UMS®

PROJECT 790		DRAWING 605	REV 8
SCALE 1/1	EST.WT.	SH 2 OF 2	2:15PM 11-16-2001

Table of Contents

Table of Contents (Continued)

Table of Contents (Continued)

Table of Contents (Continued)

Table of Contents (Continued)

Table of Contents (Continued)

Table of Contents (Continued)

Table of Contents (Continued)

Table of Contents (Continued)

List of Figures

List of Figures (Continued)

List of Figures (Continued)

List of Figures (Continued)

List of Figures (Continued)

List of Figures (Continued)

List of Tables

List of Tables (Continued)

List of Tables (Continued)

List of Tables (Continued)

List of Tables (Continued)

List of Tables (Continued)

List of Tables (Continued)

List of Tables (Continued)

List of Tables (Continued)

List of Tables (Continued)

List of Tables (Continued)

List of Tables (Continued)

List of Tables (Continued)

List of Tables (Continued)

List of Tables (Continued)

List of Tables (Continued)

List of Tables (Continued)

List of Tables (Continued)

List of Tables (Continued)

transportation normal conditions of transport and hypothetical accident conditions. The basket can be loaded with up to 24 intact PWR fuel assemblies or up to 56 intact BWR fuel assemblies. Some design features are common to both the PWR and BWR fuel baskets and some features are unique to each basket, as described in the following paragraphs.

The common design features between the PWR and BWR basket structure designs are the top and bottom weldments, support disks, heat transfer disks, fuel tubes, tie rods and nuts, and split spacers. When complete, the basket structure is a rigid cylindrical structure. The base of the structure is the stainless steel bottom weldment.

Either 8 (PWR) or 6 (BWR) stainless steel tie rods are welded to the bottom weldment. The tie rods are used to mechanically join the bottom weldment with the top weldment and hold in place all layers of the support disks and heat transfer disks. Each weldment is designed to support the entire basket structure for all loads. The axial loads are bounded by hypothetical accident condition top/bottom-end drop loads. The fuel assemblies are self-supporting in the axial direction.

The basket structure is assembled by stacking the support disks and the heat transfer disks over the tie rods, each separated by either a spacer or split spacer and washer. The system of multiple support disks is designed to support the fuel assemblies and fuel tubes for all lateral loads. The lateral loads are bounded by hypothetical accident condition side-drop loads. The heat transfer disks do not transmit structural loads (other than self-weight) for any load condition.

The support disks satisfy structural design criteria requirements at temperatures that result from either the normal conditions of transport or hypothetical accident. The aluminum heat transfer disks enhance thermal performance of the basket structure by augmenting its overall heat the conduction properties.

The support disks in the PWR basket are separated and supported at 4.92-in. center-to-center intervals by tie rods and spacer nuts at eight locations. The heat transfer disks are located in the central region of the basket and supported by the eight tie rods and spacer nuts. The number of support disks and heat transfer disks in the PWR basket varies depending upon the class of fuel (Class 1, 2, or 3 PWR fuel) the basket is designed to contain. The PWR fuel tubes are encased by BORAL poison plates on each of the four sides.

The support disks in the BWR basket are separated and supported at 3.83-in. center-to-center intervals by tie rods and spacer nuts at six locations. The heat transfer disks are located in the central region of the basket and supported by the six tie rods and spacer nuts. As is the case for the PWR basket, the number of support disks and heat transfer disks in the BWR basket varies depending upon the class of fuel (Class 4 or Class 5 BWR fuel) the basket is designed to contain. Three types of tubes are designed to contain BWR fuel: tubes with BORAL on two sides, tubes with BORAL one side, and tubes with no BORAL.

2.1.1.4 Impact Limiters

The Universal Transport Cask packaging includes two removable, cup-shaped impact limiters, which absorb the energy of a cask drop impact through the crushing of redwood and balsa wood.

Prior to shipment, the upper impact limiter is bolted to the top forging with 16 retaining rods, washers, and nuts. Likewise, the lower impact limiter is bolted to the bottom plate with 16 retaining rods, washers, and nuts. Both impact limiters are designed to limit impact loads on the cask and its contents resulting from either the normal conditions of transport or hypothetical accident drop scenarios. The impact limiters are fabricated from redwood and balsa wood wedge-shaped sections glued together to form a cylindrical shape. The wood impact-absorbing medium is completely enclosed in a stainless steel shell that is fabricated from 0.25-in. thick stainless steel plate.

The maximum normal condition of transport (1-ft free drop) impact load is calculated to be 17.1g in the bottom end drop orientation. The design load used in all normal conditions of transport impact calculations is 20g. The maximum hypothetical accident condition (30-ft free drop) impact load is calculated to be 57.8g in the top end drop orientation. A design load of 60g is used in all hypothetical accident condition impact calculations.

2.1.1.5 GTCC Waste Canister and Basket

The GTCC waste canister is identical in design to the spent fuel transportable storage canister described in Section 2.1.1.2. The GTCC waste basket is designed to ASME Code, Section III, Subsection NF and conforms to the applicable load combinations and buckling criteria of Regulatory Guide 7.8, and NUREG/CR-6322, respectively. Exceptions to applicable code requirements for these components are shown in Table 2.1.2-1.

Table 2.1.2-1 Exceptions to Codes and Standards (Continued)

Code Section	ASME SECTION III, SUBSECTION NB CODE EXCEPTIONS (Continued)
	Transportable Storage Canister (Continued)
Paragraph NB-5230 Radiographic or Ultrasonic Weld Examination (Structural Lid to Canister Shell)	The structural lid to canister shell weld will be verified by either ultrasonic examination (UT) or by progressive liquid penetrant examination (PT). If progressive PT examination is used, it must include the root and final layers, and each intermediate (approximately) 3/8-inch of weld depth. If UT is used, it will be followed by a final surface PT examination. For either examination, the maximum, undetectable flaw size is demonstrated to be smaller than the critical flaw size. The critical flaw size is determined in accordance with ASME Code, Section XI methods. The examination of the weld will be performed by qualified personnel per ASME Code Section V, Articles 5 (UT) and 6 (PT) with acceptance per ASME Code Section III, NB-5332 (UT) per 1997 Addenda, and NB-5350 for (PT).
Paragraph NB-5230 Radiographic or Ultrasonic Weld Examination (Shield Lid to Canister Shell and Port Covers to Shield Lid)	A root and final liquid penetrant examination has been specified because a radiographic examination cannot be performed since the canister is loaded with spent fuel and ultrasonic examination of these weld joints is not indicated because of the joint configuration. In addition, ultrasonic examination would require close proximity to the canister shield lid, which would expose personnel to high dose rates. Two welds close all leak paths through the canister shield and structural lids. In addition, the shield lid weld is pressure tested and helium leak tested to confirm its integrity.
Article NB-6111 Pressure Testing	A hydrostatic or pneumatic test of the Transportable Storage Canister is not performed at the time of fabrication because the canister (pressure vessel) is not closed until it is loaded with the spent fuel or radioactive waste that it holds for storage and transport. The canister is leak tested and pressure tested (following fuel loading) during the canister closure operations.
Article NB-7000 Overpressure Protection	No overpressure protection is provided since the function of the canister is to confine radioactive material. The canister is designed to withstand an internal pressure that considers 100% fuel rod failure and the maximum accident temperature.
Article NB-8000 Nameplates, Stamping and Reports	The Transportable Storage Canister is not Code stamped and no reports are completed that arc associated with these activities.

Table 2.1.2-1 Exceptions to Codes and Standards (Continued)

Code Section	**ASME SECTION III, SUBSECTION NG CODE EXCEPTIONS**
	Spent Fuel Basket Assembly
NG-2000 ASME Approved Material Supplier	Materials will be supplied by NAC-approved suppliers with Certified Material Test Reports in accordance with NB-2000 requirements.
Article NG-8000 Nameplates, Stamping and Reports	The Internal Fuel Basket Assembly is not Code stamped and no reports are completed that are associated with these activities.

Code Section	**ASME SECTION III, SUBSECTION NF CODE EXCEPTIONS**
	GTCC Waste Basket Assembly
NF-2000 ASME Approved Material Supplier	Materials will be supplied by NAC approved suppliers with Certified Material Test Reports in accordance with NF-2000 requirements.
Article NF-8000 Nameplates, Stamping and Reports	The Internal GTCC Waste Basket Assembly is not Code stamped and no reports are completed that are associated with these activities.

Upper Bound Magnitudes for Compressive Stresses and In-Plane Shear Stresses

From Section-1600 of Code Case N-284-1, as an upper limit, the compressive stresses, S_i ($i = \phi$ or θ), must be less than the yield strength, S_y, divided by the appropriate factor of safety ($S_i < S_y/FS$). Similarly, for shear, $S_{\phi\theta}$, must be less than or equal to 0.6 S_y divided by the appropriate factor of safety ($S_{\phi\theta} < 0.6\ S_y/FS$). As discussed earlier in this section, the factor of safety is 2.0 for normal transport and 1.34 for hypothetical accident conditions. Under no circumstances may the values for the upper bound magnitudes of compressive stresses and in-plane shear stresses be exceeded. However, satisfying these limits alone is not sufficient to demonstrate that buckling does not occur; the interaction equations must also be satisfied.

Interaction Equations

Elastic and inelastic interaction equations must be satisfied for all states of compressive and in-plane shear stress. The interaction equations for cylindrical shells are directly available from Paragraph 1713.1.1 and Paragraph 1713.2.1 of Code Case N-284-1. Once a stress state is established for a specific shell, plasticity reduction factors can be determined and all appropriate interaction equations checked. Elastic interaction equations must be satisfied and, if any of the uniaxial critical stress values exceed the proportional limit of the fabricated material, the inelastic interaction equations must also be satisfied.

2.1.2.5.4 Creep Considerations at Elevated Temperatures

Structural components of the Universal Transport Cask and the canister are fabricated from stainless steel, which does not experience creep below temperatures of 700°F. The canister is the package structural component exposed to the highest temperatures, which remain below 700°F. Therefore, the potential for creep is essentially zero. Design considerations relative to the creep failure mode are therefore satisfied.

2.1.2.5.5 Impact Limiter Deformation Limits

The Universal Transport Cask impact limiters are designed to crush and, thereby, absorb the kinetic energy of the cask acquired during a free-drop accident. The geometry of the impact limiters and the crush characteristics of the energy-absorbing material are designed to limit the deceleration forces applied to the cask.

As shown in Table 2.6.7.5-6, the Universal Transport Cask impact limiters limit the maximum deceleration experienced by the cask body equal to or less than 57.8 g for all impact conditions. The deceleration force is a function of the crush strength of the energy-absorbing material in the impact limiter and the area of crush. The impact limiter must provide a sufficient depth of energy-absorbing material so that all of the kinetic energy of the package is absorbed (cask is stopped) before the limiter is crushed to its solid "stacked" height (approximately 30% of the initial depth).

2.6.1.1 Summary of Pressures and Temperatures

The maximum normal condition temperatures are summarized in Table 3.4-1 for the various PWR and BWR cask components. Summaries of pressures for the PWR and BWR canister and cask configurations are listed in Tables 2.6.1.1-1 and 2.6.1.1-2, respectively. The Maximum Normal Operating Pressure (MNOP), as defined in NUREG-1617 [57], Table 3.4-4, is 6.91 psig (Section 3.4.4).

2.6.1.2 Thermal Expansion Evaluation

The differential thermal expansions between the basket disks and the canister and the canister and the cask are evaluated based on bounding results from the PWR thermal analyses. In performing the calculations, nominal dimensions of the various components are used. The data used in the evaluation are presented in Chapter 1.0.

All thermal expansions are calculated using the following relation:

$$\Delta l = l_0 \, \alpha \, \Delta T$$

where Δl is the resulting change in linear dimension, l_0 is the original dimension, α the material thermal expansion coefficient, and ΔT temperature differential. The original dimensions are expressed in terms of room temperature, so the calculated temperature differences are based on 70°F environment temperature.

2.6.1.2.1 Canister/Cask Radial Thermal Expansion

The maximum canister shell temperature is 408°F. The thermal expansion coefficient of Type 304L stainless steel at 400°F is 9.19E-6 in/in-°F [21]. The increase in diameter of the canister is then

$$\Delta d = d_0 \, \alpha \, \Delta T = 67.06 \text{ (9.19E-6 in/in-°F) (408 - 70)} = 0.208 \text{ in.}$$

The canister diameter increases to 67.06 + 0.208 = 67.268 in.

Since this diameter is smaller than the nominal diameter of the cask cavity (67.61 in.), a diametrical clearance of 67.61 - 67.268 = 0.342 in. is assured during normal operating conditions even without considering the thermal expansion of the cask inner shell.

2.6.1.2.2 Canister/Cask Axial Thermal Expansion

The maximum canister shell temperature is 408°F. This temperature is conservative to use for the axial expansion since a temperature gradient exists along the length of the canisters. The thermal expansion coefficient of Type 304L stainless steel at 400°F is 9.19E-6 in/in-°F. The longest canister configuration is PWR Class 3 with a length of 191.95 in. The increase in length of the canister is then

$$\Delta l = l_0\, \alpha\, \Delta T = 191.95\ (9.19E\text{-}6\ \text{in/in-°F})\ (408 - 70) = 0.60\ \text{in.}$$

The canister length increases to 191.95 + 0.60 = 192.55 in.

The minimum cask shell temperature is conservatively assumed to be 150°F (bounding case since the temperature in forging is 250°F). The thermal expansion coefficient of Type 304 stainless steel at 70°F is 8.46E-6 in/in-°F. The cask cavity is 192.5 in. in length. The increase in length of the cask cavity is then

$$\Delta l = 192.5\ (8.46E\text{-}6\ \text{in/in-°F})\ (150 - 70) = 0.13\ \text{in.}$$

The cask cavity length increases to 192.5 + 0.13 = 192.63 in. The resulting axial gap is 192.63 - 192.55 = 0.08 in. Therefore, the canister and cask will expand axially and not bind during normal transport conditions.

2.6.1.3 Stress Calculations and Comparison to Allowable Stresses

The stresses throughout the cask body are calculated for the individual and combined loading conditions . The loading conditions are: (1) 150 psig internal pressure (including bolt preload); (2) thermal heat (100°F) loads; and (3) gravity. Stress results for the individual loading case of 150 psig internal pressure (including bolt preload) are documented in Tables 2.6.1.3-1 and 2.6.1.3-2. Stress results for the thermal loading case are documented in Table 2.6.1.3-3. Stress results for the individual gravity cases are documented in Table 2.6.1.3-4 and 2.6.1.3-5. The conventions used for the stress summary tables are:

Table 2.6.1.1-1 Summary of Canister Pressures During Normal Conditions of Transport

Condition	Canister Internal Pressure (PWR)	Canister Internal Pressure (BWR)
Normal (3% Rod Failure)	6.15 psig	3.47 psig
Pressure used for Canister Analysis	25 psig	25 psig

Table 2.6.1.1-2 Summary of Cask Pressures During Normal Conditions of Transport

Pressure Condition	Cask Cavity Internal Pressure (PWR)	Cask Cavity Internal Pressure (BWR)
Normal (3% Rod Failure)	6.91 psig	3.65 psig
Cask Lid Closure Analysis	80 psig	80 psig
Cask Body Finite Element Analysis	150 psig	150 psig

Table 2.6.1.3-1 P_m Stresses—150 psig Internal Pressure, Heat (100°F)

		Cylindrical Stress Components (ksi)							Allowable Stress	
Section	Angle	S_X	S_Y	S_Z	S_{XY}	S_{YZ}	S_{XZ}	SI (ksi)	(ksi)	MS
1	180	-0.1	0.0	0.9	-0.2	0.0	0.0	1.2	20.0	15.43
2	180	0.0	0.0	1.1	-0.2	-0.1	0.0	1.3	20.0	14.89
3	105	0.3	0.5	0.6	0.4	-0.3	-0.5	1.4	20.0	13.74
4	20	-1.0	0.1	-1.7	-0.4	-0.3	-0.4	2.3	20.0	7.65
5	10	-0.5	-0.1	-1.5	0.0	0.0	0.0	1.4	20.0	13.13
6	0	-0.7	-0.1	-2.2	0.2	0.0	0.0	2.2	20.0	8.16
7	0	-1.0	2.7	-2.3	-0.1	0.1	0.0	5.1	20.0	2.95
8	0	2.5	0.0	-3.6	0.2	0.3	-0.4	6.2	20.0	2.22
9	0	-3.7	0.5	-5.6	1.5	0.3	-0.2	6.7	20.0	2.00
10	0	0.1	-7.8	-6.3	0.4	0.3	-0.4	8.1	19.1	1.37
11	0	-2.4	-11.7	-8.6	1.6	0.2	-0.4	9.9	19.1	0.93
12	0	-3.3	5.5	-3.6	0.5	0.3	0.1	9.1	19.1	1.09
13	0	-1.1	8.5	-2.3	0.8	0.3	0.1	10.9	19.1	0.75
14	0	-3.7	-0.6	-5.2	-1.2	0.1	-0.1	5.0	19.7	2.93
15	0	-0.5	0.0	-4.5	0.9	0.1	-0.3	5.3	19.7	2.73
16	50	0.4	0.4	0.2	1.4	1.2	0.3	3.7	19.7	4.34
17	0	-0.1	4.6	1.1	0.0	0.2	0.2	4.7	19.7	3.18
18	0	-0.1	5.4	0.9	0.0	0.1	0.2	5.6	19.7	2.53
19	0	-0.1	5.8	0.8	0.0	0.0	0.2	5.9	19.7	2.33
20	0	-0.1	5.6	0.9	0.0	-0.1	0.2	5.8	19.7	2.41
21	0	-0.1	5.0	1.1	-0.1	-0.1	0.2	5.1	19.7	2.88
22	0	-0.1	3.3	1.1	-0.2	-0.3	0.1	3.5	19.7	4.64
23	90	1.9	1.3	-0.1	1.3	0.0	0.0	3.0	19.1	5.29
24	0	-0.3	2.5	4.3	0.0	0.4	0.4	4.7	19.1	3.06
25	0	-0.3	4.8	3.7	0.0	0.2	0.4	5.1	19.1	2.72
26	0	-0.3	5.9	3.6	0.0	0.1	0.4	6.3	19.1	2.04
27	0	-0.3	6.4	3.7	0.0	0.0	0.4	6.7	19.1	1.85
28	0	-0.3	6.1	3.6	0.0	-0.1	0.4	6.4	19.1	1.98
29	0	-0.3	5.0	3.6	0.0	-0.2	0.4	5.4	19.1	2.56
30	0	-0.3	3.1	3.9	-0.1	-0.3	0.4	4.4	19.1	3.34
31	90	3.1	1.6	-0.1	-1.4	-0.1	0.0	4.0	19.1	3.73
32	70	1.4	-0.7	0.3	-1.2	-0.8	0.5	3.6	20.0	4.50
33	50	0.8	0.4	-0.9	-0.4	-0.5	0.6	2.5	20.0	7.08
34	60	2.8	1.6	1.4	-1.9	-1.4	1.4	5.2	20.0	2.82
35	90	1.7	0.3	0.2	-0.7	-0.3	0.0	2.2	20.0	8.28
36	180	-0.3	-0.5	3.9	-0.8	-0.1	-0.6	5.2	20.0	2.83
37	0	-0.8	-0.1	-0.4	-0.1	0.0	0.0	0.7	20.0	26.51
38	0	-0.8	-0.1	-0.6	-0.3	0.0	0.0	0.9	20.0	20.38
39	10	-0.8	-0.1	-0.7	-0.3	0.1	0.0	0.9	20.0	21.07
40	80	1.1	1.7	-0.2	-0.4	1.7	0.1	4.0	20.0	4.03
41	30	-1.2	0.0	-1.1	-0.1	-0.1	0.1	1.3	20.0	14.56

Note: Includes cask lid bolt preload.

Table 2.6.1.3-2 $P_m + P_b$ Stresses—150 psig Internal Pressure, Heat (100°F)

		Cylindrical Stress Components (ksi)							Allowable Stress	
Section	Angle	S_X	S_Y	S_Z	S_{XY}	S_{YZ}	S_{XZ}	SI (ksi)	(ksi)	MS
1	180	1.8	0.1	4.4	-0.2	0.0	-0.1	4.3	30.0	6.00
2	180	0.0	0.0	3.1	-0.2	-0.1	-0.2	3.2	30.0	8.36
3	180	-0.9	-0.1	1.7	0.3	0.0	-0.2	2.8	30.0	9.72
4	20	-1.0	1.2	-1.4	-0.2	-0.3	-0.4	2.9	30.0	9.37
5	40	-2.3	-0.1	-4.5	0.0	0.0	0.0	4.3	30.0	5.91
6	0	-1.1	-0.2	-4.7	0.2	0.0	-0.1	4.6	30.0	5.59
7	0	2.5	6.6	-1.7	0.4	0.2	-0.1	8.4	30.0	2.57
8	0	5.8	10.9	0.5	0.4	0.4	-0.2	10.5	30.0	1.85
9	0	1.7	17.8	0.9	0.4	0.5	-0.1	16.9	30.0	0.77
10	0	2.6	-6.9	-5.1	-0.5	0.3	-0.5	9.7	28.7	1.97
11	0	4.9	-8.7	-5.3	1.0	0.3	-0.7	13.9	28.7	1.07
12	0	-6.6	4.7	-4.6	-0.1	0.2	0.2	11.3	28.7	1.55
13	0	-6.8	6.7	-4.4	0.8	0.4	0.3	13.6	28.7	1.11
14	0	-5.7	6.3	-3.9	-0.5	0.2	0.2	12.0	29.6	1.46
15	0	4.3	11.4	0.0	1.0	0.3	-0.2	11.6	29.6	1.54
16	40	0.9	1.1	0.9	2.0	2.5	0.9	6.4	29.6	3.59
17	0	-0.1	7.3	8.0	0.0	0.0	0.8	8.2	29.6	2.60
18	0	-0.1	2.2	-7.4	0.0	0.2	-0.5	9.7	29.6	2.05
19	0	-0.1	2.4	-7.9	0.0	0.0	-0.5	10.3	29.6	1.86
20	0	-0.1	2.5	-7.2	0.0	-0.2	-0.5	9.7	29.6	2.06
21	0	-0.1	7.6	7.5	0.0	0.1	0.7	7.8	29.6	2.80
22	40	0.8	1.3	0.9	-2.0	-2.6	0.9	6.6	29.6	3.48
23	0	-0.3	0.9	-2.6	0.8	0.9	-0.3	4.3	28.7	5.70
24	0	-0.2	4.9	8.7	0.0	0.1	0.8	9.0	28.7	2.19
25	0	-0.2	7.3	10.5	0.0	0.0	1.0	10.8	28.7	1.64
26	0	-0.2	9.1	12.0	0.0	0.0	1.1	12.4	28.7	1.31
27	0	-0.2	9.8	12.8	0.0	0.0	1.2	13.2	28.7	1.17
28	0	-0.2	9.3	12.5	0.0	0.0	1.2	12.9	28.7	1.22
29	0	-0.2	7.9	11.4	0.0	-0.1	1.1	11.9	28.7	1.42
30	0	-0.2	4.9	9.7	0.0	-0.1	0.9	10.1	28.7	1.85
31	0	-0.2	1.2	4.4	-0.5	-0.2	0.4	4.8	28.7	5.01
32	50	1.2	-1.0	0.8	-2.1	-2.0	0.9	6.5	30.0	3.60
33	50	1.1	-1.5	-2.5	-1.7	-1.7	0.7	6.2	30.0	3.83
34	0	-0.2	6.3	-2.0	0.6	-0.7	-0.3	8.5	30.0	2.54
35	0	1.0	-0.2	-3.0	0.6	-0.6	-0.3	4.4	30.0	5.82
36	180	-0.8	-0.6	3.6	-1.3	-0.4	-0.7	5.9	30.0	4.10
37	0	-6.9	-0.2	-8.1	-0.1	0.0	0.0	7.9	30.0	2.79
38	0	-4.6	-0.2	-7.2	-0.3	0.0	-0.1	7.0	30.0	3.28
39	0	-2.8	0.5	-6.2	-0.7	0.1	-0.1	6.9	30.0	3.36
40	80	5.1	6.7	1.7	-0.5	1.7	0.3	6.1	30.0	3.88
41	0	-2.4	-0.2	-1.3	0.2	0.0	0.1	2.2	30.0	12.37

Note: Includes cask lid bolt preload.

Table 2.6.1.3-3 Thermal (Q) Stresses—Heat (100°F)

Section	Angle	Cylindrical Stress Components (ksi)						SI (ksi)
		S_X	S_Y	S_Z	S_{XY}	S_{YZ}	S_{XZ}	
1	80	4.5	2.9	0	0.3	0	0	4.6
2	0	3.4	4.2	0.1	-0.1	0.1	-0.1	4.1
3	180	7.3	5.3	7.3	-0.1	-0.3	3	6
4	0	7	-0.6	-4	0.3	0.7	-0.4	11.1
5	0	-5.3	-1.5	-0.3	-0.9	-0.2	0.2	5.3
6	0	-2.7	-1.5	-0.1	-0.1	0	0	2.6
7	0	-4.5	-2.2	-8.4	-0.2	-0.1	-1.8	6.9
8	0	-4.5	-2.2	-8.4	-0.2	-0.1	-1.8	6.9
9	0	-0.4	-1.4	-9.6	0.1	0	-0.9	9.3
10	70	-1	1.5	2.1	-0.8	0.3	-0.3	3.5
11	50	0.6	2.2	2.7	-1.1	1.3	-0.7	4.1
12	20	0	2.1	3.3	-0.4	0.5	-0.2	3.6
13	0	0.4	2.2	3.2	-0.3	0	0.4	3
14	20	0	2.1	3.3	-0.4	0.5	-0.2	3.6
5	0	0.4	2.2	3.2	-0.3	0	0.4	3
16	0	-0.1	3.3	1.9	-0.3	0.1	0.1	3.5
17	0	-0.1	4.7	3.5	-0.5	0.1	0	5
18	0	-0.2	5	3.5	-0.5	0	0	5.3
19	0	-0.2	5.1	3.4	-0.5	0	0	5.3
20	0	-0.2	5.2	3.5	-0.5	0	0	5.5
21	0	-0.2	5.1	3.4	-0.5	-0.1	0	5.4
22	0	-0.1	3.4	2.5	-0.3	-0.1	-0.1	3.6
23	0	-0.3	-1	-5.1	0.1	0.2	-0.2	4.9
24	0	-0.2	-3	-6	0.3	0.4	0	5.9
25	0	-0.1	-5.3	-12	0.5	0.2	0	11.9
26	0	-0.2	-5.6	-13.7	0.5	0.1	0	13.6
27	0	-0.1	-5.1	-13.8	0.5	0	0	13.8
28	0	-0.1	-5.4	-14	0.5	0	0	13.9
29	0	-0.3	-6.2	-14	0.6	-0.1	0	13.7
30	0	-0.3	-6.3	-12.3	0.6	-0.2	0	12
31	0	-1	-3.7	-8	0.3	-0.6	-0.1	7.2
32	10	-0.2	0.6	3.2	0	0.1	-0.2	3.4
33	10	3.7	2.5	5.7	-0.1	0	-1	3.6
34	0	0.2	-2	-4.4	0	-0.5	-0.5	4.8
35	0	0	-0.7	-2.5	0.1	-0.1	-0.1	2.5
36	0	-0.2	1.4	-1.4	-0.2	-0.1	0	2.9
37	150	-2.7	-2.9	0	0.8	0	0	3.6
38	180	-2.7	-2.6	0	0.1	0	0	2.7
39	120	0.4	-0.3	-2.9	-0.1	-0.1	0.2	3.4
40	180	-1.4	1.6	0.7	0.4	0.1	0.3	3.2
41	10	0	2.8	5.5	0	0.3	0.1	5.5

Table 2.6.1.3-4 P_m Stresses—1-*g* Gravity Load, Heat (100°F)

Section	Angle	Cylindrical Stress Components (ksi) S_X	S_Y	S_Z	S_{XY}	S_{YZ}	S_{XZ}	SI (ksi)	Allowable Stress (ksi)	MS
1	120	0	0	0	-0.1	0	0	0.1	20	171.86
2	10	-0.1	-0.1	0	0	0	0	0.1	20	159.51
3	105	0	0	0	-0.1	0	0	0.1	20	134.04
4	10	-0.2	-0.3	-0.1	0	0	-0.1	0.2	20	79.35
5	10	-0.1	-0.1	0	0	0	0	0.1	20	137.89
6	0	-0.2	-0.2	0	0	0	0	0.2	20	97.38
7	0	-0.2	-0.3	0.1	0	0	0	0.4	20	51.3
8	10	-0.2	-0.4	-0.1	0	0	-0.1	0.4	20	51.99
9	10	-0.3	-0.5	-0.1	0	0	0.1	0.4	20	48.43
10	0	-0.3	-0.6	-0.5	0	0	0	0.3	19.1	59.26
11	0	-0.3	-0.7	-0.7	0	0	0.1	0.5	19.1	39.49
12	10	-0.4	-0.4	0.4	0	0	0	0.8	19.1	22.75
13	0	-0.3	-0.3	0.6	0	0	0	0.9	19.1	20.64
14	10	-0.4	-0.5	-0.2	0	0	-0.1	0.4	19.7	46.2
15	0	-0.2	-0.5	-0.1	0	0	0.1	0.4	19.7	45.37
16	50	0	0.1	0.1	0	-0.2	0	0.4	19.7	51.63
17	0	0	0.1	0.3	0	0	0	0.3	19.7	65.82
18	0	0	0.1	0.4	0	0	0	0.4	19.7	50.07
19	0	0	0.1	0.4	0	0	0	0.4	19.7	44.87
20	0	0	0.1	0.4	0	0	0	0.4	19.7	44.76
21	0	0	0.1	0.4	0	0	0	0.4	19.7	51.02
22	40	0	0.3	0.1	0	0.1	0	0.4	19.7	48.46
23	40	0	-0.1	0	0	-0.2	0	0.4	19.1	46.8
24	50	0	0	0	0	-0.2	0	0.4	19.1	49.05
25	60	0	0	0	0	-0.1	0	0.3	19.1	73.8
26	0	0	0.1	0.3	0	0	0	0.3	19.1	56.11
27	0	0	0.1	0.4	0	0	0	0.4	19.1	50.04
28	0	0	0.1	0.3	0	0	0	0.4	19.1	52.47
29	0	0	0.1	0.3	0	0	0	0.3	19.1	65.85
30	60	0	0	0	0	0.2	0	0.3	19.1	55.47
31	50	0	0.5	0	0	0.2	0	0.7	19.1	26
32	60	0	0.6	0	0	0.2	0.1	0.7	20	25.92
33	60	-0.4	0.7	0.1	-0.1	0.1	0.1	1.1	20	17.42
34	60	0.3	1	-0.2	0	0.2	0.1	1.3	20	14.56
35	70	-0.2	0.7	-0.1	0	0.2	0.3	1.1	20	16.64
36	180	1	1.4	-0.3	0.1	0	0.3	1.8	20	10.21
37	0	-0.3	-0.2	0	0	0	0	0.3	20	58.15
38	120	-0.3	-0.3	0	0	0	0	0.3	20	58.7
39	80	-0.2	-0.4	-0.8	0.1	0	0	0.6	20	32.53
40	80	-1.6	-2	-3.3	0.1	0	-1.1	2.9	20	5.89
41	0	-0.2	-0.1	-0.1	0	0	0	0.2	20	118.62

Note: Includes cask lid bolt preload.

Table 2.6.1.3-5 $P_m + P_b$ Stresses —1-g Gravity Load, Heat (100°F)

Section	Angle	Cylindrical Stress Components (ksi) S_X	S_Y	S_Z	S_{XY}	S_{YZ}	S_{XZ}	SI (ksi)	Allowable Stress (ksi)	MS
1	165	0	0.1	0	0	0	0	0.1	30	205.04
2	180	0	0.2	0	0	0	0	0.2	30	169.16
3	90	0.1	0	0.1	-0.1	-0.1	0	0.3	30	116.23
4	10	-0.1	-0.3	0	0	0	0	0.3	30	108.33
5	40	-0.1	-0.2	0	0	0	0	0.2	30	170.82
6	0	-0.2	-0.3	0	0	0	0	0.3	30	117.62
7	0	-0.2	-0.4	0.2	0	0	0	0.5	30	53.59
8	0	-0.1	-0.3	0.4	0	0	-0.1	0.7	30	40.85
9	0	0.1	-0.1	0.8	0	0	0	0.9	30	31.38
10	0	-0.2	-0.5	-0.4	0	0	0	0.3	28.7	84.53
11	0	0	-0.5	-0.5	0	0	0.1	0.6	28.7	48.05
12	10	-0.5	-0.4	0.3	0	0	0	0.9	28.7	31.69
13	0	-0.6	-0.4	0.4	0	0	0	1	28.7	26.44
14	10	-0.5	-0.4	0.4	0	0	0	0.9	29.6	32.69
15	0	0.1	-0.1	0.8	0	0	0.1	1	29.6	29.72
16	50	0	0.1	0.1	0	-0.2	0	0.5	19.7	38.96
17	0	0	0.4	0.4	0	0	0	0.4	19.7	43.82
18	0	0	0.5	0.5	0	0	0	0.6	19.7	34.63
19	0	0	-0.4	0.2	0	0	0	0.6	19.7	31.28
20	0	0	0.5	0.6	0	0	0	0.6	19.7	31.84
21	0	0	0.4	0.5	0	0	0	0.5	19.7	36.74
22	40	0	0.4	0.3	0	0.2	0	0.6	29.6	48.36
23	40	0	-0.1	0	0	-0.3	0	0.6	28.7	47.05
24	40	0	0.1	0	0	-0.3	0	0.5	19.1	36.34
25	0	0	0.4	0.3	0	0	0	0.4	19.1	42.84
26	0	0	0.5	0.5	0	0	0	0.5	19.1	35.54
27	0	0	0.5	0.5	-0.1	0	0	0.6	19.1	32.61
28	0	0	0.5	0.5	-0.1	0	0	0.6	19.1	33.46
29	0	0	0.5	0.4	0	0	0	0.5	19.1	37.41
30	50	0	0.2	0.1	0	0.2	0	0.4	19.1	41.75
31	40	0	0.6	0.1	0	0.3	0	0.8	28.7	33.62
32	50	0	0.6	-0.3	0	0.2	0.1	1	30	29.8
33	70	-0.8	0.4	-0.7	-0.2	0.2	0.1	1.4	30	20.34
34	50	0	0.6	-1.4	0	0.3	-0.1	2.1	30	13.55
35	70	-0.3	0.5	-1.1	0	0.4	1.5	3.1	30	8.56
36	70	3.2	1.9	1	0.1	0.2	0.4	2.3	30	11.88
37	0	-3.7	-3.6	0	0	0	0	3.7	30	7.06
38	30	-3.9	-3.7	-0.1	0	0	0	3.8	30	6.82
39	70	3.6	2.7	-1.2	0	0	0	4.7	30	5.32
40	0	-3.1	-6.3	-9.8	0.2	-0.1	0.3	6.7	30	3.45
41	0	-0.3	-0.1	0	0	0	0	0.4	30	82.5

Note: Includes cask lid bolt preload.

2.6.2 Cold

The Universal Transport Cask body and closure lid are analyzed for structural adequacy in accordance with the requirements of 10 CFR 71.71(c)(2), "Cold (normal condition of transport)." The cask is loaded and ready for shipment in the horizontal position, with an ambient temperature environment of -40°F, an analyzed internal pressure of 150 psig, no decay heat load, no solar insolation, and in still air and shade. Note that although the Cold condition is associated with the minimum internal pressure, an internal pressure of 150 psig, which corresponds to the maximum internal pressure, is conservatively used.

2.6.2.1 Summary of Pressures and Temperatures

The minimum normal condition temperatures are summarized in Table 3.4-2 for the various PWR and BWR cask components . Maximum internal pressures generated in the canister and cask are listed in Table 2.6.1.1-1 and 2.6.1.1-2. Closure bolts are qualified for a maximum pressure of 80 psig (Section 2.6.7.6). The Maximum Normal Operating Pressure (MNOP), as defined by NUREG-1617, Table 3.4-4 [57], is 6.91 psig (Section 3.4.4).

2.6.2.2 Thermal Expansion Evaluation

The discussion presented in Section 2.6.1.2 bounds the worst differential thermal expansion conditions since the evaluation results in higher temperatures. According to Section 2.6.1.2, thermal expansion of Universal Transport Cask is less than the minimum clearance between components.

2.6.2.3 Stress Calculations and Comparison to Allowable Stresses

The stresses throughout the cask body are calculated for the individual and combined loading conditions . The loading conditions are: (1) 150 psig internal pressure (including bolt preload); (2) cold (-40°F) thermal loads; and (3) gravity. Stress results for the individual loading case of 150 psig internal pressure (including bolt preload) are documented in Tables 2.6.2.3-1 and 2.6.2.3-2. Stress results for the thermal loading case is documented in Table 2.6.2.3-3. Stress results for the individual gravity cases are documented in Table 2.6.2.3-4 and 2.6.2.3-5. The conventions used for the stress summary tables are:

1. All stresses are in ksi.
2. Section stress locations are shown in Figures 2.10.2.2-1 through 2.10.2.2-4
3. The stress intensities (SI) presented in the tables represent the maximum SI occurring at any circumferential location or the specified section. The stress components correspond to the section having the largest SI.
4. Angles shown in the tables are in degrees and they identify the circumferential location where the maximum stress intensity occurs. These angles are measured from the x-axis rotating about the y-axis.
5. Any stress component that is shown to be less than 0.1 ksi, defined as being 0 ksi.
6. The stress intensities shown in the tables are rounded to the nearest 0.1 ksi. The margins of safety are calculated prior to rounding the stress intensities.
7. "Cold (-40°F)" refers to -40°F ambient temperature, no solar insolation and no decay heat applied to the cask in still air.
8. Stresses are reported in a cylindrical system and X, Y, Z correspond to radial, circumferential and axial respectively.

These tables document the primary membrane (P_m), primary membrane plus primary bending ($P_m + P_b$), primary plus secondary stresses (P + Q), and critical P_m, $P_m + P_b$, and P + Q stresses in accordance with the criteria presented in Regulatory Guide 7.6. As described in Section 2.6.7, procedures have been implemented to document the nodal and sectional stresses as well as to determine the critical stress summary for all cask components.

For the individual loading condition of internal pressure, the maximum calculated primary membrane stress intensity is 10.9 ksi and the maximum calculated primary membrane plus bending stress intensity is 16.9 ksi, . For the individual cold thermal loading condition, the peak stress is 0.5 ksi. For the individual gravity loading condition (including cask lid bolt preload), the maximum calculated primary membrane stress intensity is 1.9 ksi and the maximum calculated primary membrane plus bending stress intensity is 4.7 ksi except in regions affected by bolt preload. Conservatively combining the maximum stress without regard to location for the internal pressure and gravity load cases, the maximum calculated primary membrane stress intensity is 12.8 ksi, the maximum calculated primary membrane plus primary bending stress intensity is 21.6 ksi, and the maximum calculated primary plus secondary stress is 22.1 ksi.

Using the conservatively calculated stresses, the minimum margin of safety for the P_m. $P_m + P_b$, and P + Q stresses in the cask for the cold condition are:

Stress State	Max. Stress (ksi)	Allowable Stress (ksi)	Margin of Safety
P_m	12.8	20.0	+ 0.6
$P_m + P_b$	21.6	30.0	+ 0.4
P + Q	22.1	57.4	+ 1.6

Since the margins of safety are all positive, the Universal Transport Cask satisfies the requirements of 10 CFR 71.71(c)(2) for the cold condition.

Table 2.6.2.3-1 P_m Stresses—150 psig Internal Pressure; Cold (-40°F)

Section	Angle	Cylindrical Stress Components (ksi)						SI (ksi)	Allowable Stress (ksi)	MS
		S_X	S_Y	S_Z	S_{XY}	S_{YZ}	S_{XZ}			
1	180	-0.1	0.0	0.9	-0.2	0.0	0.0	1.2	20.0	15.57
2	180	0.0	0.0	1.1	-0.2	-0.1	0.0	1.2	20.0	15.03
3	105	0.3	0.5	0.6	0.4	-0.3	-0.5	1.3	20.0	13.88
4	20	-1.0	0.1	-1.7	-0.4	-0.3	-0.4	2.3	20.0	7.69
5	10	-0.5	-0.1	-1.5	0.0	0.0	0.0	1.4	20.0	13.20
6	0	-0.7	-0.1	-2.2	0.2	0.0	0.0	2.2	20.0	8.17
7	0	-1.0	2.7	-2.3	-0.1	0.1	0.0	5.1	20.0	2.95
8	0	2.5	0.0	-3.6	0.2	0.3	-0.4	6.2	20.0	2.23
9	0	-3.7	0.5	-5.6	1.5	0.3	-0.2	6.7	20.0	2.00
10	0	0.1	-7.8	-6.3	0.4	0.3	-0.4	8.1	20.0	1.48
11	0	-2.5	-11.7	-8.6	1.6	0.2	-0.4	9.9	20.0	1.02
12	0	-3.3	5.5	-3.6	0.5	0.3	0.1	9.1	20.0	1.20
13	0	-1.1	8.5	-2.3	0.8	0.3	0.1	10.9	20.0	0.84
14	0	-3.7	-0.6	-5.2	-1.1	0.1	-0.1	5.0	20.0	2.99
15	0	-0.4	0.1	-4.5	0.9	0.1	-0.3	5.3	20.0	2.79
16	50	0.4	0.4	0.2	1.4	1.2	0.3	3.7	20.0	4.46
17	0	-0.1	4.6	1.0	0.0	0.2	0.2	4.7	20.0	3.25
18	0	-0.1	5.4	0.9	0.0	0.1	0.2	5.6	20.0	2.59
19	0	-0.1	5.7	0.8	0.0	0.0	0.2	5.9	20.0	2.39
20	0	-0.1	5.6	0.9	0.0	-0.1	0.2	5.8	20.0	2.46
21	0	-0.1	5.0	1.1	-0.1	-0.1	0.2	5.1	20.0	2.93
22	0	-0.1	3.4	1.1	-0.1	-0.3	0.1	3.5	20.0	4.69
23	90	1.9	1.3	-0.1	1.3	0.0	0.0	3.1	20.0	5.56
24	0	-0.3	2.5	4.3	0.0	0.4	0.4	4.7	20.0	3.22
25	0	-0.3	4.8	3.7	0.0	0.2	0.4	5.2	20.0	2.85
26	0	-0.3	6.0	3.6	0.0	0.1	0.4	6.4	20.0	2.15
27	0	-0.3	6.4	3.7	0.0	0.0	0.4	6.8	20.0	1.95
28	0	-0.3	6.1	3.6	0.0	-0.1	0.4	6.5	20.0	2.09
29	0	-0.3	5.1	3.6	0.0	-0.2	0.4	5.4	20.0	2.69
30	0	-0.3	3.1	4.0	-0.1	-0.4	0.4	4.4	20.0	3.51
31	90	3.1	1.7	-0.1	-1.4	-0.1	0.0	4.1	20.0	3.92
32	70	1.4	-0.7	0.3	-1.2	-0.8	0.5	3.6	20.0	4.51
33	50	0.8	0.4	-0.9	-0.4	-0.5	0.6	2.5	20.0	7.08
34	60	2.9	1.6	1.4	-1.9	-1.4	1.4	5.3	20.0	2.78
35	90	1.7	0.3	0.2	-0.7	-0.3	0.0	2.2	20.0	8.19
36	180	-0.3	-0.5	3.9	-0.8	-0.1	-0.6	5.3	20.0	2.79
37	0	-0.8	-0.1	-0.4	-0.1	0.0	0.0	0.7	20.0	26.30
38	0	-0.8	-0.1	-0.6	-0.3	0.0	0.0	0.9	20.0	20.32
39	10	-0.8	-0.1	-0.7	-0.3	0.1	0.0	0.9	20.0	21.09
40	80	1.2	1.8	-0.2	-0.4	1.7	0.1	4.1	20.0	3.90
41	30	-1.2	0.0	-1.1	-0.1	-0.1	0.1	1.3	20.0	14.69

Note: Includes cask lid bolt preload.

Table 2.6.2.3-2 $P_m + P_b$ Stresses—150 psig Internal Pressure; Cold (-40°F)

		Cylindrical Stress Components (ksi)							Allowable Stress	
Section	Angle	S_X	S_Y	S_Z	S_{XY}	S_{YZ}	S_{XZ}	SI (ksi)	(ksi)	MS
1	180	1.8	0.1	4.3	-0.2	0.0	-0.1	4.3	30.0	6.06
2	180	0.0	0.0	3.0	-0.2	-0.1	-0.2	3.2	30.0	8.45
3	180	-0.9	-0.1	1.7	0.3	0.0	-0.2	2.8	30.0	9.83
4	20	-1.0	1.2	-1.4	-0.2	-0.3	-0.4	2.9	30.0	9.40
5	40	-2.3	-0.1	-4.5	0.0	0.0	0.0	4.3	30.0	5.93
6	0	-1.1	-0.2	-4.7	0.2	0.0	-0.1	4.5	30.0	5.61
7	0	2.5	6.6	-1.7	0.4	0.2	-0.1	8.4	30.0	2.57
8	0	5.8	10.9	0.5	0.3	0.4	-0.2	10.5	30.0	1.85
9	0	1.7	17.8	0.9	0.4	0.5	-0.1	16.9	30.0	0.77
10	0	2.6	-6.9	-5.1	-0.5	0.3	-0.5	9.7	30.0	2.10
11	0	4.9	-8.8	-5.3	1.0	0.3	-0.7	13.9	30.0	1.16
12	0	-6.6	4.6	-4.6	-0.1	0.2	0.2	11.2	30.0	1.67
13	0	-6.8	6.6	-4.4	0.8	0.4	0.3	13.6	30.0	1.21
14	0	-5.7	6.3	-3.9	-0.4	0.2	0.2	12.0	30.0	1.50
15	0	4.3	11.3	0.0	1.0	0.3	-0.2	11.6	30.0	1.60
16	40	0.9	1.1	0.9	2.0	2.5	0.9	6.4	30.0	3.70
17	0	-0.1	7.3	7.9	0.0	0.0	0.8	8.2	30.0	2.67
18	0	-0.1	2.2	-7.4	0.0	0.2	-0.5	9.7	30.0	2.10
19	0	-0.1	2.4	-7.9	0.0	0.0	-0.5	10.4	30.0	1.90
20	0	-0.1	2.5	-7.2	0.0	-0.2	-0.5	9.7	30.0	2.10
21	0	-0.1	7.6	7.5	0.0	0.1	0.7	7.8	30.0	2.86
22	40	0.8	1.3	0.9	-2.0	-2.5	0.9	6.5	30.0	3.59
23	0	-0.3	0.9	-2.6	0.8	0.9	-0.3	4.3	30.0	6.02
24	0	-0.2	5.0	8.7	0.0	0.1	0.8	9.0	30.0	2.32
25	0	-0.2	7.4	10.5	0.0	0.0	1.0	10.9	30.0	1.74
26	0	-0.2	9.2	12.1	0.0	0.0	1.1	12.5	30.0	1.39
27	0	-0.2	9.9	12.9	0.0	0.0	1.2	13.3	30.0	1.25
28	0	-0.2	9.4	12.6	0.0	0.0	1.2	13.0	30.0	1.30
29	0	-0.2	8.0	11.6	0.0	-0.1	1.1	12.0	30.0	1.51
30	0	-0.2	4.9	9.8	0.0	-0.2	0.9	10.1	30.0	1.96
31	0	-0.2	1.2	4.4	-0.5	-0.2	0.4	4.8	30.0	5.23
32	50	1.2	-1.1	0.8	-2.1	-2.0	0.9	6.5	30.0	3.63
33	50	1.1	-1.6	-2.5	-1.7	-1.7	0.8	6.2	30.0	3.84
34	0	-0.2	6.3	-2.0	0.6	-0.8	-0.3	8.5	30.0	2.54
35	90	3.3	0.6	0.6	-0.8	-1.4	-0.1	4.4	30.0	5.76
36	180	-0.8	-0.6	3.7	-1.3	-0.4	-0.7	5.9	30.0	4.05
37	0	-7.0	-0.2	-8.2	-0.1	0.0	0.0	8.0	30.0	2.74
38	0	-4.7	-0.2	-7.3	-0.3	0.0	-0.1	7.1	30.0	3.22
39	0	-2.9	0.5	-6.3	-0.7	0.1	-0.1	7.0	30.0	3.29
40	80	5.2	6.9	1.7	-0.5	1.7	0.3	6.3	30.0	3.78
41	0	-2.4	-0.2	-1.3	0.2	0.0	0.1	2.2	30.0	12.44

Note: Includes cask lid bolt preload.

Table 2.6.2.3-3 Thermal (Q) Stresses— Cold (-40°F)

Section	Angle	Cylindrical Stress Components (ksi)						SI (ksi)
		S_X	S_Y	S_Z	S_{XY}	S_{YZ}	S_{XZ}	
1	10	-0.1	0.0	0.0	0.0	0.0	0.0	0.1
2	10	-0.1	0.0	-0.1	0.0	0.0	0.0	0.1
3	105	0.0	0.0	0.1	0.1	0.0	-0.1	0.2
4	90	0.0	0.0	0.0	0.1	0.0	-0.1	0.2
5	0	-0.2	0.0	-0.1	0.0	0.0	0.0	0.2
6	0	-0.2	0.0	-0.1	0.0	0.0	0.0	0.2
7	0	-0.3	0.0	-0.2	-0.1	0.0	0.0	0.3
8	0	-0.3	0.0	-0.2	-0.1	0.0	0.0	0.3
9	0	0.0	0.2	-0.1	0.0	0.0	0.0	0.3
10	105	0.0	0.0	0.0	0.1	0.0	-0.1	0.2
11	180	-0.1	0.0	0.0	0.1	0.0	0.0	0.2
12	10	-0.3	0.2	-0.2	0.0	0.0	0.0	0.5
13	0	-0.1	0.3	-0.1	0.0	0.0	0.0	0.4
14	10	-0.3	0.2	-0.2	0.0	0.0	0.0	0.5
15	0	-0.1	0.3	-0.1	0.0	0.0	0.0	0.4
16	90	0.0	0.0	0.0	0.1	0.0	0.0	0.2
17	90	0.0	0.0	0.0	0.1	0.0	0.0	0.2
18	180	0.0	-0.1	0.0	0.0	0.0	0.0	0.1
19	180	0.0	-0.1	0.0	0.0	0.0	0.0	0.1
20	180	0.0	-0.1	0.0	0.0	0.0	0.0	0.1
21	180	0.0	-0.1	-0.1	0.0	0.0	0.0	0.1
22	70	0.0	0.0	0.0	-0.1	0.0	0.0	0.2
23	0	0.0	-0.1	-0.2	0.0	0.0	0.0	0.2
24	90	0.0	0.0	0.0	0.1	0.0	0.0	0.1
25	90	0.0	0.0	0.0	0.1	0.0	0.0	0.1
26	90	0.0	0.0	0.0	0.0	0.0	0.0	0.1
27	180	0.0	-0.1	0.0	0.0	0.0	0.0	0.1
28	180	0.0	-0.1	0.0	0.0	0.0	0.0	0.1
29	180	0.0	-0.1	0.0	0.0	0.0	0.0	0.1
30	90	0.0	0.0	0.0	0.0	0.0	0.0	0.1
31	90	0.0	0.0	0.0	0.0	0.0	0.0	0.1
32	90	0.0	0.0	0.0	-0.1	0.0	0.0	0.2
33	105	-0.1	0.0	0.0	-0.1	0.0	-0.1	0.3
34	180	0.0	0.2	0.1	0.0	0.0	0.0	0.2
35	90	-0.1	0.0	0.0	-0.1	0.0	0.0	0.2
36	0	-0.1	0.1	-0.3	0.0	0.0	0.0	0.3
37	0	-0.2	0.0	0.0	0.0	0.0	0.0	0.2
38	0	-0.2	0.0	-0.1	0.0	0.0	0.0	0.2
39	0	0.1	0.0	-0.1	0.1	0.0	0.0	0.2
40	0	0.2	-0.2	-0.1	0.1	0.0	0.0	0.4
41	0	-0.1	0.1	-0.2	-0.1	0.0	0.0	0.3

Table 2.6.2.3-4 P_m Stresses—1-g Gravity Load; Cold (-40°F)

		Cylindrical Stress Components (ksi)							Allowable Stress	
Section	Angle	S_X	S_Y	S_Z	S_{XY}	S_{YZ}	S_{XZ}	SI (ksi)	(ksi)	MS
1	0	-0.1	0	0	0	0	0	0.1	20	174.28
2	0	-0.1	-0.1	0	0	0	0	0.1	20	159.51
3	30	-0.1	-0.2	0	0	0	0	0.2	20	127.21
4	10	-0.2	-0.3	-0.1	0	0	-0.1	0.3	20	71.02
5	0	-0.1	-0.1	0	0	0	0	0.1	20	141.45
6	0	-0.2	-0.2	0	0	0	0	0.2	20	94.15
7	0	-0.2	-0.3	0.1	0	0	0	0.4	20	48.19
8	10	-0.1	-0.4	0	0	0	-0.1	0.4	20	46.8
9	0	-0.3	-0.5	0	0	0	0.1	0.5	20	41.17
10	0	-0.2	-0.6	-0.4	0	0	0	0.3	19.1	56.8
11	0	-0.3	-0.7	-0.7	0	0	0.1	0.4	19.1	48.38
12	0	-0.4	-0.4	0.5	0	0	0	0.9	19.1	20.28
13	0	-0.3	-0.3	0.7	0	0	0.1	1	19.1	18.98
14	0	-0.4	-0.5	-0.1	0	0	-0.1	0.5	19.7	40.11
15	0	-0.2	-0.5	-0.1	0	0	0.1	0.5	19.7	39.56
16	60	0	0	0	0	-0.2	0	0.3	19.7	55.68
17	0	0	0.1	0.3	0	0	0	0.4	19.7	55.13
18	0	0	0.1	0.4	0	0	0	0.4	19.7	44.84
19	0	0	0.1	0.5	0	0	0	0.5	19.7	41.42
20	0	0	0.1	0.5	0	0	0	0.5	19.7	41.96
21	0	0	0.1	0.4	0	0	0	0.4	19.7	48.01
22	40	0	0.3	0.2	0	0.1	0	0.4	19.7	47.6
23	40	0	-0.1	0	0	-0.2	0	0.4	19.1	50.73
24	50	0	0	0	0	-0.2	0	0.4	19.1	52.56
25	0	0	0.1	0.3	0	0	0	0.3	19.1	63.23
26	0	0	0.1	0.4	0	0	0	0.4	19.1	49.04
27	0	0	0.1	0.4	0	0	0	0.4	19.1	45.45
28	0	0	0.1	0.4	0	0	0	0.4	19.1	48.69
29	0	0	0.1	0.3	0	0	0	0.3	19.1	62.06
30	60	0	0	0	0	0.2	0	0.4	19.1	51.33
31	50	0	0.5	0	0	0.3	0	0.7	19.1	25.22
32	60	0	0.6	0	0	0.2	0.1	0.7	20	25.85
33	60	-0.4	0.7	0.1	-0.1	0.1	0.1	1.1	20	17.26
34	60	0.3	1	-0.2	0	0.3	0.1	1.3	20	14.17
35	70	-0.2	0.7	-0.1	0	0.2	0.3	1.2	20	15.98
36	180	1.1	1.6	-0.2	0.1	0	0.3	1.9	20	9.43
37	0	-0.4	-0.3	0	0	0	0	0.4	20	51.41
38	180	-0.4	-0.3	0	0	0	0	0.4	20	51.53
39	80	-0.3	-0.4	-0.8	0.1	0	-0.1	0.6	20	33.72
40	80	-1.6	-2	-3.4	0.1	0	-1.2	3	20	6.64
41	0	-0.2	-0.1	0	0	0	0	0.2	20	96.75

Note: Includes cask lid bolt preload.

Table 2.6.2.3-5 $P_m + P_b$ Stresses—1-g Gravity Load; Cold (-40°F)

Section	Angle	Cylindrical Stress Components (ksi)						SI (ksi)	Allowable Stress (ksi)	MS
		S_X	S_Y	S_Z	S_{XY}	S_{YZ}	S_{XZ}			
1	180	-0.1	0.1	0	0	0	0	0.2	30	149.45
2	20	-0.2	-0.2	0	0	0	0	0.2	30	152.69
3	30	-0.2	-0.2	0	0	0	0	0.3	30	118
4	10	-0.3	-0.3	-0.1	0	0	-0.1	0.3	30	99.67
5	0	-0.2	-0.2	0	0	0	0	0.2	30	143.72
6	0	-0.2	-0.3	0	0	0	0	0.3	30	98.57
7	0	-0.2	-0.3	0.3	0	0	0	0.6	30	49.13
8	0	-0.1	-0.2	0.5	0	0	-0.1	0.8	30	38.62
9	0	0.1	-0.1	0.9	0	0	0	1	30	28.82
10	0	-0.1	-0.5	-0.4	0	0	-0.1	0.4	28.7	69.04
11	0	0.1	-0.5	-0.5	0	0	0	0.6	28.7	47.89
12	0	-0.6	-0.4	0.4	0	0	0	1	28.7	26.6
13	0	-0.7	-0.4	0.5	0	0	0	1.2	28.7	23.39
14	0	-0.5	-0.4	0.5	0	0	0	1.1	29.6	27.02
15	0	0.1	-0.1	0.9	0	0	0.1	1	29.6	27.73
16	50	0	0.2	0.1	0	-0.2	0	0.5	19.7	40.89
17	0	0	0.4	0.5	0	0	0	0.5	19.7	38.44
18	0	0	0.5	0.6	-0.1	0	0	0.6	19.7	31.52
19	0	0	-0.4	0.3	0	0	0	0.7	19.7	29.11
20	0	0	0.5	0.6	-0.1	0	0	0.6	19.7	30.07
21	0	0	0.4	0.5	0	0	0	0.6	19.7	34.83
22	40	0	0.4	0.3	0	0.2	0	0.6	29.6	47.38
23	30	0	-0.2	0.1	0	-0.3	0	0.6	28.7	48.69
24	40	0	0.1	0.1	0	-0.2	0	0.5	19.1	38.1
25	0	0	0.4	0.4	0	0	0	0.5	19.1	41.19
26	0	0	-0.4	0.2	0	0	0	0.6	19.1	33.53
27	0	0	-0.4	0.2	0	0	0	0.6	19.1	30.74
28	0	0	-0.4	0.2	0	0	0	0.6	19.1	32.46
29	0	0	0.5	0.4	0	0	0	0.5	19.1	36.7
30	50	0	0.2	0.1	0	0.2	0	0.5	19.1	39.29
31	40	0	0.6	0.1	0	0.4	0	0.9	28.7	32.45
32	50	0	0.6	-0.3	0	0.2	0	1	30	30.11
33	70	-0.8	0.4	-0.6	-0.2	0.3	0.1	1.4	30	20.07
34	50	0	0.6	-1.4	0	0.3	-0.1	2.1	30	13.3
35	70	-0.3	0.5	-1.1	0	0.4	1.5	3.2	30	8.25
36	180	-0.4	0.7	-2	0.1	0	0.1	2.7	30	10.21
37	0	-3.8	-3.6	0	0	0	0	3.8	30	6.92
38	30	-4	-3.8	-0.1	0	0	0	3.9	30	6.67
39	70	3.5	2.7	-1.1	0	0	0	4.7	30	5.41
40	0	-3.2	-6.4	-9.9	0.2	-0.1	0.4	6.7	30	3.49
41	0	-0.3	-0.2	0	0	0	0	0.3	30	109.17

Note: Includes cask lid bolt preload.

2.6.3 Reduced External Pressure

The drop in atmospheric pressure to 3.5 psia, as specified in 10 CFR 71.71(c)(3), effectively results in an additional internal pressure in the cask of 11.2 psig (14.7 -3.5 = 11.2). However, stresses are conservatively calculated for a 150 psig internal pressure as presented in Section 2.6.1.3. The maximum stress intensities in the cask due to the 150 psig pressure plus gravity are calculated to be a primary membrane stress of 12.7 ksi with a margin of safety of +0.6 and a primary membrane plus bending stress of 21.6 ksi with a margin of safety of +0.4. Therefore, the requirements of 10 CFR 71.71(c)(3) are met.

2.6.4 Increased External Pressure

An increased external pressure of 20 psia (5.3 psig external pressure), as specified in 10 CFR 71.71(c)(4), has a negligible effect on the Universal Transport Cask because of the thick outer shell and end closures of the cask. Conservatively, applying a 20 psig external pressure to the neutron shield shell produces a compressive hoop stress. With a radius of 46.055 in. (cask outer radius of 82.61/2 plus 4.75 in. to outer neutron shell) and a thickness of 0.25 in., the calculated hoop stress is 3,685 psi. This stress is low compared to the material strength and will result in no adverse impact on the performance of the cask. Based on these observations, the requirements of 10 CFR 71.71 (c)(4) are met.

2.6.5 Vibration

The effect of vibrations normally incident to transportation is considered to be negligible for the Universal Transport Cask. This conclusion is based on the following factors:

1. The minimum natural frequency of the cask is conservatively calculated as 228 Hertz [28] (Table 36, Case 4a). The determination of this natural frequency is made considering only the stiffness of the cask outer shell and the total cask weight of 159,898 lb for the case of a free cylinder. The most significant periodic impulse load occurs as the two closest rail car wheels pass over a rail junction. A maximum speed for rail transportation of 140 miles/hour or 205 feet/second [56] is very conservatively assumed. The duration between pulses is 0.024 seconds, which corresponds to a frequency of 1/0.024 = 42 hertz. This is significantly below the fundamental frequency of the cask. Consequently, vibrational excitation is considered to be insignificant.

2. The calculated stresses due to vibrations normally incident to transportation are much smaller than the calculated stresses for the normal transport 1-ft drop event.

The following analysis documents the second factor mentioned above.

It is conservatively assumed that the normal transport vibration acceleration is equal to the equivalent acceleration which will produce the normal vertical loading imposed on the tiedown devices by 10 CFR 71.45 (b)(1). This regulation specifies a load factor of 2.0 to be applied to the package weight; therefore, it is assumed that the tiedown devices and the cask must resist an imposed 2.0 g vibration acceleration. From the 1-*g* stress evaluation presented in Section 2.6.1.3, the maximum stress produced in the cask is 6,700 psi. Scaling the stress for 2 *g*, the maximum stress intensity is 13,400 psi.

The maximum stress intensity range for normal transport vibration is obtained by multiplying the maximum stress intensity from the 1g normal condition by the acceleration values from vibration . Thus the maximum stress intensity in the cask for the 2 *g* loading is S_{max} = 13,400 psi and S_{min} = -13,400 psi. The allowable alternating stress intensity for austenitic stainless steel is determined as the 10^{11} cycle value from the ASME Boiler and Pressure Vessel Code, Section III, Appendices, Table I-9.2.2 [17]. This value is S_a = 23,700 psi; therefore, the margin of safety for the critical component of the Universal Transport Cask for normal transport vibration is:

$$MS = (S_a/S_{alt}) - 1 = (23{,}700/13{,}400) - 1 = +0.77$$

where S_{alt} = ½ of the total applied stress range.

The rotation pockets serve as the rear tiedown for the Universal Transport Cask during normal transport. The rotation pocket is the critical tiedown component for all three load axes; the front of the cask is supported in a cradle and restrained vertically by a band attached to the cradle. The critical component on the rotation pocket is the attachment weld between the pocket and the cask outer shell, which has a maximum shear stress of 28,546 psi. This shear stress is produced by the 10.2 *g* resultant from the combined longitudinal and vertical shock (10.0 *g* longitudinal and 2.0 *g* vertical) tiedown load components (Section 2.5.2).

The ratio of the normal transport vibration acceleration to the resultant acceleration for the combined longitudinal and vertical shock is used to ratio the stresses. The alternating shear stresses are S_{max} = (2.0/10.2)(28,546) = 5,597 psi and S_{min} = -(2.0/10.2)(28,546) = -5,597 psi. The margin of safety for the rotation pocket as a rear tiedown device for normal transport is:

$$MS = (S_a/S_{alt}) - 1 = (23{,}700/5{,}597) - 1 = +3.2$$

Therefore, the Universal Transport Cask satisfies the requirements for normal vibration incident to transportation as required by 10 CFR 71.71(c)(5).

2.6.6 Water Spray

Water causes negligible corrosion of the stainless shell of the Universal Transport Cask, and the cask contents are protected in the sealed cavity. A water spray as specified in 10 CFR 71.71(c)(6) has no adverse impact on the package. The cask surface temperature specified during the water spray is between 100°F and -20°F. Consequently, the induced thermal stress in the cask components is less than the thermal stresses that occur during the extreme temperature conditions for normal transport. Therefore, the requirements of 10 CFR 71.71(c)(6) are satisfied.

2.6.7 Free Drop (1-Foot): Cask Body Analysis

The free drop scenario outlined by 10 CFR 71.71(c)(7) requires the Universal Transport Cask to be structurally adequate for a 1-ft drop (normal conditions of transport) onto a flat, essentially unyielding horizontal surface in the orientation that inflicts the maximum damage to the cask. In the following subsections, the cask body, impact limiters, closure lid and bolts, neutron shield shell, and upper ring components are evaluated for the end, side, and corner-drop orientations.

Evaluation of each drop orientation is accomplished by using finite element analysis techniques. A complete description of the 3D model used to analyze the cask body is presented in Appendix 2.10.2. Appendix 2.10.2 also describes the loadings applied to the finite element model, the thermal conditions considered, and the locations of the sections on the cask body that are evaluated. The results of each drop orientation listed above are presented in this section. The impact limiters and the impact limiter attachments are evaluated in Section 2.6.7.5 for all loading conditions and orientations.

The analysis is performed using a 20g acceleration for the end and side drops. Using a 20g acceleration provides a bounding analysis, as it exceeds the calculated g-loads for the end and side drop events shown in Table 2.6.7.5-3.

For normal conditions, the one-ft drop is not a sufficient height to rotate the cask to an oblique orientation following a drop. Therefore, oblique drop orientations are not considered a credible event, and are not included in these analyses.

Only the analyses for enveloping structural conditions, representing the more restrictive of either the PWR or BWR fuel payload configuration are presented. Where necessary, a composite payload of the PWR configuration decay heat load and the BWR configuration weight is used for the cask body analysis. This composite configuration imposes larger impact loads on the cask components and raises the component temperatures, thereby lowering the material strength, resulting in a more restrictive loading configuration than either the PWR or BWR payload configurations would impose.

2.6.7.1 One-Foot End Drop

In accordance with the requirements of 10 CFR 71.71, the Universal Transport Cask is structurally evaluated for the normal condition of transport 1-ft end-drop. In this event, the cask (equipped with an impact limiter over each end) falls a distance of 1 ft onto a flat, unyielding, horizontal surface. The cask strikes the surface in a vertical position; consequently, an end impact on the bottom end or top end of the cask occurs. The analysis is performed using a 20g acceleration, which provides a bounding analysis as it exceeds the calculated g-loads for the end drop event shown in Table 2.6.7.5-3.

Stress results for the 1-ft top-and bottom-end-drop combined loading are documented in Tables 2.6.7.1-1 through 2.6.7.1-16. These tables document the primary membrane (P_m), primary membrane plus primary bending ($P_m + P_b$), primary membrane plus primary bending plus secondary peak stress (P + Q), and critical (P_m, $P_m + P_b$, and P + Q) stresses in accordance with the criteria presented in Regulatory Guide 7.6.

As shown in Tables 2.6.7.1-1 through 2.6.7.1-8, the margins of safety for the primary stress intensity category are positive for all of the 1-ft top-end-drop conditions. The most critically stressed component in the system is the top forging for the top-end-drop. The minimum margin of safety for P_m stress intensity for the top-end-drop condition is found to be 1.66 as documented in Table 2.6.7.1-5. The minimum margin of safety for $P_m + P_b$ stress intensity for the top-end-drop condition is found to be 1.17, as documented in Table 2.6.7.1-6. The minimum margin of safety for the P + Q stresses (2.43) occurs in the inner shell, as documented in Table 2.6.7.1-8.

As shown in Tables 2.6.7.1-9 through 2.6.7.1-16, the margins of safety for the primary stress intensity category are positive for all of the 1-ft bottom-end-drop conditions. The most critically stressed components in the system are the cask body ligaments for the bottom-end-drop. The minimum margin of safety for P_m stress intensity for the bottom end-drop condition is found to be 0.74, as documented in Table 2.6.7.1-13. The minimum margin of safety for $P_m + P_b$ stress intensity for the bottom-end-drop condition is found to be 1.29, as documented in Table 2.6.7.1-14. The minimum margin of safety for the P + Q stresses (2.49) occurs in the inner shell as documented in Table 2.6.7.1-16.

Because the margins of safety are all positive, the Universal Transport Cask satisfies the requirements of 10 CFR 71.71(c)(7) for the 1-ft end-drop (normal transport) condition.

Table 2.6.7.1-1 P_m Stresses—1-Foot Top End-Drop, Bolt Preload, Internal Pressure

Section	Angle	Cylindrical Stress Components (ksi)						SI (ksi)	Allowable Stress (ksi)	MS
		S_X	S_Y	S_Z	S_{XY}	S_{YZ}	S_{XZ}			
1	70	0.3	0.3	0	0	0	0.1	0.4	20	44.31
2	180	0.3	0.3	0	0	0	0.1	0.4	20	48.47
3	180	0.2	0.4	0.2	0	0	0.2	0.4	20	48.37
4	180	0.3	0.2	0.3	0	0	0.3	0.6	20	35.02
5	180	-0.1	-0.1	-0.2	0	0	0	0.1	20	157.23
6	80	-0.1	-0.1	-0.1	0	0	0.1	0.2	20	92.5
7	0	-0.1	0.1	0.5	0	0	0.1	0.7	20	28.2
8	180	1.1	0	-0.2	-0.1	0	0.4	1.5	20	12.06
9	105	-0.7	-0.6	-0.2	-0.1	0.1	0.4	0.9	20	21.26
10	135	0.8	-0.5	-1.6	-0.1	0	0.6	2.7	19.1	6.1
11	135	0.2	-1.1	-2.8	-0.1	0.1	0.6	3.3	19.1	4.85
12	80	0.2	0.1	0.8	-0.1	0	0	0.8	19.1	24.3
13	80	0.7	0.4	1.4	-0.1	-0.1	0.1	1	19.1	17.24
14	135	-0.2	-0.1	0.5	0	0	-0.2	0.8	19.7	24.06
15	80	0.6	0.1	0.5	-0.1	-0.1	0.1	0.6	19.7	33.05
16	0	0	1	0.1	-0.1	0	0	1	19.7	18.04
17	0	0	1.3	-0.1	-0.1	0	0	1.5	19.7	12.58
18	0	-0.1	1.6	-0.3	-0.2	0	0	1.9	19.7	9.33
19	0	-0.1	2	-0.5	-0.2	0	0	2.5	19.7	6.79
20	0	-0.1	2.8	-0.8	-0.3	0	0	3.7	19.7	4.39
21	0	-0.1	4.1	-1.2	-0.4	0	0	5.3	19.7	2.72
22	0	-0.2	5.6	-1.8	-0.6	0	0.1	7.4	19.7	1.66
23	105	-0.1	0.2	-0.6	0	0.2	0.2	1	19.1	18.69
24	120	-0.1	1.5	-0.7	0	0.1	0	2.2	19.1	7.59
25	0	-0.1	1.1	-0.9	-0.1	0	0	2	19.1	8.44
26	0	-0.2	0.9	-1.2	-0.1	0	0	2.1	19.1	8.06
27	0	-0.2	0.7	-1.5	0	0	0	2.2	19.1	7.82
28	0	-0.2	0	-1.7	0.1	0	0	1.7	19.1	10.23
29	10	-0.2	-1.2	-1.9	0	0	0	1.7	19.1	10.2
30	20	-0.2	-2.8	-1.9	0	-0.1	0	2.6	19.1	6.41
31	90	-0.4	-3	-1.7	0.1	-0.5	0.1	2.8	19.1	5.87
32	0	-0.3	4.3	-2	-0.5	0	-0.3	6.4	20	2.1
33	0	1.1	2.9	-1.9	-0.2	0	-0.6	5	20	3.02
34	0	3.4	3.3	-3.1	-0.1	0.1	1.2	7	20	1.87
35	180	-0.6	1.5	-2.1	0.3	-0.2	0.2	3.8	20	4.31
36	0	1.5	1	-3.2	0	0.3	0.1	4.8	20	3.18
37	0	-0.3	-0.2	-1.2	0	0.2	0.6	1.4	20	12.85
38	0	-0.3	-0.2	-1.1	0	0.2	0.5	1.3	20	14.86
39	0	-0.1	-0.5	-3.1	0	0.1	0.2	3	20	5.7
40	0	-2	-2	-6.2	0	-0.1	-1.2	4.8	20	3.15
41	135	-0.2	-0.2	-0.6	0	0	0.2	0.5	20	40.25

Table 2.6.7.1-2 $P_m + P_b$ Stresses—1-Foot Top End-Drop, Bolt Preload, Internal Pressure

		Cylindrical Stress Components (ksi)							Allowable Stress	
Section	Angle	S_X	S_Y	S_Z	S_{XY}	S_{YZ}	S_{XZ}	SI (ksi)	(ksi)	MS
1	70	1.4	1.8	0	0	0	0.1	1.8	30	15.46
2	180	0.4	1	0	0.1	0	0.1	1.1	30	27.25
3	180	0.7	0.5	0.7	0	0	0.5	0.9	30	31.7
4	180	0.6	0.5	0.6	0	-0.1	0.5	1	30	27.87
5	180	1.3	1	-0.2	0	0	0	1.4	30	19.94
6	120	0.7	1	0	0	0	0.1	1.1	30	27.04
7	0	-1.8	-0.4	-0.3	-0.1	0	0.1	1.6	30	18.24
8	135	0.3	-0.9	-2.5	-0.1	0	0.4	3	30	8.96
9	135	0.3	0.7	3.4	0	0.1	0.1	3.1	30	8.58
10	135	1.6	0	-1	-0.1	0	0.5	2.8	28.7	9.25
11	135	2	-0.2	-2.1	-0.1	0	0.7	4.3	28.7	5.7
12	105	-0.7	-0.2	0.4	-0.1	0	-0.1	1.1	28.7	23.98
13	120	-0.6	-0.1	1	-0.1	0	0.1	1.6	28.7	16.74
14	180	-0.4	-0.1	0.7	0	0.1	-0.2	1.3	29.6	22.42
15	80	1.5	0.7	1.6	-0.1	-0.2	0.2	1.2	29.6	24.18
16	20	-0.1	1	0	0	-0.1	0	1.1	29.6	25.85
17	20	-0.1	1.5	-0.1	0	0	0	1.6	29.6	18.08
18	30	-0.1	1.8	-0.2	0	0	0	2	29.6	13.45
19	0	0	2.2	-0.5	-0.2	0	0	2.7	29.6	9.91
20	20	-0.2	3.2	-0.7	0	0	0	3.9	29.6	6.66
21	0	0	4.3	-1.2	-0.4	0	0	5.5	29.6	4.36
22	10	-0.3	5.1	-3.8	0	0.1	0.1	8.9	29.6	2.32
23	80	-0.1	0.3	-0.6	0	0.2	0.1	1	28.7	27.23
24	180	-0.2	1.7	-0.7	0.2	0	0	2.5	28.7	10.56
25	0	-0.2	1.5	-0.8	-0.1	0	0	2.3	28.7	11.71
26	0	-0.2	1.4	-1.1	-0.1	0	0	2.4	28.7	10.78
27	0	-0.2	1.3	-1.3	-0.1	0	0	2.6	28.7	9.99
28	0	-0.3	0.6	-1.5	0	0	0	2.2	28.7	12.27
29	0	-0.3	-1.9	-2.1	0.2	0	0	1.9	28.7	14.24
30	20	-0.1	-3.3	-2.3	0	-0.1	0	3.2	28.7	8.08
31	0	-0.6	-4.6	-6.3	0.4	0.1	0.2	5.8	28.7	3.95
32	0	-0.6	4	-3.2	-0.5	0	-0.2	7.2	30	3.14
33	0	-0.5	1.7	-4.2	-0.2	0	-0.4	6	30	4.04
34	0	-0.2	-0.9	-14	0	-0.1	-0.3	13.8	30	1.17
35	0	-1	1.4	-3.3	-0.2	0.2	1.2	5.3	30	4.63
36	0	-0.7	-0.3	-5.9	0	0.4	0.1	5.6	30	4.35
37	10	1	2.9	-0.8	0	0.1	0.6	3.8	30	6.91
38	0	2.7	0.1	-1.3	0.2	0.3	0.5	4.3	30	6.05
39	0	4.8	1.4	-2.9	0.2	0.2	-0.2	7.7	30	2.88
40	0	-4.6	-5.4	-13.4	0	0	-0.1	8.7	30	2.43
41	135	0.1	-0.3	-1.1	0	0	0.2	1.2	30	23.27

Table 2.6.7.1-3 $P_m + P_b + Q$ Stresses—1-Foot Top End-Drop, Bolt Preload, Internal Pressure, Thermal Hot

Section	Angle	Cylindrical Stress Components (ksi)							Allowable Stress	MS
		S_X	S_Y	S_Z	S_{XY}	S_{YZ}	S_{XZ}	SI (ksi)	(ksi)	
1	80	5.8	4.4	0	0.3	0	0	5.8	60	9.28
2	0	4	5.2	-0.1	-0.1	0.1	0	5.3	60	10.41
3	10	-3.2	3.2	-0.1	0.1	0	0.2	6.5	60	8.28
4	0	7	-0.9	-4.4	0.3	0.6	-0.5	11.6	60	4.15
5	0	-4.7	-1.8	-0.5	-0.9	0.2	-0.2	4.5	60	12.2
6	0	-1.8	-0.1	-0.3	-0.2	0	0.1	1.7	60	33.7
7	0	-1.7	-0.3	-3.4	-0.1	-0.1	-0.8	3.5	60	15.99
8	0	-1.7	-0.3	-3.4	-0.1	-0.1	-0.8	3.5	60	15.99
9	40	-1.3	-0.5	-3	-1	1.3	0.4	4.3	60	13.08
10	0	-0.8	0.1	-3.3	-0.2	-0.2	-0.1	3.5	57.4	15.38
11	40	-1.3	-0.5	-3	-1	1.3	0.4	4.3	57.4	12.46
12	0	-0.6	2	4.5	-0.3	0.1	-0.2	5.2	57.4	10.11
13	0	-0.7	1.3	2.1	-0.3	0.1	-0.2	2.9	57.4	19.05
14	0	-0.6	2	4.5	-0.3	0.1	-0.2	5.2	59.1	10.45
15	90	-0.1	1.8	2.6	-0.1	-0.3	0	2.8	59.1	20.38
16	0	-0.1	3.4	1.7	-0.3	0.1	0.1	3.6	59.1	15.5
17	0	-0.1	5.3	3	-0.5	0.1	0	5.5	59.1	9.66
18	0	-0.2	5.9	2.7	-0.6	0	0	6.2	59.1	8.48
19	0	-0.2	6.5	2.3	-0.7	0	0	6.8	59.1	7.74
20	0	-0.2	7.4	2.1	-0.7	0	0	7.7	59.1	6.64
21	0	-0.2	8.4	1.4	-0.8	0	0	8.8	59.1	5.75
22	0	-0.2	8.7	1.4	-0.8	-0.1	0	9	59.1	5.55
23	0	-0.2	0.1	-5	0	0.2	0	5.2	57.4	10.08
24	0	-0.9	0.8	-6.6	-0.1	0.5	0	7.5	57.4	6.63
25	0	-0.3	-3.1	-12.7	0.3	0.3	0	12.5	57.4	3.59
26	0	-0.4	-3.6	-14.8	0.4	0.1	0	14.4	57.4	2.97
27	0	-0.3	-3.2	-15.2	0.4	0.1	0	15	57.4	2.83
28	0	-0.3	-4	-15.5	0.4	0	0	15.3	57.4	2.76
29	0	-0.6	-5.8	-15.8	0.6	-0.1	0	15.3	57.4	2.75
30	0	-0.6	-7.4	-14.6	0.7	-0.2	0	14	57.4	3.1
31	0	-1.5	-7	-14.2	0.5	-0.5	0	12.8	57.4	3.48
32	0	-0.2	5.4	-2.4	-0.6	0.1	-0.7	8.1	60	6.37
33	0	0.3	3	-6	-0.3	-0.1	-0.6	9	60	5.66
34	0	0.4	-2.5	-16.8	0.2	-0.5	0.4	17.2	60	2.49
35	0	-0.2	-0.8	-12.4	0.1	0.1	0.6	12.3	60	3.86
36	0	5.7	4.1	-2.3	0.1	0.2	0.2	8	60	6.48
37	10	-3.1	-4.5	-0.8	-0.2	0.2	0.4	3.8	60	14.79
38	135	-5.8	-2.6	-0.7	0.3	0	0.2	5.1	60	10.67
39	0	1.3	-2.9	-15.7	0.4	0.3	0.5	17.1	60	2.5
40	0	0.1	-2.4	-13.8	0.3	0.2	0.1	13.9	60	3.3
41	0	-0.2	2.8	6.3	-0.3	0.2	0.1	6.6	60	8.13

Table 2.6.7.1-4 $P_m + P_b + Q$ Stresses—1-Foot Top End-Drop, Bolt Preload, Internal Pressure, Thermal Cold

		Cylindrical Stress Components (ksi)							Allowable Stress	
Section	Angle	S_X	S_Y	S_Z	S_{XY}	S_{YZ}	S_{XZ}	SI (ksi)	(ksi)	MS
1	0	0.7	3.4	-0.1	-0.4	-0.1	0.2	3.5	60	15.99
2	0	1.3	2.9	0	-0.1	0	0.1	3	60	19.28
3	10	-4.2	1.8	-0.4	0.3	0	0.4	6.1	60	8.9
4	0	11.6	-0.7	-1.2	0.5	1	-1.1	13.9	60	3.33
5	0	-3.3	-2.3	-0.3	-0.4	0.1	-0.1	3.2	60	17.77
6	135	-2.4	-2.3	-0.3	0.3	0	0	2.4	60	24.06
7	180	-2	0.5	-0.5	0.3	0	0.2	2.6	60	21.87
8	30	0.3	-0.9	-3.6	-0.7	0.6	1.7	5.4	60	10.05
9	40	-4.3	-3.4	-6.6	-1	1.4	1.1	5.1	60	10.79
10	30	0.3	-0.9	-3.6	-0.7	0.6	1.7	5.4	57.4	9.56
11	30	0.3	-0.9	-3.6	-0.7	0.6	1.7	5.4	57.4	9.56
12	10	-3.8	-0.1	1.5	-0.2	0.3	0.4	5.4	57.4	9.62
13	10	-0.2	1.1	2.5	-0.2	0.2	0.8	3.2	57.4	17.16
14	10	-3.8	-0.1	1.5	-0.2	0.3	0.4	5.4	59.1	9.95
15	40	4.2	2.5	4.1	-0.6	-0.3	0.6	2.6	59.1	21.39
16	0	-0.1	3.3	1.7	-0.3	0.1	0.1	3.5	59.1	16.08
17	0	-0.1	5.4	2.8	-0.5	0.1	0	5.6	59.1	9.58
18	0	-0.2	6.1	2.5	-0.6	0	0	6.4	59.1	8.3
19	0	-0.2	6.6	2.1	-0.7	0	0	6.9	59.1	7.57
20	0	-0.2	7.5	1.8	-0.7	0	0	7.8	59.1	6.58
21	0	-0.2	8.4	1.2	-0.8	-0.1	0	8.7	59.1	5.77
22	0	-0.5	4.2	-4.6	-0.5	0.1	-0.1	8.8	59.1	5.73
23	0	-0.2	-0.7	-5.5	0.1	0.3	0.1	5.3	57.4	9.9
24	0	-1	1.6	-6.7	-0.2	0.6	0	8.4	57.4	5.85
25	0	-0.3	-3.4	-14	0.3	0.3	0	13.8	57.4	3.17
26	0	-0.4	-3.9	-16.2	0.4	0.2	0	15.8	57.4	2.62
27	0	-0.2	-3.5	-16.6	0.4	0.1	0	16.4	57.4	2.5
28	0	-0.3	-4.3	-17	0.5	0	0	16.7	57.4	2.43
29	0	-0.6	-6	-17.3	0.6	-0.1	0	16.7	57.4	2.43
30	0	-0.7	-7.6	-15.9	0.7	-0.3	0	15.3	57.4	2.75
31	0	-1.5	-6.6	-14.5	0.5	-0.6	0	13	57.4	3.41
32	0	-0.2	5.1	-3	-0.6	0.1	-0.7	8.4	60	6.17
33	0	0.3	3	-6	-0.3	-0.1	-0.6	9.1	60	5.59
34	0	0.3	-2.3	-16	0.2	-0.6	0.4	16.3	60	2.68
35	0	-0.2	-0.7	-12.3	0.1	0.1	0.6	12.2	60	3.93
36	0	6	4.5	-1.8	0.1	0.2	0.4	7.9	60	6.61
37	10	-2.9	-4.2	-0.8	-0.1	0.2	0.4	3.5	60	16.04
38	135	-6	-2.9	-0.7	0.3	0	0.2	5.4	60	10.2
39	0	1.3	-2.4	-15.3	0.3	0.3	0.5	16.6	60	2.61
40	0	0	-2	-13.6	0.3	0.2	0	13.6	60	3.43
41	10	-0.7	1.6	3.2	0	0.3	0.3	4.0	60	13.86

Table 2.6.7.1-5 Critical P_m Stress Summary (ksi)—1-Foot Top End-Drop, Bolt Preload, Internal Pressure

Component	Section	Angle	SI (ksi)	Allowable Stress (ksi)	Margin of Safety
1	4	180	0.6	20	35.02
2	8	180	1.5	20.0	12.06
3	11	135	3.3	19.1	4.85
4	14	135	0.8	19.7	24.06
5	21	0	5.3	19.7	2.72
6	22	0	7.4	19.7	1.66
7	23	105	1	19.1	18.69
8	30	20	2.6	19.1	6.41
9	31	90	2.8	19.1	5.87
10	34	0	7	20	1.87
11	40	0	4.8	20	3.15
12	41	135	0.5	20	40.25

Table 2.6.7.1-6 Critical $P_m + P_b$ Stress Summary (ksi)—1-Foot Top End-Drop, Bolt Preload, Internal Pressure

Component	Section	Angle	SI (ksi)	Allowable Stress (ksi)	Margin of Safety
1	1	70	1.8	30	15.46
2	9	135	3.1	30	8.58
3	11	135	4.3	28.7	5.7
4	14	180	1.3	29.6	22.42
5	21	0	5.5	29.6	4.36
6	22	10	8.9	29.6	2.32
7	23	80	1	28.7	27.23
8	30	20	3.2	28.7	8.08
9	31	0	5.8	28.7	3.95
10	34	0	13.8	30	1.17
11	40	0	8.7	30	2.43
12	41	135	1.2	30	23.27

Table 2.6.7.1-7 Critical $P_m + P_b + Q$ Stress Summary (ksi)—1-Foot Top End-Drop, Bolt Preload, Internal Pressure, Impact, Thermal Hot

Component	Section	Angle	SI (ksi)	Allowable Stress (ksi)	Margin of Safety
1	4	0	11.6	60	4.15
2	5	0	4.5	60	12.2
3	12	0	5.2	57.4	10.11
4	14	0	5.2	59.1	10.45
5	21	0	8.8	59.1	5.75
6	22	0	9	59.1	5.55
7	23	0	5.2	57.4	10.08
8	29	0	15.3	57.4	2.75
9	31	0	12.8	57.4	3.48
10	34	0	17.2	60	2.49
11	39	0	17.1	60	2.5
12	41	0	6.6	60	8.13

Table 2.6.7.1-8 Critical $P_m + P_b + Q$ Stress Summary (ksi)—1-Foot Top End-Drop, Bolt Preload, Internal Pressure, Impact, Thermal Cold

Component	Section	Angle	SI (ksi)	Allowable Stress (ksi)	Margin of Safety
1	4	0	13.9	60	3.33
2	8	30	5.4	60	10.05
3	10	30	5.4	57.4	9.56
4	14	10	5.4	59.1	9.95
5	21	0	8.7	59.1	5.77
6	22	0	8.8	59.1	5.73
7	23	0	5.3	57.4	9.9
8	29	0	16.7	57.4	2.43
9	31	0	13	57.4	3.41
10	34	0	16.3	60	2.68
11	39	0	16.6	60	2.61
12	41	10	4	60	13.86

Table 2.6.7.1-9 P_m Stresses—1-Foot Bottom End-Drop, Bolt Preload, Internal Pressure

Section	Angle	Cylindrical Stress Components (ksi)						SI	Allowable Stress	Margin of
		S_X	S_Y	S_Z	S_{XY}	S_{YZ}	S_{XZ}	(ksi)	(ksi)	Safety
1	180	-0.3	-1	0.1	0.1	0	0	1.1	20	16.48
2	180	-0.1	-0.7	0.1	-0.2	0	0	0.8	20	23.91
3	180	0	-5	-1.1	-0.1	0.4	0	5	20	3
4	180	-1.1	-3.5	0	-0.2	0.5	-0.2	3.7	20	4.42
5	180	0.5	-0.9	0.7	0.6	0.3	0	2	20	9.13
6	0	0.6	-0.6	0.7	0	0.1	0	1.4	20	13.68
7	0	0.5	-1.5	0.4	0.7	0	0	2.5	20	7.03
8	180	1.2	-2.5	-0.1	-1.7	0	0.2	5	20	3
9	180	2.1	-2.9	-0.2	0.6	0.3	0.3	5.3	20	2.8
10	180	4	-2.5	0.8	-4.4	-0.2	0.5	11	19.1	0.74
11	180	6.2	-2.6	1.2	-0.3	0.3	0.7	8.9	19.1	1.14
12	180	3.3	-0.8	1.6	2.2	0.6	0.3	6.1	19.1	2.13
13	180	6.7	1.6	3.3	-0.8	0.4	0.5	5.5	19.1	2.49
14	180	0.8	-3.4	0.2	1.8	0.6	0.1	5.7	19.7	2.44
15	180	3.7	-3.4	1.1	-0.9	0.3	0.3	7.4	19.7	1.67
16	0	-0.1	-1.8	4	-0.1	0	0.4	5.8	19.7	2.38
17	0	-0.1	-1.5	2.6	0	0	0.3	4.1	19.7	3.82
18	0	-0.1	-1.3	1.8	0	0	0.2	3.1	19.7	5.33
19	0	0	-1.1	1.4	0	0	0.2	2.5	19.7	6.78
20	0	0	-1	1.2	0	0	0.1	2.2	19.7	7.95
21	0	0	-0.8	1	0	0	0.1	1.8	19.7	9.98
22	0	0	-0.6	1	0	0	0.1	1.6	19.7	11.1
23	90	-3	-1.7	-0.3	-0.4	0	0.1	2.8	19.1	5.9
24	0	-0.3	-2.1	-2.1	0	0	-0.2	1.9	19.1	9.06
25	0	-0.3	-2	-0.7	0	0	-0.1	1.8	19.1	9.74
26	0	-0.2	-1.9	0.3	0	0	0	2.2	19.1	7.8
27	0	-0.2	-1.7	0.9	0	0	0	2.6	19.1	6.33
28	0	-0.2	-1.5	1.1	0	0	0.1	2.6	19.1	6.47
29	0	-0.1	-1.3	1.2	0	0	0.1	2.5	19.1	6.76
30	0	-0.1	-1	1.4	0	0	0.1	2.4	19.1	6.96
31	0	-0.1	-0.8	2.1	0	0	0.2	2.9	19.1	5.6
32	0	0	-0.5	1.4	0.1	0	0.1	2	20	9.18
33	0	-0.6	-0.1	1.5	0.1	0	0.2	2.1	20	8.55
34	0	0	-0.8	2.1	0	0	0.2	2.9	20	6
35	0	0.1	-0.2	1.4	0.3	-0.1	0.1	1.8	20	9.86
36	80	1.2	-0.4	-0.1	0.1	-0.8	0.2	2.4	20	7.46
37	30	-0.2	0	-0.2	0.1	-0.1	0	0.4	20	56.13
38	70	-0.2	0	-0.2	0.1	-0.2	0	0.4	20	43.87
39	0	-0.2	-1.1	-0.4	0.2	0.1	0	1	20	19.91
40	80	0.9	1.6	-0.1	-0.4	1.7	0.1	3.9	20	4.06
41	180	-0.4	-4.8	-0.1	-0.4	0.1	-0.1	4.8	20	3.17

Table 2.6.7.1-10 $P_m + P_b$ Stresses—1-Foot Bottom End-Drop, Bolt Preload, Internal Pressure

Section	Angle	Cylindrical Stress Components (ksi)						SI (ksi)	Allowable Stress (ksi)	Margin of Safety
		S_X	S_Y	S_Z	S_{XY}	S_{YZ}	S_{XZ}			
1	180	0.1	-1.1	1.3	0	-0.1	-0.1	2.4	30	11.44
2	180	1.2	-0.7	1.6	-0.2	0	0.1	2.3	30	11.94
3	180	-2.1	-6.5	-1	-0.1	0.5	-0.2	5.6	30	4.32
4	180	-2.3	-6.6	-1.3	-0.1	0.5	-0.2	5.5	30	4.42
5	0	0.8	-0.5	4	-0.5	0.1	0.3	4.7	30	5.37
6	120	3.6	-0.4	4.4	0	0	1	5.5	30	4.46
7	0	1.9	-2.6	0.2	0.4	0	-0.1	4.6	30	5.57
8	180	1.6	-2.4	0	-3.3	-0.1	0.3	7.7	30	2.9
9	180	5	-1.3	1.1	1.2	0.3	0.5	6.9	30	3.36
10	180	5.8	0.4	2.3	-5.6	-0.2	0.5	12.5	28.7	1.29
11	180	5.2	-5.1	0.4	-2.6	0.3	0.7	11.6	28.7	1.47
12	180	2.9	-0.7	1.4	3.3	0.6	0.3	7.6	28.7	2.79
13	180	11.7	4	5.5	-2.4	0.4	0.8	9.3	28.7	2.08
14	0	-0.3	-6.9	-1.1	-0.9	0.3	-0.1	6.9	29.6	3.31
15	180	-1.8	-9.5	-2.2	0.3	0.2	0.1	7.8	29.6	2.79
16	20	0.3	-1.9	3.7	0	0.1	1.4	6.2	29.6	3.79
17	20	0.2	-1.3	2.5	0	0	1	4.3	29.6	5.95
18	20	0.1	-1.2	1.8	0	0	0.7	3.3	29.6	8.05
19	20	0.1	-1	1.4	0	0	0.6	2.7	29.6	10.11
20	20	0.1	-0.9	1.2	0	0	0.5	2.3	29.6	11.74
21	20	0.1	-0.7	1	0	0	0.4	1.9	29.6	14.74
22	0	0	-1	0.8	0	0	0.1	1.8	29.6	15.13
23	180	-0.6	-5.6	-4	0	0.3	0.5	5.1	28.7	4.59
24	0	-0.3	-2.1	-2.7	0	0	-0.3	2.5	28.7	10.67
25	180	-0.4	-1.4	0.7	0	0	0	2.1	28.7	12.94
26	0	-0.2	-1.7	0.9	0	0	0	2.6	28.7	9.97
27	0	-0.2	-1.6	1.5	0	0	0.1	3	28.7	8.47
28	0	-0.2	-1.3	1.5	0	0	0.1	2.9	28.7	8.92
29	0	-0.2	-1.1	1.6	0	0	0.1	2.7	28.7	9.51
30	0	-0.2	-0.9	1.7	0	0	0.1	2.6	28.7	10.12
31	0	-0.1	-1.1	2.1	0	0	0.2	3.3	28.7	7.78
32	0	0	-0.8	1.4	0.1	0	0.1	2.3	30	12.23
33	10	-1.3	-1.6	0.9	0.3	-0.1	0.4	2.7	30	9.94
34	0	-0.1	-1.6	1.9	-0.1	0	0.2	3.5	30	7.49
35	0	0.4	-1.8	1.3	1.7	-0.2	0.1	4.2	30	6.17
36	80	1.1	0.1	-0.7	0.3	-1.2	0.3	2.8	30	9.83
37	0	-2.1	0	-1.6	0.1	0	0	2.1	30	13.41
38	20	-3.4	-0.1	-2.7	0.1	0	0.3	3.4	30	7.77
39	0	3.8	-1.4	2.6	0	0.1	-0.2	5.3	30	4.68
40	10	1.7	7.2	4.3	-1.6	0.3	0.5	6.5	30	3.63
41	180	0.6	-6.4	-0.2	-0.9	0	0	7.3	30	3.14

Table 2.6.7.1-11 $P_m + P_b + Q$ Stresses—1-Foot Bottom End-Drop, Bolt Preload, Internal Pressure, Impact, Thermal Hot

Section	Angle	Cylindrical Stress Components (ksi)						SI (ksi)	Allowable Stress (ksi)	Margin of Safety
		S_X	S_Y	S_Z	S_{XY}	S_{YZ}	S_{XZ}			
1	0	-2.5	-1.2	3	-0.5	-0.3	1	5.9	60	9.09
2	180	0.2	-0.9	1.8	-0.1	0	-0.2	2.8	60	20.54
3	180	1.1	-5	1.8	-1	0.5	-0.2	7.1	60	7.48
4	0	-9.4	-0.8	3.9	1.3	1.1	0.7	13.8	60	3.34
5	0	-0.3	-1	6.2	-0.3	-0.3	1.2	7.5	60	6.97
6	180	-2.4	-0.7	1.6	0	-0.1	-0.5	4.1	60	13.77
7	0	-6.2	-14.7	-3.4	-2.4	0.2	0.3	12	60	4
8	0	-6.2	-14.7	-3.4	-2.4	0.2	0.3	12	60	4
9	0	-0.7	-17.6	-2.8	-1.5	0.2	-0.2	17.2	60	2.49
10	180	5.3	2.3	4.8	-4.1	0.3	-0.1	8.8	57.4	5.51
11	180	0.9	-2.2	2	-2.1	0.4	-0.2	5.6	57.4	9.27
12	180	2.1	0.3	3.4	2.1	0.4	-0.1	4.8	57.4	10.94
13	180	9.3	3.4	6.7	-2.1	0.6	0.1	7.4	57.4	6.77
14	0	0	-6.6	0.8	-0.8	0.2	0.1	7.5	59.1	6.93
15	0	-0.1	-8.4	0.5	0.2	0	0.1	8.9	59.1	5.67
16	0	-0.1	-0.4	6.5	0	-0.1	0.6	6.9	59.1	7.51
17	0	-0.2	1.4	6.6	0	0	0.7	6.9	59.1	7.55
18	0	-0.2	1.7	6.2	0	0	0.6	6.5	59.1	8.1
19	0	-0.2	1.8	5.8	0	0	0.6	6.1	59.1	8.67
20	0	-0.2	2	5.7	0	0	0.6	6	59.1	8.92
21	0	-0.2	2.2	5.2	0	0	0.5	5.4	59.1	9.89
22	0	-0.1	0.6	3.2	-0.2	0.1	0.3	3.4	59.1	16.42
23	0	-0.7	-9.8	-3.3	-0.3	0	-0.3	9.2	57.4	5.27
24	0	-0.4	-8.2	-3.5	0	-0.4	-0.4	7.9	57.4	6.29
25	0	-0.4	-13.9	-4.5	0	-0.2	-0.5	13.6	57.4	3.23
26	0	-0.4	-15.5	-4	0	-0.1	-0.4	15.1	57.4	2.8
27	0	-0.2	-15.4	-3	0	0	-0.3	15.2	57.4	2.78
28	0	-0.2	-15.3	-3.2	0	0	-0.3	15.1	57.4	2.81
29	0	-0.5	-15.1	-3.9	0	0.1	-0.4	14.7	57.4	2.91
30	0	-0.5	-13.1	-3.7	0	0.3	-0.3	12.7	57.4	3.51
31	0	-0.9	-7.7	-0.4	-0.1	0.6	0	7.4	57.4	6.72
32	0	-0.1	-1.4	1.9	-0.4	0	0.3	3.4	60	16.48
33	0	0.1	-1	2.5	0	0.1	0.2	3.5	60	16.02
34	0	-1	-5.8	-0.6	-0.9	0.4	0.2	5.5	60	9.94
35	0	0	-9.8	-0.9	0.5	0	-0.1	9.9	60	5.08
36	0	0	-1.6	2.9	0.4	-0.1	0.3	4.7	60	11.88
37	150	-3.6	0	-4.9	0	0	-0.4	5	60	11
38	70	-3.8	-0.1	-5.1	0.1	-0.1	0.7	5.3	60	10.4
39	0	-1.1	-1.6	2.9	-1.2	0.3	0.1	5.5	60	9.97
40	60	0.6	5.4	-3.2	-0.8	1.6	3.3	11.2	60	4.37
41	180	-0.2	-1.7	2.2	1.1	0.6	-0.3	4.8	60	11.57

Table 2.6.7.1-12 $P_m + P_b + Q$ Stresses—1-Foot Bottom End-Drop, Bolt Preload, Internal Pressure, Impact, Thermal Cold

Section	Angle	Cylindrical Stress Components (ksi)						SI (ksi)	Allowable Stress (ksi)	Margin of Safety
		S_X	S_Y	S_Z	S_{XY}	S_{YZ}	S_{XZ}			
1	180	0.3	-1	1.4	0	-0.1	0	2.5	60	23.23
2	180	1.3	-0.7	1.7	-0.2	0	0.1	2.4	60	23.9
3	180	-2.6	-7.1	-1.4	0	0.5	-0.2	5.8	60	9.36
4	180	-2.6	-7.1	-1.4	0	0.5	-0.2	5.8	60	9.36
5	0	1.2	-0.5	3.9	-0.1	0.1	0.1	4.4	60	12.67
6	120	3.7	-0.3	4.6	0	0	1	5.6	60	9.74
7	0	0.5	-3.9	-0.6	0.2	0	-0.1	4.5	60	12.48
8	180	2.8	-5.2	-0.5	-3.1	0.2	0.5	10.2	60	4.91
9	180	6.2	-1.2	1.4	1.4	0.1	0.6	8	60	6.51
10	180	5.9	1.5	2.5	-5.1	0	0.4	11.2	57.4	4.12
11	180	2.8	-5.2	-0.5	-3.1	0.2	0.5	10.2	57.4	4.65
12	180	2.9	-0.2	1.6	2.9	0.5	0.3	6.7	57.4	7.51
13	180	11.8	4	5.6	-2.4	0.6	0.7	9.5	57.4	5.04
14	0	-0.1	-7.1	-1.2	-1	0.3	-0.1	7.4	59.1	7.04
15	180	0	-9.5	-1.6	-0.2	0.2	0.2	9.6	59.1	5.17
16	20	0.3	-2	3.6	0	0.1	1.4	6.1	59.1	8.64
17	20	0.2	-1.4	2.5	0	0	1	4.2	59.1	13.04
18	30	0.4	-1.2	1.5	0	0	0.9	3.2	59.1	17.33
19	20	0.1	-1	1.4	0	0	0.5	2.6	59.1	21.65
20	20	0.1	-0.9	1.2	0	0	0.5	2.2	59.1	25.36
21	150	0.2	-0.8	0.7	0	0	-0.5	1.8	59.1	31.79
22	0	0	-1.1	0.7	0	0	0.1	1.8	59.1	32.29
23	180	-0.6	-5.5	-4	0	0.3	0.5	5.1	57.4	10.3
24	0	-0.3	-2.1	-2.6	0	0	-0.3	2.4	57.4	23.26
25	180	-0.4	-1.3	0.8	0	0	0	2.1	57.4	26.16
26	0	-0.2	-1.7	1	0	0	0.1	2.7	57.4	20.52
27	0	-0.2	-1.5	1.5	0	0	0.1	3.1	57.4	17.63
28	0	-0.2	-1.3	1.6	0	0	0.1	3	57.4	18.39
29	0	-0.2	-1.1	1.7	0	0	0.1	2.8	57.4	19.31
30	0	-0.1	-0.9	1.8	0	0	0.2	2.7	57.4	20.19
31	0	-0.1	-1.1	2.3	0	0	0.2	3.5	57.4	15.57
32	0	0	-0.8	1.4	0.1	0	0.1	2.2	60	26.09
33	10	-1.7	-2.1	0.6	0.4	-0.1	0.4	3.1	60	18.18
34	0	-0.1	-1.4	2	0	0	0.2	3.4	60	16.56
35	0	0.1	-7.9	-0.6	0.5	-0.1	-0.1	8.1	60	6.45
36	80	1.2	-1.2	0.2	0	-0.5	0.2	2.6	60	22.3
37	50	-2	0	-1.9	0.1	-0.1	0.3	2.2	60	25.8
38	20	-3.6	-0.1	-2.8	0.1	0	0.3	3.6	60	15.48
39	0	-0.6	-1.2	1.2	-1	0.2	0	3.2	60	18.01
40	10	-3.5	4.3	1.4	-1.4	0.3	0.9	8.4	60	6.14
41	180	0.6	4.3	1.9	-0.9	0.1	-0.2	4.2	60	13.45

Table 2.6.7.1-13 Critical P_m Stress Summary (ksi)—1-Foot Bottom End-Drop, Bolt Preload, Internal Pressure

Component	Section	Angle	SI (ksi)	Allowable Stress (ksi)	Margin of Safety
1	3	180	5.0	20	3.0
2	9	180	5.3	20	2.8
3	10	180	11.0	19.1	0.74
4	15	180	7.4	19.7	1.67
5	16	0	5.8	19.7	2.38
6	22	0	1.6	19.7	11.1
7	23	90	2.8	19.1	5.9
8	28	0	2.6	19.1	6.47
9	31	0	2.9	19.1	5.6
10	34	0	2.9	20	6.0
11	40	80	3.9	20	4.06
12	41	180	4.8	20	3.17

Table 2.6.7.1-14 Critical $P_m + P_b$ Stress Summary (ksi)—1-Foot Bottom End-Drop, Bolt Preload, Internal Pressure

Component	Section	Angle	SI (ksi)	Allowable Stress (ksi)	Margin of Safety
1	3	180	5.6	30	4.32
2	8	180	7.7	30	2.9
3	10	180	12.5	28.7	1.29
4	15	180	7.8	29.6	2.79
5	16	20	6.2	29.6	3.79
6	22	0	1.8	29.6	15.13
7	23	180	5.1	28.7	4.59
8	27	0	3.0	28.7	8.47
9	31	0	3.3	28.7	7.78
10	35	0	4.2	30	6.17
11	40	10	6.5	30	3.63
12	41	180	7.3	30	3.14

Table 2.6.7.1-15 Critical $P_m + P_b + Q$ Stress Summary (ksi)—1-Foot Bottom End-Drop, Bolt Preload, Internal Pressure, Thermal Hot

Component	Section	Angle	SI (ksi)	Allowable Stress (ksi)	Margin of Safety
1	4	0	13.8	60	3.34
2	9	0	17.2	60	2.49
3	10	180	8.8	57.4	5.51
4	15	0	8.9	59.1	5.67
5	16	0	6.9	59.1	7.51
6	22	0	3.4	59.1	16.42
7	23	0	9.2	57.4	5.27
8	27	0	15.2	57.4	2.78
9	31	0	7.4	57.4	6.72
10	35	0	9.9	60	5.08
11	40	60	11.2	60	4.37
12	41	180	4.8	60	11.57

Table 2.6.7.1-16 Critical $P_m + P_b + Q$ Stress Summary (ksi)—1-Foot Bottom End-Drop, Bolt Preload, Internal Pressure, Thermal Cold

Component	Section	Angle	SI (ksi)	Allowable Stress (ksi)	Margin of Safety
1	4	180	5.8	60	9.36
2	8	180	10.2	60	4.91
3	10	180	11.2	57.4	4.12
4	15	180	9.6	59.1	5.17
5	16	20	6.1	59.1	8.64
6	22	0	1.8	59.1	32.29
7	23	180	5.1	57.4	10.3
8	27	0	3.1	57.4	17.63
9	31	0	3.5	57.4	15.57
10	35	0	8.1	60	6.45
11	40	10	8.4	60	6.14
12	41	180	4.2	60	13.45

2.6.7.2 One-Foot Side Drop

In the 1-ft side-drop event, the cask (equipped with an impact limiter over each end) falls a distance of 1 foot onto a flat, unyielding, horizontal surface. The cask strikes the surface in a horizontal position, thereby resulting in a side impact on the cask. The types of loading involved in a side-drop event are closure lid bolt preload, internal pressure load, thermal load, and inertial body load. The analysis is performed using a 20g acceleration load, which provides a bounding analysis, since it exceeds the calculated g-loads for the one-foot side drop event shown in Table 2.6.7.5-3.

The same conditions evaluated for the end-drop are also used in the side drop evaluation. Stress results for the combined 1-ft side-impact loading condition are documented in Tables 2.6.7.2-1 through 2.6.7.2-8.

As shown in Tables 2.6.7.2-5 and 2.6.7.2-6, the margins of safety for the primary stress intensity category are positive for the 1-ft side-drop condition. The most critically stressed component in the system is the cask body ligament region. The minimum margin of safety is found to be +0.04 for primary membrane stress intensity, as documented in Table 2.6.7.2-5. The minimum margin of safety is found to be 0.4 for primary membrane plus bending stress intensity, as documented in Table 2.6.7.2-6.

As seen from the tables, the minimum margin of safety for primary plus secondary stress intensity for the 1-ft side-drop is 1.18 (Table 2.6.7.2-8).

Because the margins of safety are all positive, the Universal Transport Cask satisfies the requirements of 10 CFR 71.71(c)(7) for the 1-ft side-drop (normal transport) condition.

Table 2.6.7.2-1 P_m Stresses—1-Foot Side-Drop, Bolt Preload, Internal Pressure

Section	Angle	Cylindrical Stress Components (ksi)						SI (ksi)	Allowable Stress (ksi)	MS
		S_X	S_Y	S_Z	S_{XY}	S_{YZ}	S_{XZ}			
1	180	-0.7	1.5	0.0	0.1	0.0	0.1	2.4	20.0	7.47
2	135	0.2	1.2	0.0	-1.1	0.0	0.2	2.6	20.0	6.79
3	105	0.5	1.1	1.1	-1.0	-1.0	0.3	3.0	20.0	5.72
4	10	-4.1	-6.2	-2.1	-0.1	-0.3	-1.3	4.8	20.0	3.14
5	10	-3.0	-2.4	-0.1	0.2	0.0	0.0	2.9	20.0	5.96
6	10	-3.5	-4.2	-0.1	0.0	0.0	0.1	4.1	20.0	3.87
7	0	-4.2	-6.1	2.5	0.1	-0.2	-0.3	8.5	20.0	1.35
8	10	-1.6	-7.8	-0.4	-0.2	-0.7	-0.8	8.0	20.0	1.50
9	10	-5.2	-9.2	-0.2	0.1	-0.9	1.5	9.7	20.0	1.07
10	0	-4.5	-11.6	-10.2	0.6	-0.4	0.4	7.3	19.1	1.62
11	0	-6.1	-14.0	-15.4	0.7	-0.3	2.2	10.3	19.1	0.85
12	0	-8.3	-7.7	8.8	-0.1	-0.5	0.6	17.5	19.1	0.09
13	0	-5.2	-5.9	13.0	0.0	-0.5	1.0	18.5	19.1	0.03
14	10	-7.4	-10.6	-2.8	0.1	-0.6	-2.5	9.0	19.7	1.18
15	0	-4.4	-10.2	-2.3	0.5	-0.3	2.0	9.1	19.7	1.16
16	50	0.0	1.5	1.3	-0.1	-3.7	-0.1	7.4	19.7	1.66
17	0	-0.1	2.0	6.2	-0.3	-0.3	0.1	6.4	19.7	2.09
18	0	-0.1	1.6	7.9	-0.3	-0.2	0.0	8.1	19.7	1.43
19	0	-0.1	1.6	8.6	-0.3	0.0	0.0	8.8	19.7	1.23
20	0	-0.1	1.7	8.5	-0.3	0.1	0.0	8.6	19.7	1.28
21	0	-0.1	2.2	7.4	-0.3	0.2	-0.1	7.5	19.7	1.63
22	60	0.0	2.1	0.7	0.0	3.2	0.2	6.6	19.7	2.00
23	40	-0.2	-2.1	1.2	0.0	-3.6	0.4	7.8	19.1	1.45
24	50	-0.1	3.1	1.5	0.0	-3.7	-0.1	7.5	19.1	1.55
25	0	-0.3	4.0	5.6	-0.4	-0.3	0.0	6.1	19.1	2.15
26	0	-0.3	4.1	7.6	-0.4	-0.2	0.0	7.9	19.1	1.42
27	0	-0.3	4.2	8.4	-0.4	0.0	0.0	8.7	19.1	1.19
28	0	-0.3	4.1	8.1	-0.4	0.1	0.0	8.5	19.1	1.24
29	0	-0.3	4.0	6.9	-0.4	0.2	0.0	7.2	19.1	1.66
30	60	0.0	2.8	0.9	0.0	3.1	0.0	6.4	19.1	2.00
31	50	-0.1	2.8	1.6	0.0	4.3	0.2	8.7	19.1	1.19
32	70	0.1	2.3	-0.1	0.1	3.4	0.4	7.2	20.0	1.78
33	80	-1.0	0.9	-0.1	-0.7	2.2	0.1	4.7	20.0	3.23
34	60	0.8	2.3	1.4	0.2	3.5	0.2	7.1	20.0	1.82
35	0	-1.1	-4.8	0.4	0.3	0.0	-0.9	5.6	20.0	2.54
36	180	1.4	6.8	-0.8	0.8	0.2	1.1	8.1	20.0	1.47
37	0	-3.2	-0.4	-0.1	0.0	0.0	-0.2	3.1	20.0	5.49
38	0	-3.4	-1.7	-0.1	0.0	0.0	-0.4	3.4	20.0	4.90
39	0	-3.5	-2.8	1.0	0.0	-0.1	-0.2	4.6	20.0	3.33
40	10	-3.7	-5.5	-3.2	0.1	-0.2	-0.5	2.7	20.0	6.49
41	0	-5.0	-2.8	-1.3	-0.2	0.0	0.6	3.9	20.0	4.12

Table 2.6.7.2-2 $P_m + P_b$ Stresses—1-Foot Side-Drop, Bolt Preload, Internal Pressure

		Cylindrical Stress Components (ksi)							Allowable Stress	
Section	Angle	S_X	S_Y	S_Z	S_{XY}	S_{YZ}	S_{XZ}	SI (ksi)	(ksi)	MS
1	180	1.8	5.3	0.1	0.1	0.0	0.1	5.2	30.0	4.73
2	180	1.0	4.9	0.1	0.2	-0.1	0.1	4.8	30.0	5.22
3	90	2.7	1.3	2.5	-1.5	-1.8	1.0	5.4	30.0	4.51
4	90	2.9	1.3	2.1	-1.6	-2.0	1.3	5.8	30.0	4.22
5	60	-4.3	-5.0	-0.1	-0.4	0.0	0.0	5.0	30.0	4.96
6	0	-4.3	-6.6	-0.2	0.1	0.0	0.1	6.4	30.0	3.71
7	0	-2.5	-6.1	6.3	0.1	-0.3	-0.4	12.3	30.0	1.43
8	0	1.0	-3.5	12.0	0.2	-0.5	-1.4	15.7	30.0	0.91
9	0	1.6	-1.1	20.8	0.3	-0.6	0.0	22.6	30.0	0.33
10	0	-2.7	-10.3	-8.4	0.6	-0.3	-0.8	7.9	30.0	2.80
11	0	1.3	-10.4	-11.5	0.9	-0.4	1.2	13.4	30.0	1.24
12	10	-11.3	-8.4	7.8	0.1	-0.5	0.1	19.5	30.0	0.54
13	0	-12.3	-8.8	9.9	-0.3	-0.6	0.8	22.6	30.0	0.33
14	10	-9.1	-7.4	9.7	0.1	-0.6	-0.9	18.5	29.6	0.60
15	0	2.5	-2.2	18.3	0.3	-0.4	1.2	20.5	29.6	0.44
16	50	0.0	3.3	1.4	-0.1	-4.8	-0.1	9.8	19.7	1.02
17	0	-0.1	8.6	8.9	-0.8	-0.1	0.1	9.1	19.7	1.16
18	0	-0.1	9.9	11.2	-1.0	-0.1	0.0	11.3	19.7	0.74
19	0	-0.1	10.2	12.1	-1.0	0.0	0.0	12.3	19.7	0.60
20	0	-0.1	9.9	11.9	-1.0	0.0	0.0	12.3	19.7	0.60
21	0	0.0	8.4	10.1	-0.8	0.0	-0.1	10.2	19.7	0.94
22	40	-0.1	2.7	1.3	-0.1	4.8	0.1	9.7	29.6	2.07
23	40	-0.2	-1.5	1.7	0.0	-5.5	0.4	11.3	28.7	1.54
24	40	-0.2	4.7	1.6	-0.1	-4.8	-0.1	10.2	19.1	0.88
25	0	-0.2	10.5	8.2	-0.9	-0.1	0.0	11.3	19.1	0.69
26	0	-0.2	12.2	10.8	-1.1	-0.1	0.0	12.3	19.1	0.55
27	0	-0.2	13.0	11.9	-1.2	0.0	0.0	13.4	19.1	0.43
28	0	-0.2	12.8	11.5	-1.2	0.1	0.0	13.4	19.1	0.43
29	0	-0.2	11.7	9.9	-1.0	0.1	0.0	12.3	19.1	0.55
30	0	-0.2	9.7	6.2	-0.9	0.2	-0.1	10.1	19.1	0.90
31	40	-0.2	2.9	0.2	-0.1	6.5	0.1	13.4	28.7	1.15
32	50	0.0	2.0	-1.7	0.0	4.7	0.1	10.2	30.0	1.95
33	60	-2.1	-0.3	-2.4	-2.1	3.6	0.2	8.5	30.0	2.52
34	50	-0.1	0.5	-2.4	0.1	4.7	-0.4	10.0	30.0	2.01
35	50	-0.4	-2.2	-0.1	0.1	3.8	1.1	8.2	30.0	2.65
36	180	-0.2	5.8	-2.5	0.8	0.2	0.7	8.6	30.0	2.48
37	90	-7.0	-8.5	-0.2	-0.3	0.0	-0.1	8.4	30.0	2.56
38	180	-6.3	-7.1	-0.2	-0.1	0.0	-0.3	7.0	30.0	3.30
39	0	-2.4	-6.3	2.5	0.2	0.0	-1.3	9.1	30.0	2.28
40	0	1.7	-6.6	-3.7	0.4	0.0	1.4	8.6	30.0	2.48
41	0	-6.6	-2.9	0.7	-0.2	-0.1	0.4	7.4	30.0	3.06

Table 2.6.7.2-3 $P_m + P_b + Q$ Stresses—1-Foot Side-Drop, Bolt Preload, Internal Pressure, Thermal Hot

Section	Angle	Cylindrical Stress Components (ksi)						SI (ksi)	Allowable Stress (ksi)	MS
		S_X	S_Y	S_Z	S_{XY}	S_{YZ}	S_{XZ}			
1	90	8.2	4.3	0.1	0.1	0.0	0.1	8.1	60.0	6.40
2	180	3.2	8.3	0.0	0.3	-0.1	0.2	8.3	60.0	6.21
3	80	10.7	5.2	10.7	-0.6	-0.9	4.1	9.9	60.0	5.09
4	0	5.9	-5.6	-6.8	0.6	0.7	-1.2	13.2	60.0	3.53
5	20	-4.2	-8.9	0.2	-2.0	-0.1	0.1	9.8	60.0	5.15
6	20	-3.1	-7.6	-0.1	-2.1	0.0	0.1	8.3	60.0	6.21
7	20	1.4	-3.3	8.5	-2.7	-3.0	0.4	14.4	60.0	3.17
8	20	1.4	-3.3	8.5	-2.7	-3.0	0.4	14.4	60.0	3.17
9	10	-0.2	-3.1	15.6	-0.2	-1.5	0.5	18.9	60.0	2.18
10	0	1.0	-8.4	-9.9	0.1	-0.6	-0.6	11.2	60.0	4.36
11	0	-0.4	-10.0	-11.0	0.0	-0.4	1.5	11.2	60.0	4.36
12	0	-9.1	-5.3	13.8	-0.7	-0.2	-0.3	23.0	60.0	1.61
13	0	8.3	1.5	22.0	-0.1	-0.6	2.9	21.0	60.0	1.86
14	0	-9.1	-5.3	13.8	-0.7	-0.2	-0.3	23.0	59.1	1.57
15	0	8.3	1.5	22.0	-0.1	-0.6	2.9	21.0	59.1	1.82
16	0	-0.1	11.2	10.3	-1.1	-0.1	0.0	11.5	59.1	4.14
17	0	-0.2	14.0	14.0	-1.3	0.0	0.1	14.4	59.1	3.11
18	0	-0.2	15.2	15.8	-1.5	0.0	0.0	16.1	59.1	2.67
19	0	-0.2	15.5	16.3	-1.5	0.0	0.0	16.6	59.1	2.55
20	0	-0.2	15.3	15.9	-1.5	0.0	0.0	16.3	59.1	2.62
21	0	-0.2	13.9	13.9	-1.3	0.0	-0.1	14.3	59.1	3.14
22	0	-0.1	10.2	11.3	-1.0	0.0	-0.2	11.5	59.1	4.14
23	40	-0.2	-2.0	1.5	-0.1	-4.7	0.2	10.1	57.4	4.70
24	0	-1.1	7.8	0.3	-0.7	0.3	0.1	9.0	57.4	5.35
25	0	-2.3	11.0	1.3	-1.2	0.1	0.0	13.5	57.4	3.27
26	0	-2.5	13.2	2.1	-1.4	0.0	0.0	16.0	57.4	2.58
27	0	-2.6	14.2	2.3	-1.5	0.0	0.0	17.0	57.4	2.37
28	0	-2.6	13.7	1.6	-1.4	0.0	0.0	16.4	57.4	2.49
29	0	-2.5	12.0	0.4	-1.3	0.0	0.0	14.8	57.4	2.88
30	0	-2.2	9.2	-2.1	-1.0	0.0	0.0	11.7	57.4	3.90
31	40	-0.3	0.1	0.0	-0.1	5.9	0.0	11.8	57.4	3.86
32	50	-0.2	3.4	1.3	0.0	5.4	-0.1	11.1	60.0	4.41
33	40	2.7	1.8	5.8	-4.1	4.5	-1.0	13.0	60.0	3.60
34	60	0.1	1.1	-5.3	0.0	4.0	0.0	10.4	60.0	4.78
35	0	-0.1	-10.2	-6.4	0.8	0.6	0.1	10.3	60.0	4.84
36	180	5.0	9.0	0.0	0.7	0.0	1.7	9.8	60.0	5.15
37	150	-11.0	-11.3	-0.1	0.6	0.0	-0.1	11.5	60.0	4.22
38	180	-9.1	-10.0	-0.2	0.0	0.0	-0.1	9.8	60.0	5.15
39	0	0.6	-8.9	1.5	0.9	0.3	0.2	10.7	60.0	4.62
40	180	-1.1	4.7	-6.3	0.7	0.1	-0.3	11.1	60.0	4.41
41	10	-2.4	-2.0	15.2	0.0	0.1	-0.9	17.7	60.0	2.40

Table 2.6.7.2-4 $P_m + P_b$ + Q Stresses—1-Foot Side-Drop, Bolt Preload, Internal Pressure, Thermal Cold

		Cylindrical Stress Components (ksi)							Allowable Stress	
Section	**Angle**	**S_X**	**S_Y**	**S_Z**	**S_{XY}**	**S_{YZ}**	**S_{XZ}**	**SI (ksi)**	**(ksi)**	**MS**
1	180	1.0	5.9	-0.1	0.3	0.0	0.2	6.1	60.0	8.90
2	180	0.4	5.9	0.0	0.3	-0.1	0.2	6.0	60.0	9.07
3	90	4.8	2.7	3.6	-1.5	-2.0	2.0	6.4	60.0	8.42
4	0	9.6	-6.4	-3.5	0.7	1.0	-2.1	16.7	60.0	2.58
5	20	-5.5	-7.8	0.0	-1.0	0.0	0.0	8.2	60.0	6.30
6	0	-4.9	-8.7	-0.1	0.0	0.0	0.0	8.6	60.0	5.96
7	0	0.9	-3.6	12.1	0.0	-0.4	0.1	15.8	60.0	2.79
8	0	0.9	-3.6	12.1	0.0	-0.4	0.1	15.8	60.0	2.79
9	0	-0.4	-2.0	21.9	0.1	-0.4	0.4	23.9	60.0	1.51
10	0	3.0	-8.0	-8.4	0.5	-0.5	-0.1	11.8	60.0	4.08
11	0	-2.4	-11.8	-12.5	0.3	-0.5	2.5	11.5	60.0	4.22
12	0	-15.0	-8.4	12.0	-0.8	-0.3	0.0	27.1	60.0	1.21
13	0	10.7	1.8	24.6	0.2	-0.5	3.1	23.4	60.0	1.56
14	0	-15.0	-8.4	12.0	-0.8	-0.3	0.0	27.1	59.1	1.18
15	0	10.7	1.8	24.6	0.2	-0.5	3.1	23.4	59.1	1.52
16	0	-0.1	10.5	9.6	-1.0	-0.1	0.1	10.7	59.1	4.53
17	0	-0.2	13.5	13.4	-1.3	0.0	0.1	14.0	59.1	3.23
18	0	-0.2	15.0	15.3	-1.5	0.0	0.0	15.7	59.1	2.76
19	0	-0.2	15.3	15.8	-1.5	0.0	0.0	16.2	59.1	2.64
20	0	-0.2	15.0	15.5	-1.4	0.0	0.0	15.9	59.1	2.71
21	0	-0.2	13.4	13.6	-1.3	0.0	-0.1	13.9	59.1	3.26
22	50	-0.2	4.1	2.5	-0.1	5.4	0.1	11.1	59.1	4.33
23	30	-0.2	-3.8	1.8	-0.1	-4.2	0.5	10.3	57.4	4.59
24	0	-1.2	8.7	0.2	-0.8	0.3	0.1	10.2	57.4	4.65
25	0	-2.5	11.9	0.7	-1.3	0.2	0.0	14.7	57.4	2.91
26	0	-2.8	14.2	1.3	-1.5	0.1	0.0	17.3	57.4	2.33
27	0	-2.9	15.1	1.4	-1.6	0.0	0.0	18.3	57.4	2.14
28	0	-2.9	14.6	0.9	-1.6	0.0	0.0	17.8	57.4	2.23
29	0	-2.8	13.0	-0.3	-1.4	0.0	0.0	16.1	57.4	2.56
30	0	-2.4	10.4	-2.7	-1.1	0.0	0.0	13.2	57.4	3.33
31	40	-0.3	0.4	-0.5	-0.1	6.0	0.0	11.9	57.4	3.82
32	50	-0.1	2.8	0.9	0.0	5.4	0.0	11.0	60.0	4.46
33	40	1.6	1.0	4.6	-3.8	4.2	-0.8	12.0	60.0	3.99
34	0	-5.0	-10.0	-13.5	0.0	-0.5	-2.8	10.2	60.0	4.90
35	60	-0.1	-2.3	-5.3	0.0	4.5	0.6	9.7	60.0	5.22
36	180	5.1	9.4	0.2	0.8	0.0	2.0	10.0	60.0	5.02
37	180	-11.4	-11.2	-0.2	0.1	0.0	-0.1	11.2	60.0	4.36
38	180	-9.1	-10.0	-0.2	0.0	0.0	-0.1	9.8	60.0	5.15
39	0	0.5	-7.1	1.5	0.8	0.2	0.2	8.7	60.0	5.87
40	180	-0.7	5.2	-5.9	0.7	0.0	-0.2	11.2	60.0	4.36
41	0	-4.0	-4.0	11.6	-0.2	0.0	-1.2	15.9	60.0	2.77

Table 2.6.7.2-5 Critical P_m Stress Summary (ksi)—1-Foot Side Drop, Bolt Preload, Internal Pressure

Component	Section	Angle	SI (ksi)	Allowable Stress (ksi)	Margin of Safety
1	4	10	4.8	20	3.14
2	9	10	9.7	20	1.07
3	13	0	18.5	19.1	0.08
4	15	0	9.1	19.7	1.16
5	19	0	8.8	19.7	1.23
6	22	60	6.6	19.7	2.00
7	23	40	7.8	19.1	1.45
8	27	0	8.7	19.1	1.19
9	31	50	8.7	19.1	1.19
10	36	180	8.1	20	1.47
11	39	0	4.6	20	3.33
12	41	0	3.9	20	4.12

Table 2.6.7.2-6 Critical $P_m + P_b$ Stress Summary (ksi)—1-Foot Side-Drop, Bolt Preload, Internal Pressure

Component	Section	Angle	SI (ksi)	Allowable Stress (ksi)	Margin of Safety
1	4	90	5.8	30	4.22
2	9	0	22.6	30	0.33
3	13	0	22.6	28.7	0.33
4	15	0	20.5	29.6	0.44
5	19	0	12.3	29.6	1.40
6	22	40	9.7	29.6	2.07
7	23	40	11.3	28.7	1.54
8	27	0	13.4	28.7	1.15
9	31	40	13.4	28.7	1.15
10	32	50	10.2	30	1.95
11	39	0	9.1	30	2.28
12	41	0	7.4	30	3.06

Table 2.6.7.2-7 Critical $P_m + P_b + Q$ Stress Summary (ksi)—1-Foot Side-Drop, Bolt Preload, Internal Pressure, Thermal Hot

Component	Section	Angle	SI (ksi)	Allowable Stress (ksi)	Margin of Safety
1	4	0	12.9	60	3.66
2	7	20	14	60	3.3
3	12	0	22.4	57.4	1.56
4	14	0	22.4	59.1	1.64
5	19	0	16.2	59.1	2.64
6	22	0	11.2	59.1	4.29
7	23	40	9.8	57.4	4.88
8	27	0	16.6	57.4	2.46
9	31	40	11.5	57.4	4.01
10	33	40	12.7	60	3.74
11	40	180	10.8	60	4.54
12	41	10	17.2	60	2.49

Table 2.6.7.2-8 Critical $P_m + P_b + Q$ Stress Summary (ksi)—1-Foot Side-Drop Bolt Preload, Internal Pressure, Thermal Cold

Component	Section	Angle	SI (ksi)	Allowable Stress (ksi)	Margin of Safety
1	4	0	16.3	60	2.68
2	7	0	15.4	60	2.9
3	12	0	26.4	57.4	1.18
4	14	0	26.4	59.1	1.24
5	19	0	15.8	59.1	2.74
6	22	50	10.8	59.1	4.48
7	23	30	10	57.4	4.74
8	27	0	17.8	57.4	2.22
9	31	40	11.6	57.4	3.94
10	33	40	11.7	60	4.14
11	37	180	10.9	60	4.5
12	41	0	15.5	60	2.87

2.6.7.3 One-Foot Corner Drop

In this event, the Universal Transport Cask (equipped with an impact limiter over each end) falls a distance of 1 foot onto a flat, unyielding, horizontal surface. The cask strikes the surface on its top or bottom corner. The cask center of gravity is considered to be directly above the initial point of impact for the corner-drop condition. For the cask, the orientation angle is 23° and 23.5° for the top and bottom corner-drops, respectively.

Results for the top corner and bottom corner 1-ft drop evaluations are presented in Tables 2.6.7.3-1 through 2.6.7.3-16. For the top-corner-drop loading case including impact, bolt preload, and internal pressures the minimum margin of safety resulting from calculated P_m stress intensity is 1.54 (Table 2.6.7.3-5) and the minimum calculated $P_m + P_b$ stress intensity margin of safety is 1.11 (Table 2.6.7.3-6). As seen from the tables, the minimum margin of safety for primary plus secondary stress intensity for the 1-ft top corner-drop is 2.32 (Table 2.6.7.3-8).

For the bottom-corner-drop loading case including impact, bolt preload, and internal pressures the minimum margin of safety resulting from calculated P_m stress intensity is 0.84 (Table 2.6.7.3-13) and the minimum margin of safety resulting from calculated $P_m + P_b$ stress intensity is 1.34 (Table 2.6.7.3-14). As seen from the tables, the minimum margin of safety for primary plus secondary stress intensity for the 1-ft bottom corner-drop is 2.14 (Table 2.6.7.3-16).

Because the margins of safety are all positive, the Universal Transport Cask satisfies the requirements of 10 CFR 71.71(c)(7) for the 1-ft corner-drop (normal transport) condition.

Table 2.6.7.3-1 P_m Stresses—1-Foot Top Corner-Drop, Bolt Preload, Internal Pressure

		Cylindrical Stress Components (ksi)							Allowable Stress	
Section	Angle	S_X	S_Y	S_Z	S_{XY}	S_{YZ}	S_{XZ}	SI (ksi)	(ksi)	MS
1	180	-0.1	0.6	-0.1	0	0	0.1	0.9	20	21.74
2	180	0	0.8	0	0	0	0.1	0.9	20	20.22
3	180	0.2	1	0.1	0.1	0	0.1	1	20	18.38
4	0	-1.2	-1.9	0	0.1	0	-0.2	2	20	9.24
5	10	-1.1	-0.9	-0.1	0.1	0	0	1	20	18.67
6	0	-1.3	-1.7	-0.1	0	0	0.1	1.6	20	11.48
7	0	-1.6	-2.1	2.2	0	-0.1	-0.2	4.3	20	3.66
8	0	0.2	-3.1	0	0.3	-0.2	-0.3	3.6	20	4.54
9	40	-2.6	-2.5	0.7	0.4	-1.7	1.5	5.8	20	2.44
10	0	-2.2	-5.6	-6.7	0.3	-0.2	-0.1	4.6	19.1	3.14
11	0	-4.8	-7.8	-10.9	0.3	-0.1	1.7	7.1	19.1	1.7
12	0	-3.8	-3.3	3.1	0	-0.1	0.4	6.9	19.1	1.75
13	0	-4.1	-3.5	3.3	0	-0.1	-0.4	7.5	19.1	1.54
14	0	-2.7	-3.8	0.1	0.1	-0.1	-0.6	4	19.7	3.91
15	0	-2.6	-4.1	0.1	0.2	0	0.1	4.2	19.7	3.67
16	60	0	0	-0.1	0	-1.3	0	2.6	19.7	6.53
17	70	0	0.4	-0.7	0	-1	0	2.3	19.7	7.66
18	90	0	0.5	-1.6	0	-0.5	0	2.3	19.7	7.48
19	105	0	0.7	-1.9	0	-0.2	0	2.6	19.7	6.44
20	105	0	1.2	-1.9	0	0.1	0	3.1	19.7	5.26
21	80	0	2.2	-1.3	0	0.8	0	3.9	19.7	4.1
22	60	-0.1	3.8	-0.9	0	1.6	0.1	5.6	19.7	2.5
23	50	0	1.1	0.1	0	-2.5	0.2	5	19.1	2.8
24	0	-0.1	4.8	0.9	-0.5	-0.3	0	5	19.1	2.82
25	80	0	2.4	-0.9	0	-0.7	0	3.5	19.1	4.4
26	90	-0.1	2	-1.4	0	-0.1	0	3.4	19.1	4.58
27	90	-0.1	1.8	-1.6	0	0.2	0	3.4	19.1	4.65
28	90	-0.1	1.4	-1.5	0	0.5	0	3.1	19.1	5.21
29	70	-0.1	0.8	-1.1	0	1	0	2.7	19.1	6.03
30	50	-0.2	-0.1	-0.9	0	1.3	0	2.7	19.1	6.02
31	40	-0.3	-0.6	-1.2	0	1.7	0.1	3.6	19.1	4.38
32	70	-0.1	3.2	-1.1	0.1	1.6	0	5.3	20	2.74
33	180	0.4	2.1	-1.8	0.2	0	-0.3	4	20	4.05
34	0	1.2	0.5	-3.6	0.1	0.3	0.5	5	20	2.99
35	180	-0.4	2.3	-1.6	0.4	-0.2	0.3	4	20	3.98
36	180	1.2	3.2	-2.3	0.3	-0.2	0.7	5.7	20	2.54
37	0	-1.5	-0.3	-0.9	0	0.2	0.5	1.6	20	11.85
38	10	-1.5	-0.8	-0.5	0.1	0.1	0.4	1.3	20	14.92
39	80	-0.1	-0.7	-1.9	0	0	-0.1	1.8	20	10.25
40	80	-1.7	-1.7	-4	0	0	-1.4	3.7	20	4.47
41	0	-1.7	-1.2	-0.3	0	0	0.3	1.5	20	12.18

Table 2.6.7.3-2 $P_m + P_b$ Stresses—1-Foot Top Corner-Drop, Bolt Preload, Internal Pressure

		Cylindrical Stress Components (ksi)							Allowable Stress	
Section	Angle	S_X	S_Y	S_Z	S_{XY}	S_{YZ}	S_{XZ}	SI (ksi)	(ksi)	MS
1	180	1	2.6	0	0.1	0	0.1	2.6	30	10.39
2	180	0.1	1.9	0	0.1	0	0.1	2	30	14.23
3	90	1.1	0.5	0.6	-0.5	-0.6	0.4	1.8	30	15.22
4	90	1.1	0.5	0.4	-0.5	-0.6	0.5	2	30	13.82
5	20	-2.6	-2.5	-0.1	0	0	0	2.4	30	11.35
6	0	-2.1	-3.2	-0.1	0.1	0	0.1	3.1	30	8.69
7	0	0.2	-1.5	5.5	0	-0.1	0	7	30	3.31
8	0	3.1	0.6	9.6	0.1	-0.2	-0.3	9.1	30	2.31
9	0	1.5	1.8	15.6	0	-0.3	0.5	14.2	30	1.11
10	0	-0.7	-4.7	-5.5	0.4	-0.1	-1	5.3	28.7	4.46
11	0	0.7	-5.2	-7.9	0.5	-0.2	0.6	8.7	28.7	2.29
12	0	-4.5	-3.5	2.9	-0.1	-0.1	0.4	7.5	28.7	2.82
13	0	-6	-4	3.1	-0.1	-0.2	0.1	9.1	28.7	2.15
14	0	-3.5	-3.2	2.9	0	-0.1	0	6.4	29.6	3.61
15	0	-1.6	-2.4	4.8	0.1	-0.1	-0.7	7.3	29.6	3.04
16	50	0	0.7	0.1	0	-1.8	0	3.6	29.6	7.11
17	0	0	3.4	2.8	-0.3	-0.1	0	3.5	29.6	7.47
18	0	0	4.3	3.5	-0.4	0	0	4.4	29.6	5.67
19	0	0	4.8	3.5	-0.5	0	0	4.9	29.6	5.04
20	0	0	5.1	3.1	-0.5	0	0	5.3	29.6	4.63
21	0	0	5.3	1.8	-0.5	0	0	5.4	29.6	4.45
22	40	-0.2	3.8	-2.3	0	2.1	0.1	7.4	29.6	3.01
23	50	0	0.6	-1.4	-0.1	-3.4	0.2	7.2	28.7	3.01
24	0	0	6.6	2.3	-0.6	-0.2	0	6.7	28.7	3.30
25	0	-0.1	5.7	3	-0.5	0	0	5.9	28.7	3.85
26	0	-0.1	5.6	3.4	-0.5	0	0	5.8	28.7	3.91
27	0	-0.1	5.5	3.3	-0.5	0	0	5.7	28.7	4.03
28	0	-0.2	4.8	2.7	-0.4	0	0	5	28.7	4.74
29	60	-0.1	2.9	-0.2	0	1.1	0	3.9	28.7	6.45
30	50	-0.2	1.1	-0.5	0	1.6	0	3.7	28.7	6.86
31	40	-0.2	0.2	0.5	0	2.5	0.1	5.1	28.7	4.66
32	50	-0.3	2.9	-2.8	0	2	-0.1	7	30	3.29
33	70	0.3	2.1	-0.9	-0.9	1.6	-0.3	4.7	30	5.4
34	60	-0.1	-0.1	-8.4	0	1.7	-0.4	9	30	2.33
35	180	-0.6	2.3	-1.8	0.4	-0.3	1.1	4.9	30	5.17
36	180	-0.3	2.6	-2.9	0.4	-0.3	0.5	5.7	30	4.24
37	70	-0.5	-3	-0.8	0.4	0.1	0.6	3.1	30	8.75
38	80	3.7	0.3	-0.4	0.1	0	0.4	4.2	30	6.19
39	80	4.6	1.3	-1.6	-0.1	0	-0.3	6.3	30	3.78
40	0	-3.6	-5.6	-11.6	0.1	0	0.2	8	30	2.74
41	0	-2.5	-1.3	0.4	-0.1	0	0.3	2.9	30	9.31

Table 2.6.7.3-3 $P_m + P_b + Q$ Stresses—1-Foot Top Corner-Drop, Bolt Preload, Internal Pressure, Thermal Hot

Section	Angle	Cylindrical Stress Components (ksi)						SI (ksi)	Allowable Stress (ksi)	MS
		S_X	S_Y	S_Z	S_{XY}	S_{YZ}	S_{XZ}			
1	90	5	3.7	0	0.3	0	0.1	5	60	10.93
2	180	2.4	4.7	0	0.2	-0.1	0.1	4.7	60	11.65
3	10	-3.2	2.8	-0.1	0.3	0	0.1	6	60	8.95
4	0	7	-1.5	-4.5	0.4	0.7	-0.6	11.7	60	4.15
5	20	-1.7	-4.6	0.1	-1.3	-0.1	0	5.2	60	10.56
6	40	-2.4	-2.2	-0.2	-1.7	0	0	3.8	60	14.94
7	40	-2.1	-0.8	0.8	-1.7	-1.6	-0.6	5.5	60	9.96
8	0	1.2	-2.1	-5.4	-0.2	-0.2	1.3	7.2	60	7.35
9	30	-4.6	-4.4	-7.1	-2.1	1.8	1.1	6.6	60	8.11
10	0	3.6	-0.8	-4.5	0	-0.3	0.5	8.2	57.4	5.95
11	0	1.2	-2.1	-5.4	-0.2	-0.2	1.3	7.2	57.4	6.98
12	0	-3.9	-0.8	3.9	-0.5	0	0.2	7.9	57.4	6.27
13	40	-0.3	0.6	4.8	-1.7	-1.7	0.1	7.3	57.4	6.85
14	0	-3.9	-0.8	3.9	-0.5	0	0.2	7.9	59.1	6.5
15	40	-0.3	0.6	4.8	-1.7	-1.7	0.1	7.3	59.1	7.09
16	0	-0.1	5.7	4.1	-0.6	0.1	0.1	5.9	59.1	9.01
17	0	-0.2	8.1	5.7	-0.8	0.1	0	8.4	59.1	6.07
18	0	-0.2	8.9	5.6	-0.9	0.1	0	9.3	59.1	5.38
19	0	-0.2	9.3	4.9	-0.9	0.1	0	9.7	59.1	5.12
20	0	-0.2	9.7	3.9	-1	0.1	0	10.1	59.1	4.85
21	0	-0.2	9.8	2	-1	0.1	0	10.2	59.1	4.79
22	40	-0.4	4.8	-3.2	0	3	0	9.9	59.1	4.94
23	0	-0.3	-0.3	-4.6	0	0.2	0.2	4.3	57.4	12.23
24	0	-0.9	4.3	-4	-0.4	0.5	0	8.4	57.4	5.85
25	0	-0.4	-4.8	-11.6	0.4	0.2	0	11.2	57.4	4.11
26	0	-0.4	-5.7	-13.5	0.5	0.1	0	13.1	57.4	3.38
27	0	-2.5	6.1	-7.9	-0.8	0.1	0	14.1	57.4	3.08
28	0	-0.4	-5.9	-15	0.6	0.2	0	14.7	57.4	2.9
29	0	-0.6	-6.8	-16.2	0.6	0.2	0	15.6	57.4	2.67
30	0	-0.7	-7.1	-16	0.7	0.1	0	15.4	57.4	2.73
31	0	-1.4	-4.2	-15.4	0.3	-0.3	-0.1	14.1	57.4	3.07
32	0	-0.2	4.9	-4.6	-0.8	0.3	-0.9	9.9	60	5.08
33	0	0.3	2.7	-6.6	-0.4	0.1	-0.7	9.4	60	5.37
34	0	0	-4.8	-15.5	0.4	-0.1	0.4	15.6	60	2.84
35	0	-0.2	-5.6	-13.9	0.5	0.5	0.4	13.8	60	3.34
36	0	4.6	-1.5	-5.3	0.6	0.3	-0.7	10	60	4.98
37	180	-5.6	-1.9	-0.6	0.4	-0.1	0.4	5.1	60	10.79
38	180	-8.8	-5.1	-0.7	0.4	-0.1	0.2	8.2	60	6.31
39	80	1.2	-3.8	-10.4	0.6	0.7	0.6	11.9	60	4.05
40	0	-2.4	-9.5	-15.1	0.8	0.3	-0.7	13	60	3.63
41	10	-0.3	1.1	5.7	0	0.1	0.2	6	60	8.95

Table 2.6.7.3-4 $P_m + P_b$ + Q Stresses—1-Foot Top Corner-Drop, Bolt Preload, Internal Pressure, Thermal Cold

Section	Angle	Cylindrical Stress Components (ksi)						SI (ksi)	Allowable Stress (ksi)	MS
		S_X	S_Y	S_Z	S_{XY}	S_{YZ}	S_{XZ}			
1	0	1.2	3.5	0	-0.2	0	0.1	3.6	60	15.87
2	0	0.9	3.1	0	-0.1	0	0.1	3.1	60	18.42
3	10	-3.6	2.1	-0.4	0.4	0	0.5	5.8	60	9.35
4	0	11.1	-1.7	-1.1	0.5	1.1	-1.3	13.8	60	3.34
5	50	-3.6	-3	-0.1	-0.6	0	0	3.9	60	14.53
6	0	-2.4	-3.6	-0.1	0	0	0	3.4	60	16.56
7	10	0.4	-0.2	4.8	-0.1	-0.1	-0.1	5.1	60	10.83
8	0	-0.3	-3.8	-7	0.1	-0.2	1.9	7.7	60	6.78
9	0	-0.3	0.5	9.2	-0.1	0	0.1	9.4	60	5.36
10	0	-0.3	-3.8	-7	0.1	-0.2	1.9	7.7	57.4	6.43
11	0	-0.3	-3.8	-7	0.1	-0.2	1.9	7.7	57.4	6.43
12	0	-5.9	-2	4.4	-0.5	0	0	10.4	57.4	4.54
13	0	5.7	2.5	9.9	0	-0.1	1.2	7.7	57.4	6.45
14	0	-5.9	-2	4.4	-0.5	0	0	10.4	59.1	4.71
15	0	5.7	2.5	9.9	0	-0.1	1.2	7.7	59.1	6.68
16	0	-0.1	5.3	3.7	-0.5	0.1	0.1	5.5	59.1	9.79
17	0	-0.1	7.8	5.3	-0.8	0.1	0	8.2	59.1	6.25
18	0	-0.2	8.8	5.2	-0.9	0.1	0	9.2	59.1	5.44
19	0	-0.2	9.2	4.4	-0.9	0.1	0	9.6	59.1	5.16
20	0	-0.2	9.6	3.4	-1	0.1	0	10	59.1	4.93
21	0	-0.2	9.6	1.4	-0.9	0.1	0	10	59.1	4.93
22	30	-0.3	3.8	-4.4	0	2.8	0	9.9	59.1	4.96
23	0	-0.3	-1.3	-5.5	0.1	0.3	0.3	5.3	57.4	9.85
24	0	-1	4.7	-4.4	-0.5	0.5	0	9.2	57.4	5.21
25	0	-0.4	-4.7	-12.9	0.4	0.2	0	12.5	57.4	3.58
26	0	-0.5	-5.8	-15	0.5	0.1	0	14.6	57.4	2.93
27	0	-2.8	6.6	-9.1	-0.9	0.1	0	15.7	57.4	2.64
28	0	-0.4	-6	-16.6	0.6	0.2	0	16.3	57.4	2.51
29	0	-0.7	-6.9	-17.9	0.6	0.2	0	17.3	57.4	2.32
30	0	-0.7	-7	-17.6	0.6	0.1	0	16.9	57.4	2.39
31	0	-1.5	-4	-16.3	0.3	-0.3	-0.2	14.9	57.4	2.84
32	0	-0.3	4.2	-5.8	-0.7	0.3	-1	10.3	60	4.84
33	0	0.3	2.1	-7	-0.3	0.1	-0.8	9.2	60	5.55
34	0	0	-3.9	-15.1	0.4	-0.1	0.4	15.1	60	2.96
35	0	-0.2	-4.5	-14	0.4	0.5	0.3	13.8	60	3.35
36	0	4.7	-1.4	-6.2	0.6	0.4	-0.2	11.1	60	4.42
37	180	-6.2	-2.2	-0.6	0.3	-0.1	0.4	5.7	60	9.56
38	180	-9.4	-5.6	-0.6	0.4	-0.1	0.1	8.8	60	5.81
39	0	0.3	-7.1	-11.7	0.7	0.2	-0.2	12	60	3.98
40	0	-2.3	-8.4	-15.2	0.7	0.3	-0.7	13.1	60	3.58
41	10	-1.4	0.2	5	0	0.4	0	6.5	60	8.26

Table 2.6.7.3-5 Critical P_m Stress Summary (ksi)—1-Foot Top Corner-Drop, Bolt Preload, Internal Pressure

Component	Section	Angle	SI (ksi)	Allowable Stress (ksi)	Margin of Safety
1	4	0	2	20	9.24
2	9	40	5.8	20	2.44
3	13	0	7.5	19.1	1.54
4	15	0	4.2	19.7	3.67
5	21	80	3.9	19.7	4.1
6	22	60	5.6	19.7	2.5
7	23	50	5	19.1	2.8
8	24	0	5	19.1	2.82
9	31	40	3.6	19.1	4.38
10	36	180	5.7	20	2.54
11	40	80	3.7	20	4.47
12	41	0	1.5	20	12.18

Table 2.6.7.3-6 Critical $P_m + P_b$ Stress Summary (ksi)—1-Foot Top Corner-Drop, Bolt Preload Internal Pressure

Component	Section	Angle	SI (ksi)	Allowable Stress (ksi)	Margin of Safety
1	1	180	2.6	30	10.39
2	9	0	14.2	30	1.11
3	13	0	9.1	28.7	2.15
4	15	0	7.3	29.6	3.04
5	21	0	5.4	29.6	4.45
6	22	40	7.4	29.6	3.01
7	23	50	7.2	28.7	3.01
8	24	0	6.7	28.7	3.30
9	31	40	5.1	28.7	4.66
10	34	60	9	30	2.33
11	40	0	8	30	2.74
12	41	0	2.9	30	9.31

Table 2.6.7.3-7 Critical $P_m + P_b + Q$ Stress Summary (ksi)—1-Foot Top Corner-Drop, Bolt Preload, Internal Pressure, and Thermal Hot

Component	Section	Angle	SI (ksi)	Allowable Stress (ksi)	Margin of Safety
1	4	0	11.7	60	4.15
2	8	0	7.2	60	7.35
3	10	0	8.2	57.4	5.95
4	14	0	7.9	59.1	6.5
5	21	0	10.2	59.1	4.79
6	22	40	9.9	59.1	4.94
7	23	0	4.3	57.4	12.23
8	29	0	15.6	57.4	2.67
9	31	0	14.1	57.4	3.07
10	34	0	15.6	60	2.84
11	39	80	11.9	60	4.05
12	41	10	6	60	8.95

Table 2.6.7.3-8 Critical $P_m + P_b + Q$ Stress Summary (ksi)—1-Foot Top Corner-Drop, Bolt Preload, Internal Pressure, and Thermal Cold

Component	Section	Angle	SI (ksi)	Allowable Stress (ksi)	Margin of Safety
1	4	0	13.8	60	3.34
2	9	0	9.4	60	5.36
3	12	0	10.4	57.4	4.54
4	14	0	10.4	59.1	4.71
5	20	0	10	59.1	4.93
6	22	30	9.9	59.1	4.96
7	23	0	5.3	57.4	9.85
8	29	0	17.3	57.4	2.32
9	31	0	14.9	57.4	2.84
10	34	0	15.1	60	2.96
11	40	0	13.1	60	3.58
12	41	10	6.5	60	8.26

Table 2.6.7.3-9 P_m Stresses—1-Foot Bottom Corner-Drop, Bolt Preload, and Internal Pressure

		Cylindrical Stress Components (ksi)							Allowable Stress	
Section	Angle	S_X	S_Y	S_Z	S_{XY}	S_{YZ}	S_{XZ}	SI (ksi)	(ksi)	MS
1	180	-0.7	0.6	-0.9	0.1	0	-0.1	1.5	20	11.93
2	180	-0.4	0.8	-0.5	0.1	0	0.1	1.4	20	13.27
3	0	-1.3	-3.2	-6.4	0	-0.5	-0.2	5.2	20	2.82
4	180	-0.8	0.9	-1.8	0.2	0.2	0.3	2.8	20	6.07
5	180	-0.4	0.6	-0.8	0	0.3	-0.6	1.9	20	9.6
6	180	-0.1	0.9	-0.5	0.1	0.1	0.1	1.4	20	12.89
7	10	-1	-2.1	-0.1	-0.1	-0.2	0.3	2.1	20	8.57
8	10	2.4	0.4	-0.3	-0.6	-0.9	1.2	4.2	20	3.78
9	0	-1.6	-4.1	-3.4	0.3	-0.3	0.4	2.8	20	6.09
10	0	0.5	-3.7	-4.9	0.4	-0.1	3.4	8.7	19.1	1.19
11	0	1.4	-4.5	-8	0.5	-0.2	2.2	10.4	19.1	0.84
12	10	-1.4	-1.9	2.6	0.1	-0.5	-1.2	5	19.1	2.8
13	10	1.7	-0.5	4.8	-0.1	-0.6	0.2	5.4	19.1	2.54
14	0	-2.6	-4.3	-4.8	0.2	-0.6	-2.4	5.4	19.7	2.65
15	0	-0.4	-3.8	-4.8	0.3	-0.3	1.2	5.1	19.7	2.85
16	50	0	2.3	-1.8	0	-1.6	-0.1	5.2	19.7	2.77
17	70	0	1.1	-1.9	0	-1.1	0	3.7	19.7	4.37
18	90	0	0.4	-2.3	0	-0.5	0	2.9	19.7	5.78
19	90	0	0.1	-2.3	0	-0.2	0	2.4	19.7	7.12
20	105	0	-0.1	-2.2	0	0.1	0	2.2	19.7	8.14
21	105	0	-0.2	-1.8	0	0.3	0	1.8	19.7	9.94
22	70	0	0.4	-0.8	0	0.9	0.1	2.1	19.7	8.41
23	20	-0.2	-3.1	-2.7	0	-1	0.4	3.8	19.1	4.03
24	40	-0.1	0.8	-1.5	0	-1.5	0	3.7	19.1	4.14
25	60	-0.1	1.5	-1.2	0	-1.2	0	3.6	19.1	4.28
26	80	-0.1	2	-1.5	0	-0.8	0	3.8	19.1	4.03
27	90	-0.1	2.3	-1.7	0	-0.4	0	4	19.1	3.74
28	90	-0.1	2.4	-1.6	0	0	0	4.1	19.1	3.7
29	80	0	2.5	-1.2	0	0.4	0	3.9	19.1	3.92
30	0	-0.1	3.8	1.2	-0.4	0.2	0	4	19.1	3.74
31	40	-0.1	2.9	-0.1	0	2	0	5	19.1	2.81
32	80	0.1	0.9	-0.8	0	0.9	0.2	2.6	20	6.72
33	80	-0.8	0.9	-0.3	-0.2	0.6	0.1	2.1	20	8.45
34	60	0	1.8	0.3	0.2	1.6	0	3.6	20	4.55
35	180	-0.1	1.8	0	0.3	0	0.1	2	20	8.91
36	180	1.1	3.1	-0.5	0.3	0	0.5	3.8	20	4.27
37	10	-1.1	-0.3	-0.1	0.2	0	0	1.1	20	17.94
38	0	-1.2	-0.7	-0.1	0	0	-0.2	1.2	20	16.26
39	0	-1.2	-1	0	0	-0.1	0	1.2	20	15.19
40	80	-1.3	-2	-3	0	0	-1	2.6	20	6.57
41	0	-1.8	-1	-5	-0.1	-0.1	0.5	4.2	20	3.82

Table 2.6.7.3-10 $P_m + P_b$ Stresses—1-Foot Bottom Corner-Drop, Bolt Preload, and Internal Pressure

		Cylindrical Stress Components (ksi)							Allowable Stress	
Section	Angle	S_X	S_Y	S_Z	S_{XY}	S_{YZ}	S_{XZ}	SI (ksi)	(ksi)	MS
1	180	-0.9	1.2	-1	0.1	-0.1	-0.1	2.2	30	12.48
2	10	-2.6	-1.9	-0.2	0.1	-0.1	0.1	2.4	30	11.36
3	0	1.9	-2.4	-4.6	0.1	-0.5	0.3	6.5	30	3.58
4	0	-4.8	-4.3	-8.1	-0.1	-0.7	-0.9	4.3	30	6
5	180	-2.2	2.1	-0.4	0.4	0.2	-0.5	4.5	30	5.66
6	120	4.5	2.9	-0.3	-0.3	0	0.1	4.8	30	5.2
7	150	-2.2	1.3	-0.5	-0.1	0	0.6	3.6	30	7.26
8	0	0.9	-4.2	-6.5	0.5	-0.1	2.9	9.4	30	2.18
9	0	-3.3	-7	-11.3	0.5	-0.2	1.3	8.5	30	2.53
10	0	-0.5	-4.5	-6.6	0.4	-0.1	3.4	9.2	28.7	2.13
11	0	4.6	-2.8	-5.9	0.6	-0.2	3.1	12.3	28.7	1.34
12	0	-3	-2.6	1.8	0.1	-0.5	-2.2	6.6	28.7	3.35
13	10	-2.6	-2.2	3.3	0.1	-0.6	-0.7	6.1	28.7	3.67
14	0	-2.6	-6.4	-12.3	0.3	-0.6	-2.3	10.9	29.6	1.72
15	0	-5.4	-8.4	-15.9	0.3	-0.2	1.2	10.7	29.6	1.75
16	50	-0.1	3	-1.8	0	-2	-0.1	6.3	29.6	3.67
17	60	0	2.8	-1	0	-1.3	0	4.6	29.6	5.39
18	0	0	4.1	2.1	-0.4	0	0	4.3	29.6	5.94
19	0	0	3.9	2.7	-0.4	0	0	4.1	29.6	6.29
20	0	0	3.5	2.8	-0.4	0	0	3.6	29.6	7.16
21	0	0	2.5	2.3	-0.3	0	0	2.6	29.6	10.45
22	50	0	0.9	0.1	0	1.3	0.1	2.8	29.6	9.66
23	0	-0.4	-3.9	-6.2	0.4	-0.2	0.4	5.9	28.7	3.83
24	40	-0.2	1.2	-1.7	-0.1	-1.9	0	4.9	28.7	4.89
25	60	-0.1	3.3	-0.6	0	-1.4	0	4.8	28.7	5.01
26	0	-0.1	5.3	1.9	-0.5	0	0	5.5	28.7	4.24
27	0	-0.1	6	2.7	-0.6	0	0	6.2	28.7	3.60
28	0	-0.1	6.2	3	-0.6	0	0	6.4	28.7	3.48
29	0	-0.1	6.2	2.9	-0.6	0	0	6.3	28.7	3.52
30	0	0	6.2	2.1	-0.6	0.1	0	6.4	28.7	3.52
31	40	-0.1	3	-1	0	3	0	7.3	28.7	2.94
32	60	0.1	1	-1.6	0	1.3	0.1	3.6	30	7.29
33	70	-1.9	0.1	-2.4	-0.6	1	0.4	3.7	30	7.21
34	50	-0.1	1.6	-0.3	0	2.1	-0.1	4.6	30	5.54
35	70	-0.3	0.5	-0.6	0	1.4	1.5	4.1	30	6.26
36	180	-0.3	2.3	-2	0.4	0	0.3	4.4	30	5.83
37	0	-5.7	-5.3	-0.1	0	0	0	5.5	30	4.45
38	0	-4.4	-5.3	-0.2	0	0	-0.2	5	30	4.94
39	0	-3.1	-4.6	1.3	0	0	-0.4	5.9	30	4.11
40	0	-1.4	-6.4	-7.5	0.3	0	0.8	6.3	30	3.79
41	0	-0.3	-1	-7.2	0	0	0.9	7.1	30	3.2

Table 2.6.7.3-11 $P_m + P_b + Q$ Stresses—1-Foot Bottom Corner-Drop, Bolt Preload, Internal Pressure, Thermal Hot

		Cylindrical Stress Components (ksi)							Allowable Stress	
Section	Angle	S_X	S_Y	S_Z	S_{XY}	S_{YZ}	S_{XZ}	SI (ksi)	(ksi)	MS
1	0	-1.9	1.9	-1.2	-1	0.3	-0.4	4.5	60	12.29
2	180	2.5	2.9	-0.7	0	0	-0.1	3.6	60	15.87
3	0	0.4	-0.1	-8.4	-0.1	-0.9	0.5	9	60	5.69
4	0	6.3	-0.1	-5	0.2	-0.2	-0.3	11.4	60	4.25
5	20	-4	-9.2	-0.6	-1.4	-0.1	-0.5	9	60	5.66
6	50	-4.1	0.2	-0.6	-1.9	0	-0.1	5.7	60	9.46
7	40	-10.1	-5.9	-9.6	-2.6	-2.5	-3	10	60	4.98
8	0	3.4	-0.5	-3.9	-0.2	-0.5	4.5	11.6	60	4.18
9	0	-0.8	-4.8	-12.6	0.3	-0.8	-1.4	12.3	60	3.88
10	0	8.3	2.6	1	0	-0.6	5.3	12.9	57.4	3.44
11	0	3.4	-0.5	-3.9	-0.2	-0.5	4.5	11.6	57.4	3.95
12	50	-5.5	-1	3	-0.9	-0.4	-0.6	8.8	57.4	5.5
13	40	4.4	3.4	7.9	-2.2	-2.8	1.5	9	57.4	5.38
14	0	-0.6	-2.9	-14.1	0.2	-0.5	-1.6	13.9	59.1	3.25
15	0	-1.3	-4	-17.6	0.2	-0.2	0.8	16.3	59.1	2.62
16	0	-0.1	9.2	0.1	-0.9	0	0	9.5	59.1	5.25
17	0	-0.2	9.8	3.1	-1	-0.1	0	10.2	59.1	4.82
18	0	-0.2	9.8	4.5	-1	-0.1	0	10.2	59.1	4.8
19	0	-0.2	9.6	5.3	-1	-0.1	0	10	59.1	4.92
20	0	-0.2	9.4	5.9	-0.9	-0.1	0	9.8	59.1	5.06
21	0	-0.2	8.5	5.8	-0.8	-0.1	0	8.8	59.1	5.71
22	0	-0.1	5.7	4	-0.6	-0.1	-0.2	6	59.1	8.89
23	0	-0.8	-5	-13	0.4	-0.1	0.1	12.2	57.4	3.69
24	0	-0.5	-4.5	-10.4	0.4	0.1	0	10	57.4	4.76
25	0	-0.5	-6.4	-14.4	0.6	0	0	14	57.4	3.1
26	0	-0.5	-6.6	-15.1	0.6	-0.1	0	14.7	57.4	2.9
27	0	-0.3	-5.9	-14.5	0.6	-0.1	0	14.3	57.4	3.02
28	0	-0.3	-6	-14.2	0.6	0	0	13.9	57.4	3.12
29	0	-0.5	-6.4	-14.1	0.6	0	0	13.6	57.4	3.21
30	0	-0.5	-5.4	-12.4	0.5	-0.1	0	11.9	57.4	3.81
31	0	-0.3	-3.6	-7.9	0.3	-0.1	-0.2	7.6	57.4	6.56
32	50	-0.1	2.5	2.2	0	1.8	-0.1	4.2	60	13.13
33	40	1.2	2.1	3.5	-2.1	1.8	-0.5	6.1	60	8.89
34	0	-3	-5	-8.9	-0.2	-0.6	-1.8	6.9	60	7.66
35	60	-0.1	1	-5.9	0	1.6	0.7	7.8	60	6.74
36	70	5	2.2	0.8	1	1.4	0.8	5.7	60	9.44
37	30	-7.8	-8.1	-0.1	-1.5	0	0	9.3	60	5.45
38	60	-7.9	-5.8	-0.2	-0.3	0	-0.1	7.7	60	6.75
39	0	-1.4	4.4	-1.7	-0.3	-0.3	-1.3	7.3	60	7.26
40	70	-2.2	-2.4	-8.5	0.9	0.3	-0.6	7.1	60	7.41
41	60	-2.2	0.3	1.6	0	-1.1	-1.1	5.1	60	10.82

Table 2.6.7.3-12 $P_m + P_b + Q$ Stresses—1-Foot Bottom Corner-Drop, Bolt Preload, Internal Pressure, Thermal Cold

		Cylindrical Stress Components (ksi)							Allowable Stress	
Section	Angle	S_X	S_Y	S_Z	S_{XY}	S_{YZ}	S_{XZ}	SI (ksi)	(ksi)	MS
1	180	-2.2	0.6	-1	0.3	0	-0.2	2.9	60	19.42
2	10	-3.4	-2.6	-0.3	-0.1	-0.1	0.2	3.1	60	18.13
3	0	-5.5	-3	-11.7	-0.1	-1	-1	9.1	60	5.6
4	0	10.1	-1.9	-4.5	0.4	0.1	-1.3	14.9	60	3.04
5	10	-3.8	-6	-0.6	-0.4	-0.1	-0.4	5.5	60	9.95
6	135	-6.6	-3.1	-0.5	-0.3	0	0	6.1	60	8.87
7	180	-2.5	2	-0.7	0.5	0	0.7	4.8	60	11.44
8	0	2.3	-3.5	-8.7	0.3	-0.4	6.1	16.4	60	2.66
9	0	-3.8	-7.8	-15.9	0.3	-0.1	1.9	12.7	60	3.73
10	0	2.3	-3.5	-8.7	0.3	-0.4	6.1	16.4	57.4	2.5
11	0	2.3	-3.5	-8.7	0.3	-0.4	6.1	16.4	57.4	2.5
12	20	-3.8	-1.7	3.1	-0.3	-0.5	-1.6	7.7	57.4	6.45
13	20	11.4	4.9	10.8	-1	-1.6	2.5	9.5	57.4	5.04
14	0	-2.2	-5.8	-16.6	0.3	-0.6	-2.4	15.2	59.1	2.9
15	0	-3.5	-7.9	-22.1	0.4	-0.3	1.3	18.8	59.1	2.14
16	0	-0.1	8.8	-0.7	-0.8	-0.1	0	9.6	59.1	5.19
17	0	-0.2	9.6	2.4	-1	-0.1	0	10	59.1	4.94
18	0	-0.2	9.8	4	-1	-0.1	0	10.1	59.1	4.83
19	0	-0.2	9.6	4.9	-1	-0.1	0	10	59.1	4.92
20	0	-0.2	9.3	5.5	-0.9	-0.1	0	9.7	59.1	5.09
21	0	-0.2	8.3	5.5	-0.8	-0.1	0	8.6	59.1	5.84
22	0	-0.1	5	3.4	-0.5	-0.1	-0.2	5.2	59.1	10.32
23	0	-0.8	-7.3	-15.3	0.7	0	0.3	14.6	57.4	2.94
24	0	-0.5	-3.8	-11.6	0.4	0.1	0	11.1	57.4	4.16
25	0	-0.5	-6.4	-16	0.6	0	0	15.6	57.4	2.68
26	0	-0.5	-6.7	-16.8	0.6	-0.1	0	16.4	57.4	2.51
27	0	-2.8	6.4	-9.4	-0.8	0	0	15.9	57.4	2.61
28	0	-2.7	6.6	-8.9	-0.8	-0.1	0	15.5	57.4	2.7
29	0	-0.6	-6.5	-15.6	0.6	0	0	15.1	57.4	2.8
30	0	-0.6	-5.4	-13.7	0.5	-0.1	0	13.1	57.4	3.37
31	0	-0.3	-3.1	-8.3	0.3	-0.2	-0.2	8	57.4	6.13
32	40	-0.1	1.5	2.5	0	1.7	-0.1	3.9	60	14.51
33	40	0.6	1.7	3	-1.7	1.5	-0.4	5.2	60	10.5
34	0	-3.9	-5.5	-10.5	-0.2	-0.6	-2.1	8	60	6.52
35	0	0	-4	-6.9	0.3	0.2	0.5	7	60	7.56
36	80	6.1	2.6	2.4	0.6	0.8	0.7	4.7	60	11.72
37	30	-7.7	-7.9	-0.2	-0.9	0	0	8.5	60	6.04
38	180	-6.5	-7.3	-0.2	0	0	-0.1	7.1	60	7.49
39	0	-0.9	4.5	-1.3	-0.2	-0.3	-1	6.7	60	7.98
40	80	-1.9	-2.7	-8.1	0.6	0.2	-0.6	6.7	60	8
41	50	-0.3	0.8	4.5	0	-0.3	0.9	5.2	60	10.51

Table 2.6.7.3-13 Critical P_m Stress Summary (ksi)—1-Foot Bottom Corner-Drop, Bolt Preload, Internal Pressure

Component	Section	Angle	SI (ksi)	Allowable Stress (ksi)	Margin of Safety
1	3	0	5.2	20	2.82
2	8	80	4.2	20	3.78
3	11	0	10.4	19.1	0.84
4	14	0	5.4	19.7	2.65
5	16	50	5.2	19.7	2.77
6	22	70	2.1	19.7	8.41
7	23	20	3.8	19.1	4.03
8	28	90	4.1	19.1	3.7
9	31	40	5	19.1	2.81
10	36	180	3.8	20	4.27
11	40	80	2.6	20	6.57
12	41	0	4.2	20	3.82

Table 2.6.7.3-14 Critical $P_m + P_b$ Stress Summary (ksi)—1-Foot Bottom Corner-Drop, Bolt Preload, Internal Pressure

Component	Section	Angle	SI (ksi)	Allowable Stress (ksi)	Margin of Safety
1	3	0	6.5	30	3.58
2	8	0	9.4	30	2.18
3	11	0	12.3	28.7	1.34
4	14	0	10.9	29.6	1.72
5	16	50	6.3	29.6	3.67
6	22	50	2.8	29.6	9.66
7	23	0	5.9	28.7	3.83
8	28	0	6.4	28.7	3.52
9	31	40	7.3	28.7	2.94
10	34	50	4.6	30	5.54
11	40	0	6.3	30	3.79
12	41	0	7.1	30	3.2

Table 2.6.7.3-15 Critical $P_m + P_b + Q$ Stress Summary (ksi)—1-Foot Bottom Corner-Drop, Bolt Preload, Internal Pressure, Thermal Hot

Component	Section	Angle	SI (ksi)	Allowable Stress (ksi)	Margin of Safety
1	4	0	11.4	60	4.25
2	8	0	11.6	60	4.18
3	10	0	12.9	57.4	3.44
4	15	0	16.3	59.1	2.62
5	18	0	10.2	59.1	4.8
6	22	0	6	59.1	8.89
7	23	0	12.2	57.4	3.69
8	26	0	14.7	57.4	2.9
9	31	0	7.6	57.4	6.56
10	35	60	7.8	60	6.74
11	37	30	9.3	60	5.45
12	41	60	5.1	60	10.82

Table 2.6.7.3-16 Critical $P_m + P_b + Q$ Stress Summary (ksi)—1-Foot Bottom Corner-Drop, Bolt Preload, Internal Pressure, Thermal Cold

Component	Section	Angle	SI (ksi)	Allowable Stress (ksi)	Margin of Safety
1	4	0	14.9	60	3.04
2	8	0	16.4	60	2.66
3	10	0	16.4	57.4	2.5
4	15	0	18.8	59.1	2.14
5	18	0	10.1	59.1	4.83
6	22	0	5.2	59.1	10.32
7	23	0	14.6	57.4	2.94
8	26	0	16.4	57.4	2.51
9	31	0	8	57.4	6.13
10	34	0	8	60	6.52
11	37	30	8.5	60	6.04
12	41	50	5.2	60	10.51

2.6.7.4 One-Foot Oblique Drop

One foot is not a sufficient height to rotate the cask to an oblique orientation following a drop. Therefore, one-foot drops at oblique orientations are not considered as a credible event, and are not included in these analyses.

2.6.7.5 Impact Limiters

The Universal Transport Cask design includes removable upper and lower impact limiters to ensure that the design impact loads on the cask are not exceeded for any of the defined load conditions. These impact load conditions include the cask falling 1-ft or 30-ft and landing: (1) horizontally on its side on both impact limiters, (2) vertically on one impact limiter at either end, or (3) obliquely (including C.G. over the corner) on one impact limiter at either end.

The impact limiters decelerate the cask by applying a force in the direction opposite to the motion of the cask. The deceleration force is generated by crushing the redwood and balsa wood materials of the impact limiter between the cask and the unyielding surface. The energy absorbed during crushing is net force, the vector sum of the cask weight (downward) and the deceleration force (upward) multiplied by the distance crushed. The amount of energy that an impact limiter absorbs is calculated for various cask impact orientations, from vertical (0°) to horizontal (90°).

The impact limiter analysis is based on the assumptions that the cask impacts upon an unyielding surface and that the impact limiter remains in position on the cask during all impact events (The qualification of the impact limiter attachment is presented in Section 2.6.7.5.7).

2.6.7.5.1 Description of Impact Limiters

Each of the impact limiters on the Universal Transport Cask consists of 2 energy-absorbing materials: (1) redwood and (2) balsa wood. The wood is enclosed in a thin stainless steel shell to maintain the wood orientation during an impact. Figures 2.6.7.5-1 and 2.6.7.5-2 show the locations on the cask and the primary cross-section dimensions of the impact limiters. The upper and lower impact limiters are configured similarly to each other, except that the upper limiter has pockets for the lifting trunnions and a larger inside diameter. The approximate radius used for the backed area of the bottom impact limiter is 41.3 inches. The approximate radius of the backed area of the top impact limiter is 42.6 inches.

The outside diameter of the Universal Transport Cask upper and lower impact limiters is 124.0 inches and the height is 43.0 inches. The overlap between the cask body and the impact limiters is 11.0 inches. Sixteen 1.25-inch diameter retaining rods, attach each impact limiter to the end of the cask. The attachments are described in detail in Section 2.6.7.5.7. The height of the redwood in the end section of the impact limiter is 30.0 inches. A ring of balsa wood forms part of the end section of the impact limiter. The balsa wood ring dimensions are: inside diameter = 99.2 inches, outside diameter = 123.75 inches, and height = 21.6 inches. The bottom region of the impact limiter is a 1.5-inch thick layer of balsa wood that absorbs most of the kinetic energy in a 1-ft end-drop impact and limits the impact force for normal conditions of transport (1-ft drop). The low crush strength balsa wood is necessary because the impact area is considerably greater in a flat end impact than in any other drop orientation. The redwood and the balsa wood side ring absorb most of the energy in a corner impact and all of the energy in a side impact.

The different segments and sections comprising each limiter are bonded to each other with DAP-Weldwood resorcinol adhesive.

For each of the impact load conditions in this analysis, the impact limiters remain in position on the cask and absorb the energy of the impact; thus, they limit the impact loads to the calculated values shown in Table 2.6.7.5-6.

2.6.7.5.2 Load Conditions

The specific loading conditions for the impact limiters are defined by 10 CFR 71.71(c)(7), 10 CFR 71.73(c)(1) and Regulatory Guide 7.8, as follows:

1. 1-ft drop of the cask impacting at any angle from vertical (flat end) to corner (cask center of gravity directly above point of impact).
2. 1-ft drop of the cask in a horizontal orientation (side impact).
3. 30-ft drop of the cask in an end, side, corner, or oblique orientation.

On the basis of these loading conditions, the Universal Transport Cask impact limiters are designed for the 30-ft cask drops but with consideration of the effects of the 1-ft drops. The maximum impact forces and the maximum crush depth for the 1-ft and 30-ft cask drops are obtained from the LS-DYNA [33] analyses of the cask drops. LS-DYNA is an explicit finite element program capable of performing three-dimensional nonlinear analysis of structures

containing nonlinear material behavior such as plastic deformation of steel or crushing of wood. LS-DYNA is described in Section 2.10.1.2.

2.6.7.5.3 Tests of Impact Limiter Specimens

A series of static and dynamic crush tests was performed to define the crush properties of the redwood and the balsa wood to be used in the impact limiters.

Static Tests

The static crush tests represent the crush strength of the wood for either static loading or low strain rate crush, which would be associated with the impact velocities for a 1-foot drop. The redwood force-deflection data was obtained at room temperature for the perpendicular-to-grain direction using 44 samples and parallel-to-grain crush direction using 44 samples and for the parallel-to-grain crush direction 45 samples. These crush tests were used to define an acceptable range for the density for redwood of 23.5 +/- 3.5 lb/ft^3. An average crush stress-strain curve was obtained for each direction of crush using a least squares straight line fit. To account for the effect of low temperatures (-20°F) for redwood, as well for temperatures at 152°F, the test data was ratioed by the temperature effect shown in Figure 8 of NUREG/CR-0322 [34]. To account for fabrication tolerances and provide bounding maximum crush strength for the redwood, the cold properties are factored by 1.10. To obtain the bounding minimum crush strength, the hot properties are factored by 0.9. The static crush strength data for redwood is presented in Table 2.6.7.5-1.

For balsa wood (balsa) static properties, Figure 16 of JPL Technical Report No. 32-944 [35] shows the average crush strength of the balsa in the parallel-to-grain direction at room temperature to be 1,550 psi for a density of 10 lb/ft^3. The static balsa properties at -40°F and 152°F are obtained by factoring the room temperature crush stress-strain curve for balsa based on the temperature effect contained in Figure 15 of the JPL Technical Report. The static crush strength data for balsa is presented in Table 2.6.7.5-2.

Dynamic Tests

Dynamic crush tests are performed to establish the dynamic properties for the redwood and balsa. As in the static crush tests, the density of the redwood samples are restricted to be 23.5 +/- 3.5

lb/ft³. While static testing was not performed for balsa by NAC, the density for balsa in the tests was restricted to 8.5 +/- 1.5 lb/ft³.

The stress-strain curves for balsa and redwood are determined for two directions, perpendicular, and parallel to the grain. The test program conducted at room temperature was comprised of using 9 to 10 samples at each of five strain rates, which ranged from 25 strain/sec to 375 strain/sec. The force-deflection data for the samples having the same strain rate (for the same crush direction for the same wood) were averaged to produce a composite curve. The composite curve was reduced to a series of straight-line segments while retaining the maximum acceleration of the composite curve and the same area under the stress-strain curve. To account for the effect of temperatures, an additional series of tests was conducted at -40°F and at 200°F for three strain rates ranging over the same range employed for the room temperature evaluation. In performing the evaluation, the predominant strain rate is the 25 strain/sec for which the properties are presented in Tables 2.6.7.5-3 and 2.6.7.5-4 for the redwood and the balsa, respectively.

2.6.7.5.4 Specification for Universal Transport Cask Impact Limiters

The redwood material used for the Universal Transport Cask impact limiters must meet density, crush strength (converted from the force-deflection curve) and moisture content specifications. The density of any single redwood board shall be 23.5 ± 3.5 lb/ft³. The density of any 15° or 30° pie-shaped section of redwood shall be 22.3 ± 1.2 lb/ft³. Each 15°, pie-shaped section of redwood in the side segment of the impact limiter shall have an average static crush strength value (in the parallel-to-the-grain direction) of 5,898 ± 620 psi at 0.4 in./in. strain and 70°F. Each 30-degree, pie-shaped section of redwood in the end segment of the impact limiter shall have an average crush strength value (in the perpendicular-to-the-grain direction), of 1,190 ± 130 psi at 0.4 in./in. strain and 70°F. The moisture content of any single board shall be greater than 5% but less than 15%. The average moisture content for the lot of redwood shall be less than 12%.

The balsa wood to be used in the Universal Transport Cask impact limiters shall meet the specifications of MIL-S-7998A [38]: (1) density between 7 and 10 lb/ft³, and (2) moisture content between 5 and 15% for any one piece with an average of not more than 12% for any lot of balsa wood.

2.6.7.5.5 Impact Limiter Analysis

The primary areas of analytical evaluation required in an impact limiter analysis are (1) crush depth, (2) maximum acceleration, and (3) attachment to the cask. The crush depth and maximum acceleration are dependent on the crush strength of the crushable material, the area engaged in crushing, the geometry of the impact limiter, and the energy to be dissipated.

The LS-DYNA general purpose explicit finite element computer program is used to analyze an impact limiter for an impact event to determine the dynamics of the event, the acceleration generated during that event, and the depth of crush. A detailed description of this program is provided in Section 2.10.1.2.

The top end, top corner, and side impact analyses were performed for the finite element model shown in Figure 2.6.7.5-3 using LS-DYNA. The model in Figure 2.6.7.5-3 is a half-symmetry model and is constructed of 8-node brick and 4-node shell elements. The cask body section of the model consists of brick elements using an elastic material, while the impact limiter shells are comprised of the shell elements (see Figure 2.6.7.5-4). The elastic modulus of the cask body was adjusted to allow the cross-sectional modulus of the finite element model to be equal to that of the full-scale cask design. The weight and the CG of the finite element model correspond to that of the full-scale design. The cask contents weight, including the mass of the canister lids, is distributed in the brick elements along the length of the cask. In the full-scale cask design, the canister lids are positioned to be in contact with the cask body upper forging, which is a massive ring that is insensitive to the localized loading of the canister lids. For this reason, it is only required that the weight and CG of the finite element model accurately represent the full-scale design of the UMS® transport cask. The model contains a detailed representation of the trunnion and the cutout in the top impact limiter. The impact limiters are attached to the cask ends by beam elements corresponding to the attachment bolts for the impact limiter. The redwood and the balsa wood are modeled as an isotropic foam material. The stress-strain curves used as input into the LS-DYNA model were obtained by dynamic crush testing of the wood specimens.

For the end drop, the portion of the model limiter being crushed employs the redwood perpendicular properties, and for the corner drop, the properties for the wood include the redwood in the perpendicular direction and balsa in the parallel direction. For the side drop

condition, the impact plane and cask crushes the redwood, which is oriented in the parallel direction.

The wood impact limiter surrounding the cask consists of 24 equally spaced angular wedges separated by radial gussets fabricated from steel plates. Since a half-symmetry finite element model is used to represent the impact limiters, only 12 of the wood wedges are modeled. Out of the 12 modeled wood wedges, only 3 wedges are loaded during a 30-foot side drop. The first wedge is loaded in the parallel to grain direction. The second and third wedges are loaded between the parallel and perpendicular to grain directions.

For the wedges where the impact force is applied between the parallel and perpendicular to grain directions, Hankinson's formula (Avallone, E. A., Baumeister III, T., *Marks' Standard Handbook for Mechanical Engineers*, 9th Edition, McGraw-Hill Book Company, New York, 1987, pages 6-127) is used to determine the strength properties of wood as it varies with the orthotropic axes of the wood grain.

$$N = \frac{PQ}{P\sin^2\theta + Q\cos^2\theta}$$

Where:

N - stress induced by a load acting at an angle to the grain direction,
P = compression strength parallel to the grain direction,
Q = compression strength perpendicular to the grain direction,
θ = angle between the direction of the load and the direction parallel to the grain.

Using Hankinson's formula, stress-strain curves are generated for the second and third wedges at 15 and 30 degrees, respectively; therefore, in the LS-DYNA input files, unique stress-strain curves are applied to the 0, 15, and 30 degree wood wedges depending upon the loading angle, strain rate and temperature.

To account for the deformation of the Type 304 stainless steel shells and gussets, these components were modeled with an elasto-plastic material - LS-DYNA material Type 24 ("Piecewise_Linear_Plasticity"). The required input data for the stainless steel consists of the stress-strain data presented in Table 2.6.7.5-5.

Boundary Conditions and Initial Conditions

LS-DYNA "Surface_to_Surface" contact interfaces are employed between the cask body and the impact limiter shells. The unyielding surface is modeled as being flat using the "Rigidwall_Geometric_Flat" option in LS-DYNA. Symmetry boundary conditions are imposed on the nodes in the X-Z plane. Initial velocities of 96.3 in./sec and 527.4 in/sec were applied to the entire model to represent the 1-foot and 30-foot drops, respectively. A uniform gravitational field corresponding to 386.4 in/sec^2 is also applied in the direction of the drop.

There are three orientations considered in the evaluation of the 1-foot and the 30-foot drops: end drop, center of gravity (CG) over corner and side drop. The end drop results in the maximum axial accelerations. To establish the bounding axial accelerations, as well as the maximum axial crush depth, two end drop conditions are analyzed. To obtain the maximum acceleration, the top end drop is performed using –40°F material properties. This condition corresponds to the wood having maximum crush strength in conjunction with the largest backed area. To obtain the maximum crush depth for the end drop orientation, the bottom end drop is performed using the material properties at 200°F. The bottom end of the transport cask has a smaller area than the top end and the use of 200°F material properties corresponds to the minimum crush strength.

The corner drop (CG over corner) results in the largest crush depth of the limiter. The side drop results in the maximum acceleration in the lateral direction on the cask.

Based on the validation study provided in Section 2.6.7.5.8, the side drop condition bounds any slap down for cask designs in which L/r < 2. Therefore, only the side drop analysis is performed to determine the bounding lateral accelerations and crush depths. The bounding side drop accelerations are determined using the cold material properties (–40°F). The bounding side drop crush depths are determined using the 200°F material properties.

2.6.7.5.6 Analysis Results

To obtain results from LS-DYNA, nodes of interest are used to record output data. These nodes are located at the plane of symmetry on the outer surface of the cylinder at the end of the cask cavity. For the side drop, the nodes record the lateral acceleration, and for the end drop, the nodes record the axial acceleration. For the CG over corner orientation, the recorded acceleration corresponds to the direction of drop. The nodal output is in the form of displacement and acceleration time histories. However, the acceleration time histories contain high frequency

components, which do not represent the response of the cask to the external impact. Therefore, the time histories are filtered to obtain the true accelerations corresponding to the impact. For this evaluation, the Butterworth low-pass filter in LS-DYNA's post-processor is used with a filter frequency of 120 Hz. The filter frequency was established by performing a modal analysis of the cask finite element model. The side drop modal analysis applied a simply supported condition in the direction of the drop at each of the cask ends, which resulted in a fundamental mode at 61 Hz. For the end drop modal analysis, an axial restraint is applied to the nodes at the end of the cask, which results in a fundamental mode at 129 Hz. A filter frequency of 120 Hz is used in the acceleration calculation.

The maximum accelerations for the 1-foot and the 30-foot drops are presented in Table 2.6.7.5-6. The filtered acceleration time histories for the conditions providing the maximum accelerations for the end drop, CG over corner and side drop are shown in Figure 2.6.7.5-5, Figure 2.6.7.5-6 and Figure 2.6.7.5-7, respectively.

2.6.7.5.7 Impact Limiter Attachment Analysis

The following design criteria apply to the method of attaching the impact limiters to the cask body.

1. The impact limiters must remain attached to the cask body during normal handling and transport. Satisfaction of this criterion ensures that the limiters will be in a proper position to perform their impact-limiting function in the event of a free drop (normal or accident).

2. In a free drop (normal or accident), the limiter (or limiters) making initial contact with the unyielding surface must remain in position on the cask for the full duration of the initial impact. Satisfaction of this criterion ensures that the limiter(s) will be able to properly perform the impact-limiting function.

3. In a free drop (normal or accident) involving an initial impact on a single impact limiter, the limiter on the opposite end of the cask must remain attached to the cask during the initial impact. Satisfaction of this criterion ensures that the limiter will be in a proper position to perform its impact-limiting function in a subsequent secondary impact following the initial impact.

in a proper position to perform its impact-limiting function in a subsequent secondary impact following the initial impact.

Sections 2.6.7.5.7.1 through 2.6.7.5.7.3 demonstrate that each of these criteria is satisfied.

2.6.7.5.7.1 Impact Limiter Attachment During Normal Handling and Transport

Attachment of the impact limiters to the cask body during normal handling and transport operations is ensured by demonstrating that the attachment hardware does not yield under normal handling and transport conditions. The worst-case loading associated with normal handling and transport is a 7.5 g-load corresponding to the peak longitudinal shock loading expected as the result of rail transport (as specified by the Field Manual of the AAR [31]).

The design load, P, on the attachment is P = (7.5)(8,846) = 66,345 lb, where 8,846 lb is the weight of each impact limiter.

Analysis of Retaining Rods

Sixteen 1.25-in. diameter retaining rods are equally spaced on a bolt circle diameter of 81.8 inches for the upper limiter and 71.1 inches for the lower limiter. The attachment geometry of the impact limiters is shown in Figure 2.6.7.5-8. The retaining rods are SA-193, Grade B8S stainless steel with a yield strength of 39.8 ksi and a design stress intensity (S_m) of 13.0 ksi at 200°F (Table 2.3.5-3).

The load on each retaining rod resulting from a longitudinal shock load of 7.5 g is given as

$$P = 66{,}345/16 = 4{,}147 \text{ lb per retaining rod.}$$

The retaining rod tensile area is 0.969 in^2 in the threaded region, resulting in a tensile stress of:

$$S_t = 4{,}147/0.969 = 4{,}275 \text{ psi}$$

Each retaining rod nut is torqued to 75 ± 5 ft-lbs, resulting in a preload of 2,560 lbs. Therefore, the preload stress is (2,560 lb/0.969 in^2 =) 2,642 psi. The total stress for the longitudinal shock load of 7.5g is, therefore, 4,275 + 2,642 = 6,920 psi (6.9 ksi). For the retaining rods, the allowable stress is twice S_m, or 2 x 13.0 = 26.0 ksi. The Margin of Safety (MS) is:

$$MS = (26/6.92) - 1 = +2.76$$

Analysis of Retaining Rod Anchorage

The nut of the retaining rod is bearing on a washer that has a diameter of 5.0 in. and a thickness of 0.50 in. The washer is bearing on the bearing plate portion of the impact limiter shell, which bears on the redwood material.

The load on each of the 16 retaining rods resulting during the normal transportation condition is 4,147 + 2,560 = 6,707 lb. The bearing area between the bearing plate and the redwood material is:

$$A = (\pi/4)(5.0^2 - 3.0^2) = 12.57 \text{ in}^2.$$

The bearing pressure is:

$$p = 6{,}707/12.57 = 534 \text{ psi}$$

The perpendicular-to-the-grain compressive stress in the redwood at 2.5% strain is 750 psi. The margin of safety for compression of the redwood is

$$MS = (750/534) - 1 = +0.41.$$

The washer is made of Type 304 stainless steel and has a 1.31-inch diameter hole in the center. It is analyzed by assuming that it is simply supported along a circle having a diameter equal to the edge of the hole in the bearing plate (3.00 in.). The total load of 6,707 lb is distributed along the edge of the nut, which has an average diameter of 1.939 in. From Roark, Table 24, Case 1a, [28], the stress on the washer is:

$$S_{max} = \left(\frac{12Wa^2}{\left(a - \frac{b^2}{a}\right)t^2}\right)\left[\frac{r_o}{a}\left\{\frac{1+\nu}{2}\ln\left(\frac{a}{r_o}\right) + \frac{1-\nu}{4}\left[1-\left(\frac{r_o}{a}\right)^2\right]\right\}\right] = 24.4 \text{ ksi}$$

where:

a = 1.50 in. b = 0.655 in.
t = 0.50 in. ν = 0.31
r_o = 0.9695 in. $W = (6{,}707/(2\pi \times 0.9695)) = 1{,}101$ lb/in.

The yield strength of Type 304 stainless steel is 25.0 ksi at 200°F. The margin of safety is calculated MS = 25.0/24.4 - 1 = +0.02.

The positive margins of safety show that the attachment of the impact limiters is adequate during normal conditions of transport.

Evaluation of Impact Limiter Attachment for Vibration

During normal conditions of transport, the impact limiter attachment may be subjected to vibration induced from the combination of component natural frequency and a dynamic load forcing function dependent on the transport media. Design of the impact limiter attachment eliminates the potential for the postulated vibration loading to loosen the impact limiter attachment. Lock nuts are installed in back of each of the retaining rod attachment nuts to prevent them from becoming loose. Locking wires installed between sets of two retaining rods eliminate rotation of the impact limiter retaining rods relative to their anchorage. The combination of these two design features eliminates the potential for the impact limiter attachment to become loose as a result of postulated vibration loading during transport.

2.6.7.5.7.2 Response of Impacted Limiters During Initial Impact of Package with Ground

The second criterion applicable to the impact limiter attachments requires that the impact limiter making initial contact with the unyielding surface must remain in position on the cask for the full duration of the initial impact. To satisfy this criterion, the impact limiter(s) being crushed must not separate from the cask, although the attachment hardware (mounting plate and bolts) may fail during the impact event.

The ability of the NAC-STC impact limiter to remain in position during an impact was demonstrated with reference to several static compression tests of the NAC-STC, during which the only attachment mechanism was a strip of duct tape. All of the compression tests were performed by using eighth-scale models of the impact limiters. The results of these tests are applicable to the Universal Transport Cask.

Analytic evaluations are performed to further justify that the initially impacted Universal Transport Cask impact limiter remains in position during an impact event and properly perform its function. Results of evaluations indicate that the attachment hardware is not expected to fail

and that the cask and impact limiter do not separate even if the attachment does fail. A significant resistance to the applied separation moment exists as a result of a combination of crushing of the limiter at the cask interface and also as a result of frictional resistance that exists at the interface. This total resistance is calculated to be greater than the applied separation moment.

2.6.7.5.7.3 Response of Secondary Impact Limiter During Initial Impact of Package

The final criterion to be satisfied is that for a free drop (normal or accident) involving an initial impact on a single impact limiter. The limiter on the opposite end of the cask (secondary limiter) must remain attached to the cask during the initial impact, thus ensuring that the secondary limiter is in position to absorb the secondary impact. The secondary limiter remains in position for the full duration of the secondary impact and performs its impact-limiting function. Attachment is ensured by demonstrating that the attachment hardware (mounting plate and retaining rods) does not fail during the initial impact.

During a free drop of the cask (normal or accident) involving an initial impact on a single impact limiter, i.e., flat end, center of gravity over corner, or any oblique drop, the ground exerts an upward force on the impact limiter that strikes it. The impact limiter in turn exerts an upward force on the cask body, thus decelerating the cask body. The cask body exerts an upward force on the secondary impact limiter and decelerates it. This scenario is repeated during a rebound of the whole package: the ground exerts an upward force on the impact limiter that strikes it; the impact limiter that strikes the ground exerts an upward force on the cask body and the cask body exerts an upward force on the secondary impact limiter, thereby accelerating the whole package upwards. When the entire package is in the air, its components (the impact limiter, the cask body, and the secondary impact limiter) move with the same acceleration and velocity; no other force acts among them. Thus, it is evident that during a free-drop impact on the first impact limiter, no separation force exists between the cask body and the second impact limiter. The absence of separation forces ensures that the second impact limiter stays in position to absorb the second impact.

Analysis of the impact limiter mounting plate and retaining rods demonstrates that the impact limiter attachments provide significant resistance to any unspecified separation force on the impact limiter. This analysis provides further evidence that the secondary impact limiter will stay attached to the cask body to absorb the second impact.

2.6.7.5.8 Verification of LS-DYNA for Cask Drop Impact Limiter Evaluation

To confirm the adequacy of LS-DYNA for cask drop impact limiter analyses, the NAC-STC quarter-scale cask is modeled for a series of parametric studies. The parametric studies include: end drop, CG over corner drop, side drop and oblique drops at shallow angles, and a study of friction forces between the impact limiters and the unyielding surface, to demonstrate that the oblique drop accelerations are bounded by the side drop. Since the NAC–STC cask was drop tested at an angle of 75° (from vertical) to determine the effects of slap-down, the NAC–STC provides an acceptable benchmark for the LS-DYNA analysis methodology.

The modeling procedure and material properties described in Section 2.6.7.5.5 for the UMS® full-scale cask model were used to develop a quarter-scale model of the NAC–STC cask. The filter frequencies for the lateral drops and the end drops were selected to be 450 Hz and 550 Hz, respectively. These filter frequencies were established by performing a modal analysis of the cask model. The LS-DYNA analysis results and comparison to NAC–STC test results for the end, corner, and side drops are shown in Table 2.6.7.5-7. As the table shows, LS-DYNA adequately predicts the response of the wood impact limiters.

Additional LS-DYNA analyses were performed using this quarter-scale model of the NAC-STC cask to determine the maximum accelerations for the shallow angle drops of 75° and 85° (from vertical). Table 2.6.7.5-8 summarizes the LS-DYNA results for the NAC-STC model and provides a comparison to available test results. The table also shows that the 90° (side drop) results are bounding for a cask design in which the L/r (length to radius of gyration) is less than 2.

The oblique drop analyses for the 75° and 85° orientations of the NAC-STC quarter-scale model assumed a coefficient of friction of 0.2, which is less than a typical published value of 0.27 for a steel-steel interface with an oxide film (Marks). An additional parametric study using the LS-DYNA model showed that the bounding case is the zero friction condition, which is summarized in Table 2.6.7.5-9. The zero friction condition remains bounded by the side drop condition.

Following the completion of the NAC–STC parametric study, LS-DYNA analyses of the NAC–UMS® quarter scale test model were completed for end, corner, and side drop conditions and compared to drop test results. The NAC–UMS® quarter scale model analyses and comparison to drop test results are presented in Section 2.10.3.7.

Figure 2.6.7.5-1 Universal Transport Cask with Impact Limiters

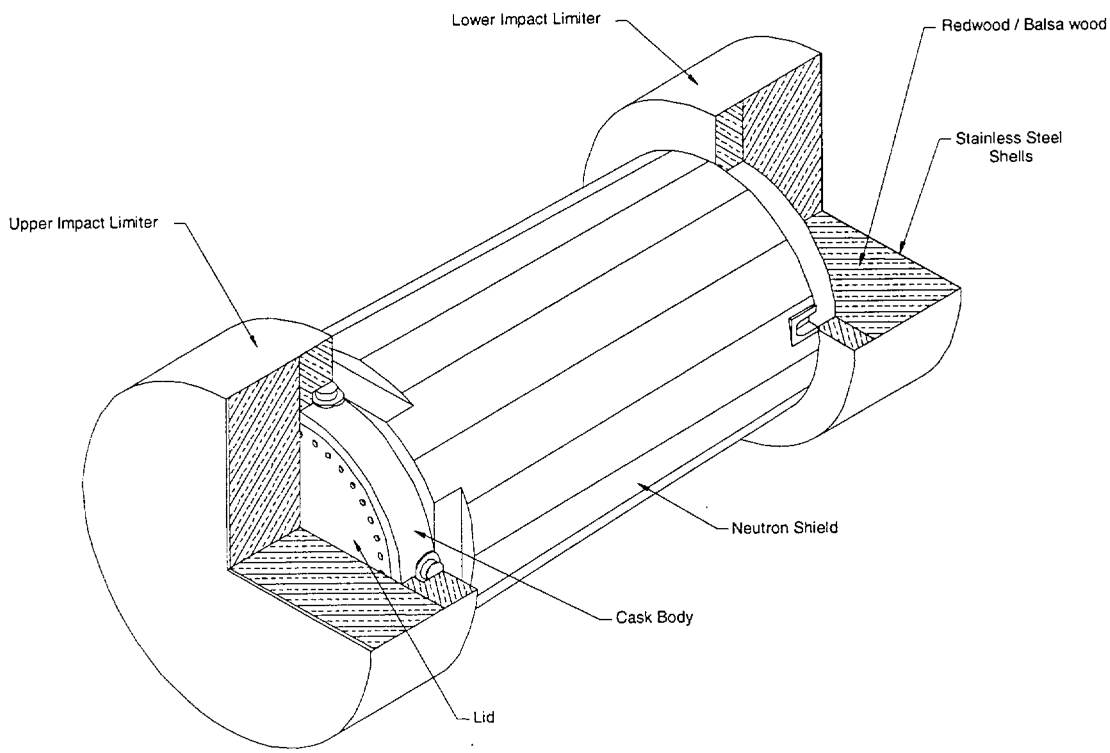

FIGURE WITHHELD UNDER 10 CFR 2.390

Figure 2.6.7.5-3 LS-DYNA Finite Element Model

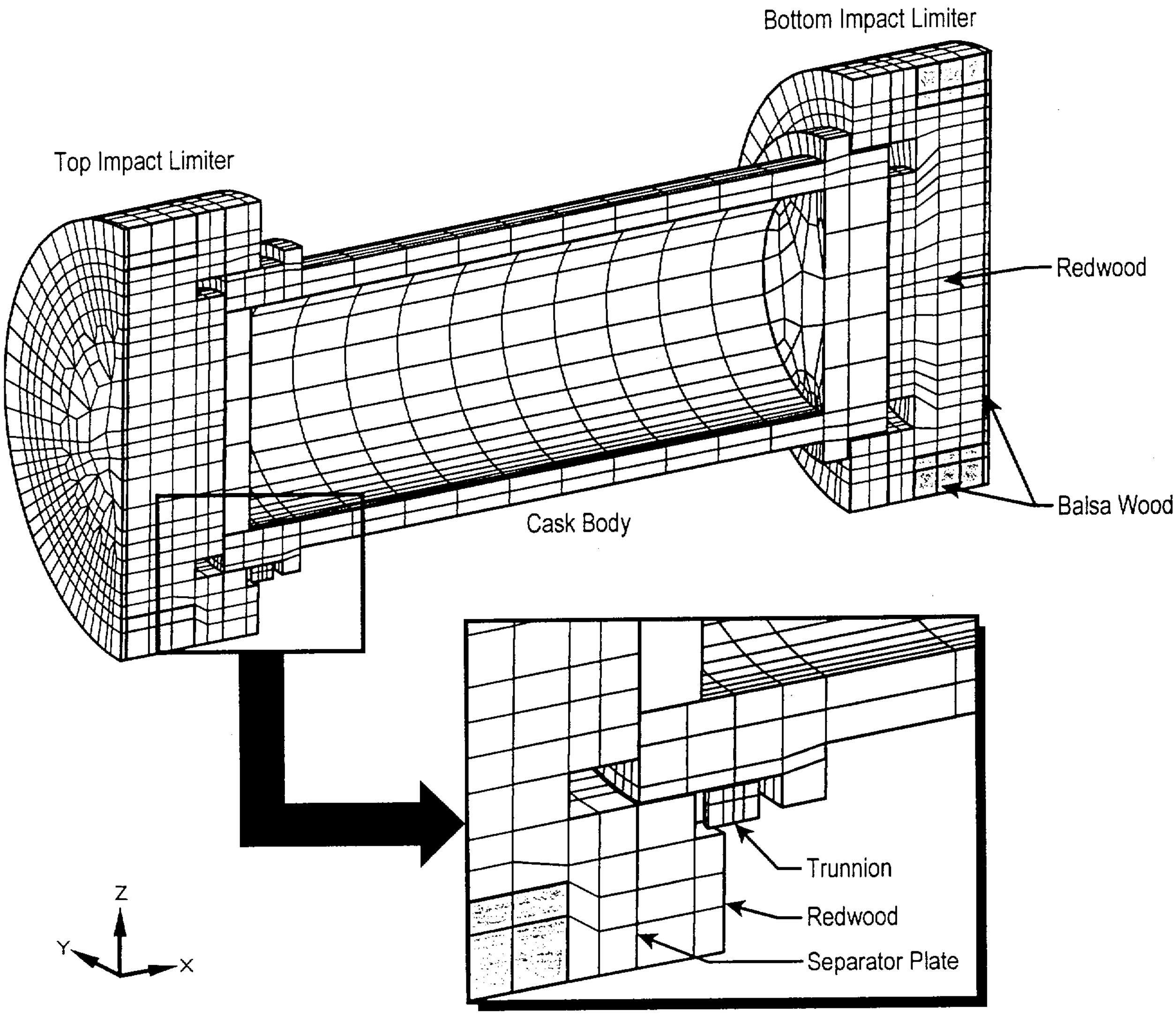

Figure 2.6.7.5-4 Impact Limiter Shell LS-DYNA Finite Element Model

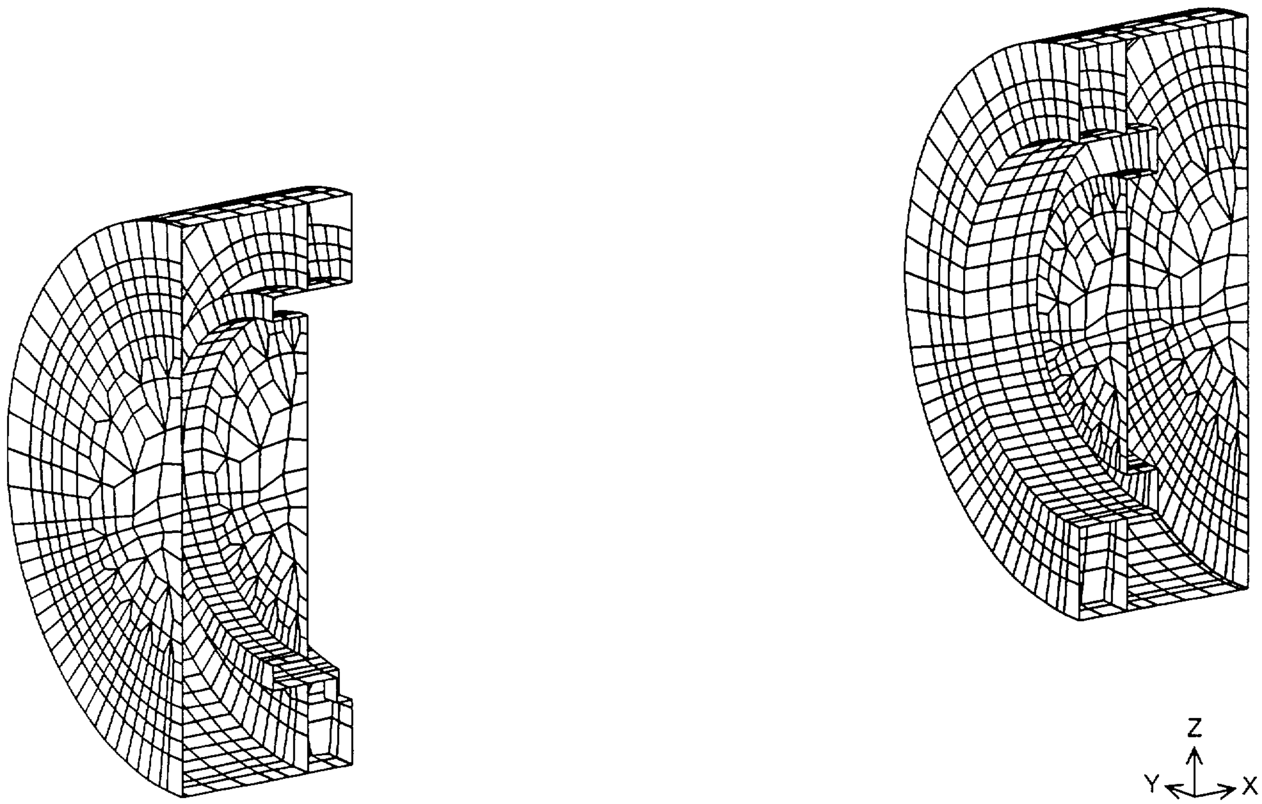

Figure 2.6.7.5-5 Acceleration Time History for the Cold Condition 30-Foot Top End Drop

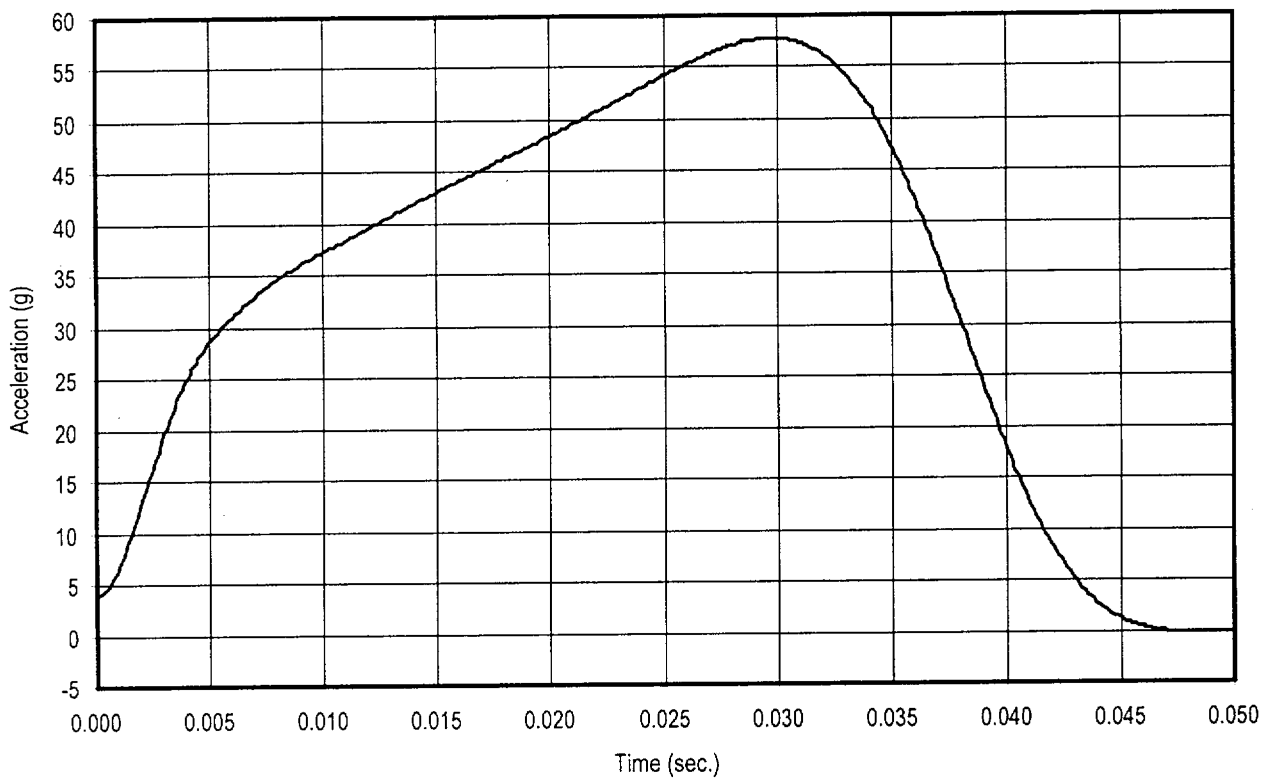

Figure 2.6.7.5-6 Acceleration Time History for the Cold Condition 30-Foot Top Corner Drop

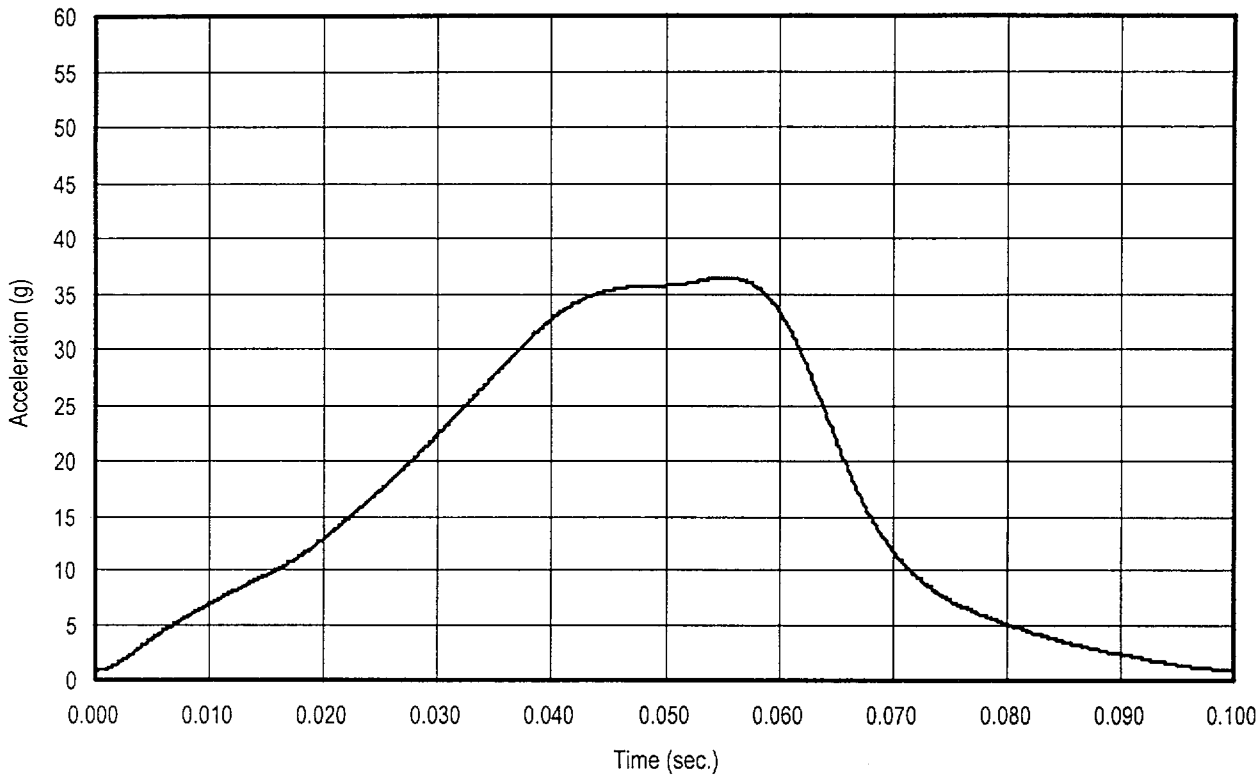

Figure 2.6.7.5-7 Acceleration Time History for the Cold Condition 30-Foot Side Drop

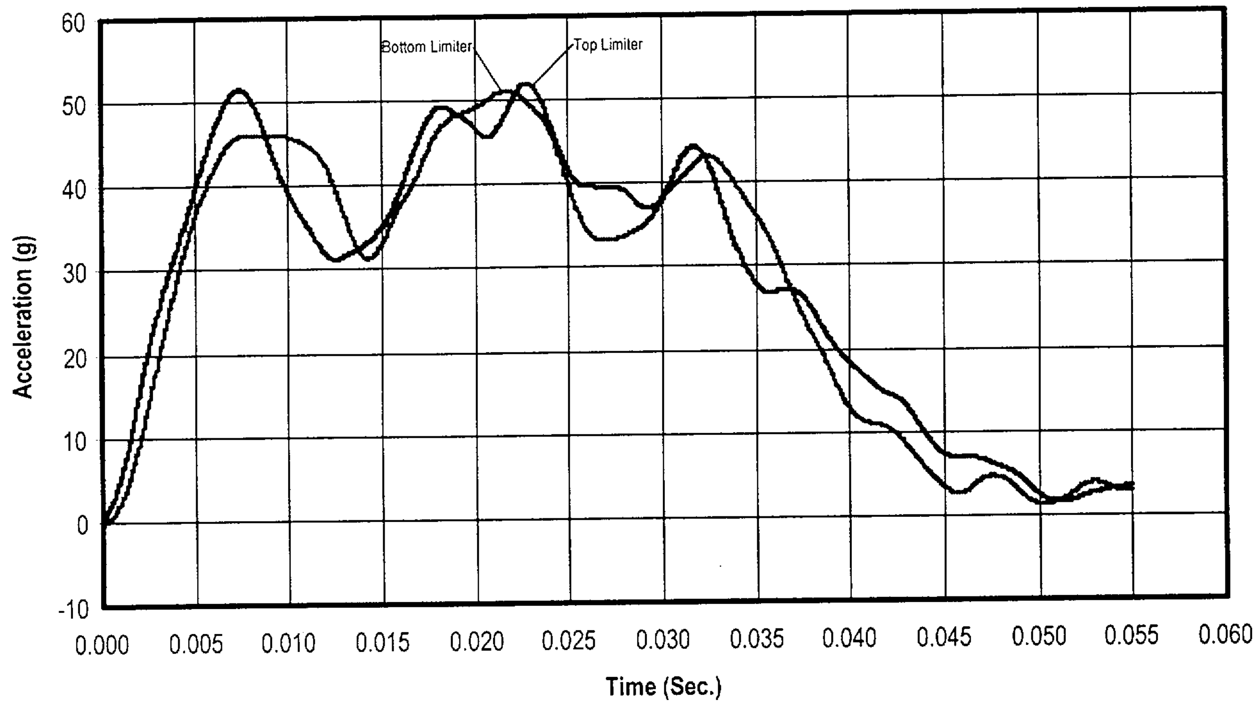

Figure 2.6.7.5-8 Impact Limiter Attachment Geometry

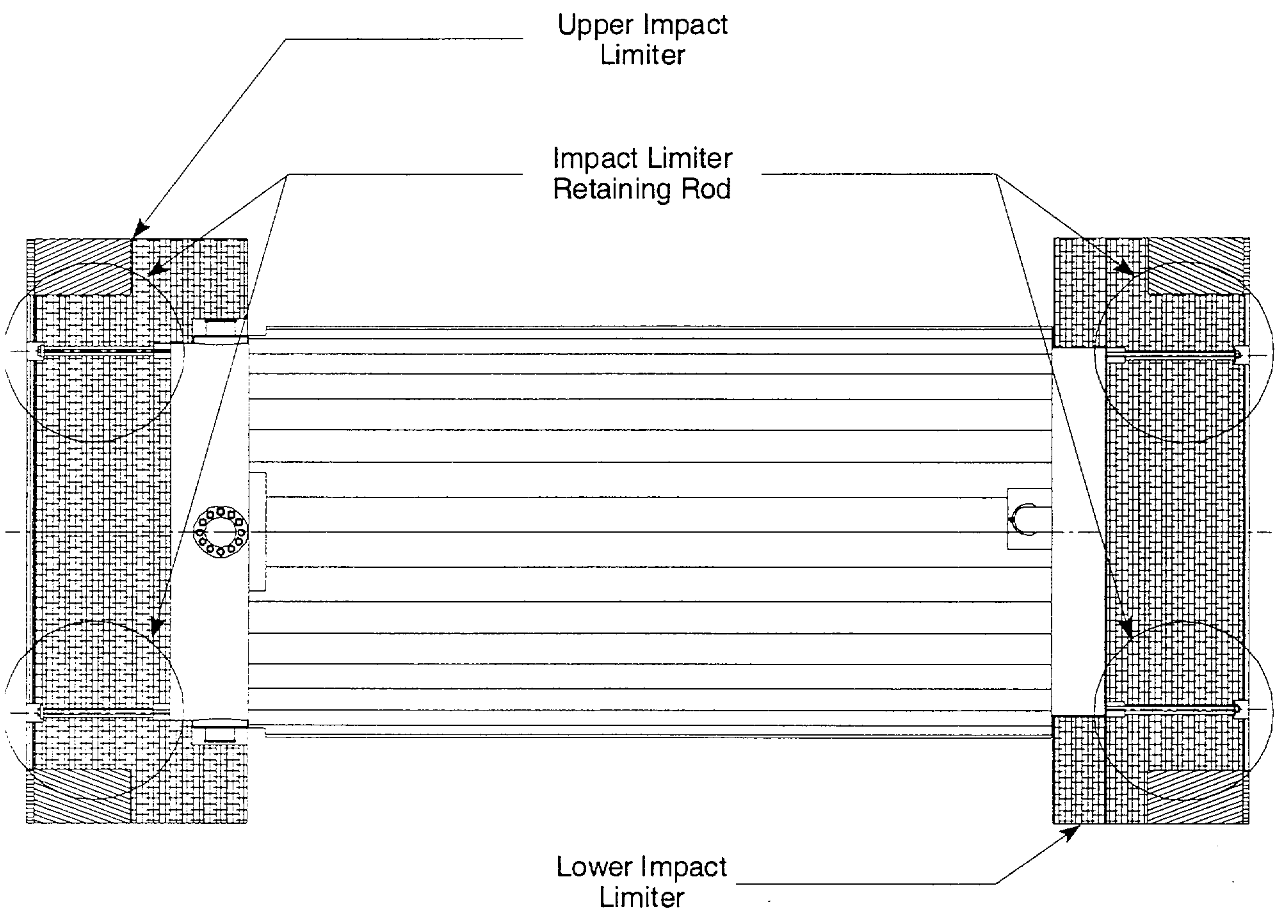

Table 2.6.7.5-1 Redwood Static Stress-Strain Properties

Strain (in/in)	Stress (psi)			
	Hot (Parallel to Grain)	Cold (Parallel to Grain)	Hot (Perpendicular to Grain)	Cold (Perpendicular to Grain)
0.000	0	0	0	0
0.100	3736	9294	542	1396
0.400	3685	8531	849	2054
0.700	10004	22085	7433	17631

Table 2.6.7.5-2 Balsa Static Stress-Strain Properties

Strain (in/in)	Stress (psi)			
	Hot (Parallel to Grain)	Cold (Parallel to Grain)	Hot (Perpendicular to Grain)	Cold (Perpendicular to Grain)
0.000	0	0	0	0
0.020	1850	2475	130	173
0.130	1676	2242	117	157
0.400	1550	2073	109	145
0.750	1550	2073	109	145
1.000	10000	13376	700	936

Table 2.6.7.5-3 Redwood Stress-Strain Properties (25 ε/sec)

Strain (in/in)	Stress (psi)			
	Hot (Parallel to Grain)	**Cold (Parallel to Grain)**	**Hot (Perpendicular to Grain)**	**Cold (Perpendicular to Grain)**
0.000	0	0	0	0
0.100	5859	8506	968	1629
0.400	4996	10734	1363	2608
0.700	15458	19683	13553	19017

Table 2.6.7.5-4 Balsa Stress-Strain Properties (25 ε/sec)

Hot (Parallel to Grain)		**Cold (Parallel to Grain)**		**Hot (Perpendicular to Grain)**		**Cold (Perpendicular to Grain)**	
Strain (in/in)	**Stress (psi)**	**Strain (in/in)**	**Stress (psi)**	**Strain (in/in)**	**Stress (psi)**	**Strain (in/in)**	**Stress (psi)**
0.000	0	0.000	0	0.000	0	0.000	0
0.067	1398	0.224	2350	0.069	101	0.069	207
0.606	900	0.625	2116	0.630	270	0.630	550

Table 2.6.7.5-5 Properties for the Impact Limiter Stainless Steel Shells

Property	**Value**
Mass Density, ρ	7.51E-04 lb-sec^2/in^4
Modulus of Elasticity, E	27.9E6 psi
Poisson's Ratio, ν	0.30

Stress-Strain Curve for Type 304 Stainless Steel

STRESS (psi)	**STRAIN (in/in)**
23,809	0.000041
28,033	0.001180
29,500	0.003180
31,970	0.007180
36,900	0.015100
42,300	0.039200
85,080	0.230000

Table 2.6.7.5-6 Summary of Peak Accelerations and Maximum Crush Depths

Drop Orientation and Conditions		Peak Acceleration (g)		Design Basis Acceleration (g)	Maximum Crush (in)	
		Top Limiter	Bottom Limiter		Top Limiter	Bottom Limiter
1-Foot	Side Drop-Cold	17.0	12.7	20	1.6	2.2
	Top End Drop-Cold	12.4	—	20	2.0	—
	Bottom End Drop Hot	—	9.6	20	—	2.0
	Corner Drop (24°) Cold	4.5	4.5	20	5.1	5.1
	Corner Drop (24°) Hot	3.9	3.9	20	6.1	6.1
30-Foot	Side Drop-Cold	52.0	51.0	60	9.9	10.2
	Side Drop-Hot	49.6	44.2	60	10.2	11.4
	Top End Drop-Cold	57.8	—	60	10.0	—
	Bottom End Drop Hot	—	40.7	60	—	11.0
	Corner Drop (24°) Cold	36.5	36.5	60	18.6	18.6
	Corner Drop (24°) Hot	35.3	35.3	60	20.2	20.2

Table 2.6.7.5-7 NAC-STC Quarter-Scale Model Impact Limiter Analysis Results Comparison to Drop Test Results

NAC-STC[1] Transport Cask Drop Orientation	Quarter-Scale Model Drop Test Accelerometer Filtered Results (g)		LS-DYNA Prediction for Accelerations Filtered Results (g)		Design Basis Accelerations (g)
	Top	Bottom	Top	Bottom	
End Drop	222	N/A	222	N/A	224.4
Side Drop	205	204	211	216	220.0
Corner Drop	117	N/A	130	N/A	220.0

1. NAC Storable Transport Cask (NAC-STC), NRC Docket 71-9235.

Table 2.6.7.5-8 Maximum Accelerations versus the Shallow Angle Drop for the NAC–STC Design

NAC-STC[1] Slap-down Drop Angle	Quarter-Scale Model Drop Test Accelerometer Filtered Results (g)		LS-DYNA Acceleration Prediction Filtered Results (g)	
	Top	**Bottom**	**Top**	**Bottom**
75 degrees	181	180	188	181
85 degrees	N/A	N/A	201	195
90 degrees	205	204	211	216

1. NAC Storable Transport Cask (NAC-STC), NRC Docket 71-9235.

Table 2.6.7.5-9 Maximum Accelerations versus the Coefficient of Friction of the Impact Plane for Slap-Down (85°) Impact for the NAC–STC Design

Coefficient of Friction	LS-DYNA Predication Filtered Results	
	Top Accelerometer	**Bottom Accelerometer**
0.0	210	198
0.2	201	195
0.3	194	194
1.0	180	192

2.6.7.6 Closure Analysis

The Universal Transport Cask closure lid and the bolts are required to satisfy two criteria: (1) calculated maximum stresses must be less than the allowable stress limit (the material yield strength is conservatively selected), and (2) lid deformation or rotation at the O-rings must be less than the elastic rebound of the O-rings. Using consistently conservative assumptions, the NUREG/CR6007 [9] analysis of the cask closure system demonstrates that the cask closure assembly satisfies the performance and structural integrity requirements of 10 CFR 71.71(c)(7) for normal conditions of transport. The NUREG/CR-6007 analysis is summarized in the following paragraphs.

NUREG/CR-6007 provides formulas for calculating bolt forces generated by all regulatory (normal and hypothetical accident) transportation loading. Specifically, the report deals with the bolt stress analysis of a circular, cylindrical cask with a flat, circular, closure lid.

To ensure positive closure, the cask has 48 bolts 2–8 UN–2A socket head cap screws fabricated from SB-637, grade N07718. Material properties are taken at 275°F for the cask lid, closure bolts, and cask wall. A maximum temperature gradient of 3°F through the thickness of the cask lid is used as well. For evaluation purposes, a maximum internal pressure of 80 psi is used.

Accelerations are based on the impact limiter analysis for normal conditions of transport. Therefore, an acceleration of 20 g (1-foot drop) is taken to be the worst case. The 20 g load is also used for the vibration case. A factor of 1.1 is used for the dynamic load. The following calculations are a summary of the NUREG/CR-6007 evaluation based on the calculated preload of 111,680 lb/bolt.

The preload on the cask lid closure bolts considers the following factors: (1) an internal pressure force on the inner lid of 80 psi; (2) the O-ring compression force; and (3) the inertial weight of the lid, canister, basket, and fuel due to the 30-ft accident corner drop conditions. Based on the above considerations, a preload of 111,680 pounds/bolt is conservatively selected for the cask lid closure bolts. A minimum torque value of 3,738 foot-pounds, develops a tensile preload force of 111,680 pounds/bolt based on the following relationship:

$$T = F\left[\frac{L}{2\pi} + \frac{d_m \mu}{2\cos\alpha} + \frac{(d+b)\mu}{4}\right] \quad [46]$$

where:

T = applied torque in inch-pounds
F = preload force in pounds
d = bolt diameter = 2.0 in
b = bolt head diameter = 3.75 in. (at the bottom of the bolt head)
d_m = mean diameter of threads = 1.9188 in
α = one-half the thread angle = 30°
μ = coefficient of friction = 0.15
N = 8 threads per inch
L = 1/N

Therefore, the minimum torque, T, required to develop the preload of 111,680 pounds/bolt is determined as:

$$T = F(0.4017) \div 12$$

$$T = 3{,}738 \text{ foot-pounds}$$

An installation torque of 3,900 ±100 foot-pounds is specified to ensure that the minimum required torque of 3,739 foot-pounds is achieved.

Maximum stresses in the closure bolt result during the top-end corner drop (23.35° from axial plane of cask) assuming the closure bolts support the full weight of the cask lid and contents. This is conservative since during a top-end drop, the cask lid is fully supported by the impact limiter; thus, the closure bolts do not carry any weight. For the following evaluation, only worst case forces and stresses are reported.

The tensile force per bolt, F_{a_pt}, due to preload and thermal is:

$$F_{a\_pt} = P_L + P_{th} = 134{,}877 \text{ pounds}$$

where P_L = 111,680 pounds, preload

P_{th} = 23,197 pounds resulting from thermal expansion

The tensile force per bolt, F_{a_al}, from all other credible loads is:

$$F_{a\_al} = P_o + P_i + P_{20} + P_v = 59{,}573 \text{ pounds}$$

where P_o = 667 pounds, load resulting from O-ring compression and operation

P_i = 6,549 lb, load resulting from internal pressure

P_{20} = 48,662 lb, load due to 20 *g* top-end corner impact.

P_v = 3,695 pounds, load resulting from 20 g vibration.

Since F_{a_pt} is greater than F_{a_al}, the total tensile bolt load, F_a, is equal to F_{a_pt}:

$$F_a = 134{,}877 \text{ pounds}$$

The shear load is

$$F_s = \left| P_i + P_{th} + P_{20} + P_v \right| = 37{,}242 \text{ pounds}$$

where P_i = 15,245 pounds, load resulting from internal pressure

P_{th} = -57,647 pounds, load resulting from temperature difference between the cask lid and upper forging

P_{20} = 1,465 pounds, load resulting from 20 g top-end corner drop

P_v = 3,695 pounds, load resulting from 20 g side vibration load

The bending moment is

M_b = -675 inch-pounds, due to thermal load (other loads do not contribute due to cask lid design);

and the load resulting from torsion is

M_t = 22,440 inch-pounds.

These loads and moments translate into the following stresses:

The tensile stress in the bolt is:

$$\sigma_a = \frac{1.2732\,F_a}{D^2} = 48{,}679 \text{ psi}$$

where D = 1.878 in., minimum bolt diameter. The shear stress is

$$\tau = \frac{1.2732\,F_s}{D^2} = 13{,}441 \text{ psi}$$

Where D = 1.878 in., minimum bolt diameter.

The bending stress is

$$\sigma_b = \frac{10.186\,M_b}{D^3} = 1{,}038 \text{ psi}$$

where D = 1.878 in., minimum bolt diameter.

The stress resulting from torsion is

$$\tau_t = \frac{5.093\,M_t}{D^3} = 17{,}249 \text{ psi}$$

where D = 1.878 in., minimum bolt diameter.

For normal conditions, Table 6.1 of NUREG/CR-6007 requires that the average tensile stress is less than S_m (where $S_m = 2/3\ S_y$), or

$$\sigma_{t(ave)} = \sigma_a = 48{,}679 \text{ psi} \le S_m = 94{,}350 \text{ psi.}$$

Table 6.1 also requires that the average shear, which is comprised of the average direct shear (τ) be less than 0.6 S_m. This is expressed as

$$\sigma_{s(ave)} = \tau = 13{,}441 \text{ psi} < 0.6\ S_m = 56{,}610 \text{ psi.}$$

For the combined state of stress that includes tension plus shear, the square of the computed average tensile stress divided by the allowable tensile stress plus the square of the average shear stress divided by the allowable shear stress must be less than 1. This is expressed as

$$\left(\frac{48{,}679}{94{,}350}\right)^2+\left(\frac{13{,}441}{56{,}610}\right)^2=0.33<1.$$

For the combined state of stress that includes tensile, shear, and bending; the bolts must have a maximum stress intensity less than 1.35 S_m (when the minimum tensile strength is greater than 100,000 psi). Therefore, the maximum stress intensity is

$$\sigma_{total}=\sqrt{\left[\left(\sigma_a+\sigma_b\right)^2+4\left(\tau_t+\tau\right)^2\right]}=78{,}989\text{ psi}<1.35\,S_m=127{,}372\text{ psi.}$$

The margin of safety for ASME SB-637, Grade N07718 closure bolts is 0.61.

2.6.7.6.1 Bolt Fatigue Evaluation

For the 2.00-inch closure bolts the fatigue life of 944 cycles is obtained from ASME Code Section III, Appendix I, Table I-9.1, Figure I-9.4 [17].

The maximum stress, S, on the cask closure bolts is:

$$S=\frac{4.0F}{A}=\frac{4.0(142{,}691)}{2.77}=206{,}053\text{ psi}\ \ (206.053\text{ ksi})$$

where:

$F = F_i + F_{th} = 119{,}494 + 23{,}197 = 142{,}691$ lb

$$F_i=\frac{12T}{\left(\frac{L}{2\pi}+\frac{d_2\mu_1}{2\cos\alpha}+\frac{(d+b)\mu_2}{4}\right)}=119{,}494\text{ lb (maximum preload force)}$$

T = 4,000 ft-lb (maximum initial torque, see Section 2.6.7.6)
F_{th} = 23,197 lb (thermal load, see Section 2.6.7.6)
A = 2.77 in^2, the cross-sectional tensile area of the bolt
4.0 = the stress reduction factor per NB-3232.3(c)

The number of cycles (N) is ([17], Table I-9.1):

$$N = N_i \left(\frac{N_j}{N_i}\right)^{\log\left(\frac{Si}{s}\right) \Big/ \log\left(\frac{Si}{sj}\right)} \text{ or, } N = 500\left(\frac{1000}{500}\right)^{\log\left(\frac{143}{103.03}\right) \Big/ \log\left(\frac{143}{100}\right)} = 944 \text{ cycles}$$

where

the maximum nominal stress (206.053 ksi) < $2.7S_m$ = 254.7 ksi, and the alternating stress (S_{alt}) is: (206.053 – 0)(0.5) = 103.027 ksi

N_i = 500 cycles

N_j = 1000 cycles

S_i = 143 ksi

S_j = 100 ksi

2.6.7.7 Neutron Shield Analysis

The Universal Transport Cask neutron shield is evaluated for two distributed-load conditions: a 1-foot end-drop event and a 1-foot side-drop event. For each of these conditions, the solid neutron shielding material applies a load on the neutron shield shell. The weights of the neutron shield shell and fins are included in the analysis. The neutron shield geometry is shown in Figure 2.6.7.7-1.

2.6.7.7.1 End Plate 1-Foot End-Drop Analysis

The primary loading on the neutron shield shell and end plates is the weight of the NS-4-FR neutron shielding material. The neutron shield is also evaluated for the impact loading of the NS-4-FR during a 1-foot bottom-end-drop event.

$$p = d_B L + d_p t, = 11 \text{ psi}$$

where:

d_B = 0.0607 lb/in^3, the density of NS-4-FR

L = 178.56 in, height of NS-4-FR material

d_p = 0.291 lb/in^3, density of Type 304 stainless steel

t = 0.5 in, plate thickness

The deceleration of the package during a 1-foot end-drop event is 20g. The impact load on the plate is calculated as PI = p(20) = 220 psi.

The material properties (conservatively taken at 300°F) for the Type 304 stainless steel shell, fins and bottom plate are:

S_u = 66,000 psi
S_y = 22,500 psi
$S_s = (0.5)S_y$ = 11,250 psi

Allowable Stresses

The allowable stress intensity for normal condition loading is (Regulatory Guide 7.6):

$$S_{allow} = \text{Axial} + \text{Bending} = 1.5\ S_m = 30{,}000\ \text{psi},$$

Where S_m is equal to 20,000 psi for Type 304 stainless steel.

Calculated Stresses

From Table 26, Case 1 [28]:

$$S_s = \frac{\beta P b^2}{t^2} = 12{,}028\,\text{psi}$$

where:

$P = P_I$ = 220 psi
a = 11.49 inch and b = 4.5 inch
t = 0.5 inch
β= 0.675

The margin of safety is:

$$MS = \frac{30{,}000}{12{,}028} - 1 = +1.49$$

For the reaction in the welds, conservatively assuming all welds are quarter-inch fillets:

$$q_w = \frac{(P)(b)(a)}{(2)(b+a)} = \frac{(220)(4.5)(11.49)}{(2)(4.5+11.49)} = 356\,lb/in$$

The allowable shear/inch is (0.707)(0.25)(Ss), or 1,988 lb/in. Therefore the Margin of Safety is:

$$MS = \frac{1,988}{356} - 1 = 4.58$$

Figure 2.6.7.7-1 Neutron Shield Geometry

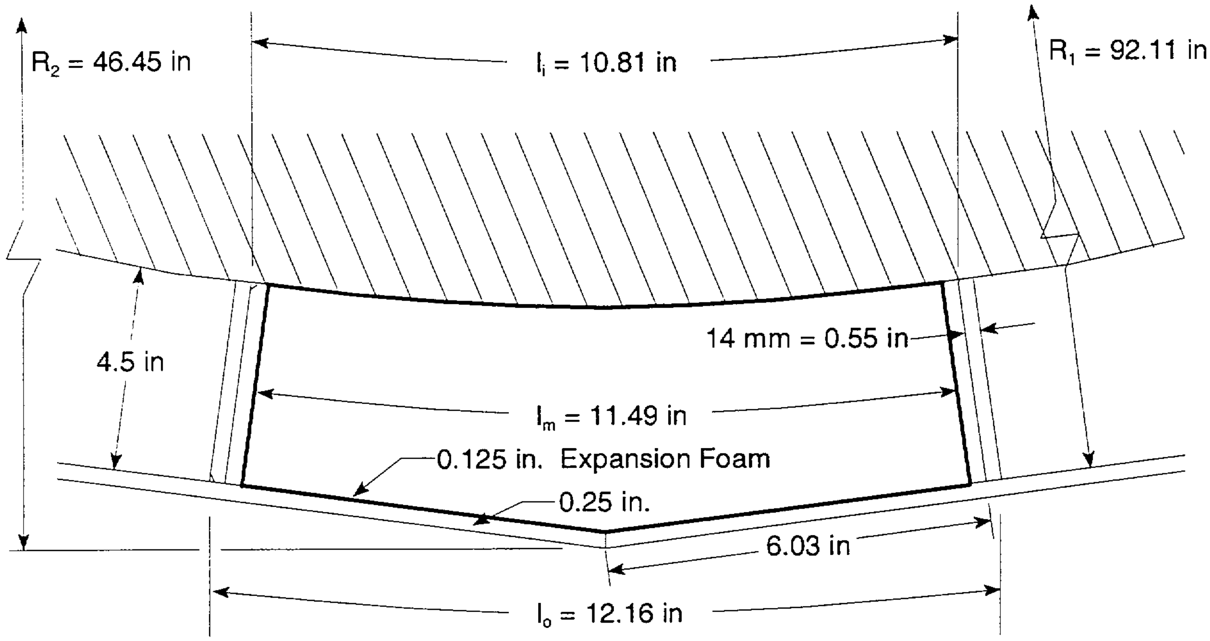

Neutron Shield Bottom Plate Attachment

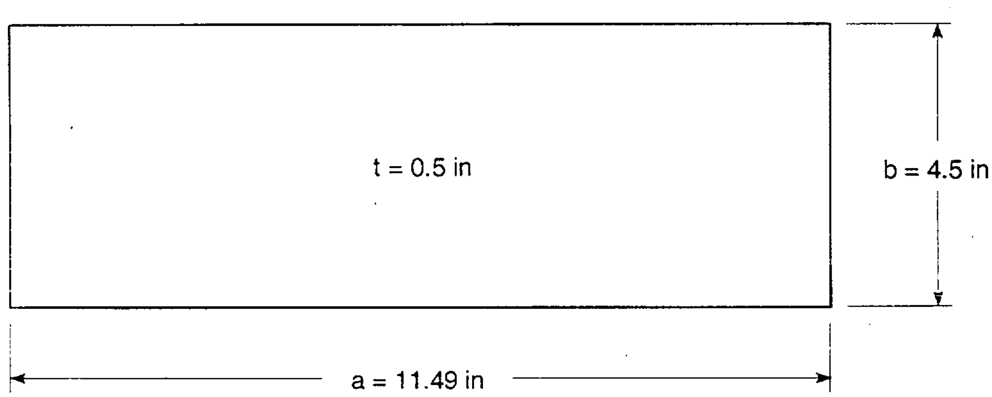

Equivalent Flat Plate Simply Supported

2.6.7.7.2 Side-Drop Analysis

This analysis assumes that the cask is subjected to a 1-foot side-drop event. The side-drop impact force is limited by the upper and lower impact limiters. For this analysis, an impact force equivalent to a 20-*g* side impact is used. The cask is stopped by the impact limiter before the neutron shield contacts the impacted surface. Therefore, the impact force is distributed through the cask body from the impact limiters. The impact deceleration force of the weight of the neutron shielding material is reacted by the neutron shield shell and fins, which transfer the load to the cask body. The NS-4-FR neutron shielding material is assumed to act as an internal pressure on the shell.

Because the structural function of the neutron shield shell and radial heat transfer fins is to support the NS-4-FR radial neutron shield, ASME Code Section III, Subsection NF [19] is used as the governing structural criteria for the evaluation of the welds connecting the radial heat transfer fins to the neutron shield shell and cask outer shell.

In addition to assuming the conservative load combination resulting from cold impact loads and thermal expansion differential between the NS-4-FR and radial fins from hot, steady-state conditions, an additional 3-psi pressure is assumed to have been created from potential gas generation (or formation) from the NS-4-FR subjected to extended service in a high temperature environment.

Following the methodology of the ASME Code, Section III criteria and cask design practice, the load on the weld joints has been categorized into the following service-level conditions:

Service Level B

1. Pressure developed on the neutron shield shell from differential radial thermal expansion of the NS-4-FR neutron shield is relative to the Type 304 stainless steel radial heat transfer fin. The thermal expansion is

$$
\begin{aligned}
T_E &= (\alpha \times L \times \Delta T)_{NS-4-FR} - (\alpha \times L \times \Delta T)_{304SS} \\
&= (4.72 \times 10^{-5})(11.49)(75) - (8.79 \times 10^{-6})(11.49)(75) \\
&= 0.033 \text{ in.}
\end{aligned}
$$

where

$\alpha_{NS\text{-}4\text{-}FR}$ = 4.72×10^{-5} in/in/°F, coefficient of thermal expansion at 158°F

α_{304SS} = 8.79×10^{-6} in/in/°F, coefficient of thermal expansion at 200°F

L = Length of the section

ΔT = 150 - 75 = 75°F, average temperature differential

Considering differential thermal expansion and 3% initial compression of the HT800 expansion foam on the inside surface of the neutron shield shell, a compressive load develops. The total compression is

$$\text{Compression} = 3\%\,(0.125) + 0.033 = 0.037 \text{ in}$$

The equivalent compression of the foam is

$$\%\ \text{Compression} = \frac{0.037}{0.125} \times 100 = 29.6\%\ .$$

Interpolating the manufacturer design information presented in Table 4.2-1, the equivalent pressure load developed on the neutron shield shell is 12.1 psi.

2. Potential pressure developed from extended service of the NS-4-FR neutron shield at high temperatures is defined as 3 psi for this evaluation.

Service Level C

1. Service Level B loads plus dynamic induced load from a postulated one foot side impact (20 *g*).

   Considering the mass of the neutron shield shell and NS-4-FR, the effective pressure load becomes

$$P = MA = (0.346)(20) = 6.9 \text{ psi}$$

where, from the dimensions provided in Fig. 2.6.7.7-1

M= [(4.5)(0.0607) + (0.25)(0.291)] x 1 = .346 lb, the mass of a 1 in^2 unit area,

A= 20 g, the acceleration during a side drop.

Service Level D

1. Service Level B loads plus dynamic induced load from a postulated 30-foot side impact (60 g). Considering the mass of the neutron shield shell and the NS-4-FR, the effective pressure load becomes

$$P = (0.346)(60) = 20.8 \text{ psi.}$$

The following evaluation is presented for two different load orientations of the fin welds. Case 1 represents the loads induced as a result of loading applied to the neutron shield and Case 2 represents loading applied to the radial heat transfer fin.

Case 1—Neutron Shield Shell Loading

Implementing the design criteria for noncontainment support structures presented in NF-3250, normal operation load service level stress in the weld region connecting the neutron shield shell to the radial heat transfer fin is evaluated using a conservative simplification of the plate and shell structure to that of a uniformly loaded beam having unit depth.

The maximum tension stress from Service Level B is:

$$S = \frac{6m}{t^2}\ 17{,}867 \text{ psi}$$

where $m = \frac{wl^2}{12} = 186.1 \text{ in.} - \text{lb}$

$t = 0.25$ in.

and $w = 12.1 + 3 = 15.1$ psi

$l = 12.16$ in.

Allowable stress limits defined in NF-3256.2 and Table NF-3522 (b)-1 for full penetration groove welds define acceptable stress for this condition load as

$$S_{all} = 1.33 \times 1.5 \times 17{,}200 = 34{,}314 \text{ psi}$$

Thus, the margin of safety is

$$MS = \frac{34{,}314}{17{,}867} - 1 = +92.$$

The maximum tension stress for Service Level C load is:

$$S = \frac{6m}{t^2} \; 26{,}024 \text{ psi}$$

where $m = \frac{wl^2}{12} = 271.1 \text{ in.} - \text{lb}$

$t = 0.25$ in.

and $w = 15.3 + 6.9 = 22.0$ psi

$l = 12.16$ in.

Allowable membrane plus bending stress limits defined in NF-3256.2 for Service Level C limits is

$$S_{all} = 1.5 \times 1.5 \times 17{,}200 = 38{,}700 \text{ psi}$$

Thus, the margin of safety is

$$MS = \frac{38{,}700}{26{,}024} - 1 = +0.49.$$

The maximum tension stress for Service Level D load is

$$S = \frac{6m}{t^2} = 31{,}850 \text{ psi}$$

As directed by NE-3256.2 for Service Level D, qualification of the structure is based on ASME Code Section III, Appendix F, [17] Paragraph F-1340, "Acceptance Criteria Using Plastic System Analysis."

Considering plastic failure of fixed-end beams with uniformly distributed load, the plastic moment then becomes (from [28] Table 15, Case 2d):

$$m = \frac{wl^2}{16} = 331.8 \text{ in.-lb}$$

where $w = 15.1 + 20.8 = 35.9$ psi

$l = 12.16$ inch

$t = 0.25$ inch

Paragraph F-1340 defines the allowable primary membrane plus primary bending stress intensity as the lesser of 1.5 ($2.4S_m$) and 1.5 ($0.7S_u$). Implementation of this criterion limits Service Level D stress to 68.8 ksi.

$$MS = \frac{68{,}800}{31{,}850.3} - 1 = +1.16 .$$

In addition to the evaluation of the maximum local bending stress in the weld region, shear stress is evaluated as follows:

Service Level	w (psi)	$S_s = \frac{wl}{2t}$ (psi)	Allowable Stress (psi)	MS
B	15.10	367	1.33 (.4S_y) = 12,700	+ Large
C	22.00	535	1.5 (.4S_y) = 14,000	+ Large
D	36.10	878	0.42 (S_u) = 28,900	+ Large

where $l = 12.16$

$t = 0.25$

Case 2—Heat Transfer Fin Loading

Following a similar method as used in the evaluation of the neutron shield shell, the heat transfer fin is evaluated by using a uniformly loaded beam with a fixed end at the cask outer shell surface and a simple support at the neutron shield shell. Because Level B load is developed from radial thermal growth of the NS-4-FR and postulated off gas pressure, Service Level B does not load the fin in the lateral direction. Tension stress developed in the fin from these radial loads is 70 psi, which is insignificant.

Lateral load from Service Level C produces the following stress:

$$S = \frac{6m}{t^2} = 2{,}135 \text{ psi}$$

where $m_{max} = \frac{wl^2}{8} = 35.3$ in.-lb

$w = (0.0607)(11.49)(20) = 13.95$ lb

$$l = \frac{92.11 - 82.61}{2} - 0.25 = 4.5 \text{ in.}$$

$$t = 0.315 \text{ in. (8 mm)}$$

From the preceding evaluation of the neutron shield shell, the service level C allowable is 38,925 psi. Therefore,

$$MS = \frac{38{,}925}{2{,}135} - 1 = \text{Large}.$$

Lateral load for Service Level D produces the following stress:

$$S = \frac{6m}{t^2} = 8{,}540 \text{ psi}$$

where $m_{max} = \frac{wl^2}{6} = 141.23$ in.-lb

$$w = (0.0607)(11.49)(60) = 41.85 \text{ lb}$$

$$l = 4.5 \text{ in.}$$

$$t = 0.315 \text{ in. (8 mm).}$$

Using the acceptance criteria for an elastic system analysis provided in the ASME Code Section III, Appendix F, Paragraph F-1332.2; ($1.5 \times 1.2S_y$ or $1.5 \times 1.55S_m < 1.5 \times .7S_u$).

$$S_{All} = 45{,}000 \text{ psi}$$

$$MS = \frac{45{,}000}{8{,}540} - 1 = 4.27$$

In addition to the evaluation of the maximum local bending stress in the weld region, shear stress is evaluated as follows:

Service Level	w (psi)	$S_s = \frac{wl}{2t}$ (psi)	Allowable Stress (psi)	MS
C	13.95	6,126	14,400	+ Large
D	41.85	377	28,900	+ Large

where $l = 4.5$ in.

$t = 0.25$ in.

Therefore, the heat transfer load path through the welds connecting the neutron shield skin to the radial heat transfer fins is maintained for all transport package normal and accident condition loads.

2.6.7.8 Upper Ring/Outer Shell Intersection Analysis

When the cask is lifted at the lifting trunnions bending stresses are induced in the upper ring and outer shell intersection region of the cask body. These stresses are evaluated by means of a closed-form ring solution (from [29], pp. 390-393). The support provided by the bolted cask lid is conservatively neglected in this analysis.

The geometry and loading of the equivalent ring are defined as follows:

F = lifting force (not including weight of impact limiter)

$$= \frac{260{,}000}{2} = 130{,}000 \text{ lb}$$

q = dead weight load per unit length

W = width of equivalent ring = 3.45 in.

r = mean radius of the equivalent ring = 40.905 in.

a = moment arm for the equivalent ring = 45.63 - 40.905 = 4.725 in.

On the basis of a total weight of 260,000 lb, q is calculated as:

$$q\,(\pi)(40.905)(2) = 260{,}000 \;\Rightarrow\; q = 1{,}011.6 \text{ lb/in.}$$

The moment and torque on the equivalent ring are given by:

$$M = \frac{T_o \sin\theta}{2} - qr^2\left(1 - \frac{\pi}{2}\sin\theta\right)$$

$$T = \frac{T_o \cos\theta}{2} - qr^2\left(\theta + \frac{\pi}{2}\cos\theta - \frac{\pi}{2}\right)$$

where theta, θ, is measured from the trunnion ($\theta = 0$) in plane perpendicular to the centerline of the cask ($0 \le \theta \le 180$).

$$T_o = (F)(a) = (130{,}000)(4.725) = 611{,}997 \text{ in-lb.}$$

Substituting for T_o, q, and r,

$$M = 3.06 \times 10^5 \sin\theta - 1.693 \times 10^6\left(1 - \frac{\pi}{2}\sin\theta\right)$$

$$T = 3.06 \times 10^5 \cos\theta + 1.693 \times 10^6\left(\theta + \frac{\pi}{2}\cos\theta - \frac{\pi}{2}\right).$$

The normal stress is treated as bending resulting from the moment acting over a cross-section.

$$\sigma = \frac{M(h/2)}{I} = 0.00511M$$

where h = 18.44 in

$$I = \frac{Wh^3}{12} = \frac{3.45 \times 18.44^3}{12} 14 = 1802.7 \text{ in}^4$$

The shear stress is (Roark's, 6th Edition, Table 20, Case 4)

$$\tau = \frac{3T}{8ab^2}\left[1 + 0.6095\frac{b}{a} + 0.8865\left(\frac{b}{a}\right)^2 - 1.8023\left(\frac{b}{a}\right)^3 + 0.9100\left(\frac{b}{a}\right)^4\right] = 0.0176T$$

where $a = \frac{h}{2} = \frac{18.44}{2} = 8.22$ in, length of longer side,

$b = \frac{w}{2} = \frac{3.45}{2} = 1.725$ in, length of shorter side.

The maximum stress intensity, where the moment and torque are functions of θ, is calculated as:

$$SI = 2\sqrt{\frac{\sigma^2}{4} + \tau^2} = 2\sqrt{(6.528 \times 10^{-6})M^2 + (3.10 \times 10^{-4})T^2}\ .$$

Resultant values of the stress intensity are evaluated in Table 2.6.7.8-1. The minimum margin of safety is:

$$MS = \frac{30{,}000}{28{,}309} - 1 = +0.06$$

where: $S_m = 20{,}000$ psi

$S_{allow} = 1.5\ S_m = 30{,}000$ psi.

Table 2.6.7.8-1 Resultant Stress Intensity Values in the Equivalent Ring

Angle [1] (degrees)	Moment (in-lb)	Torque (in-lb)	SI (psi)
0.0	$-1.693(10)^6$	$3.060(10)^5$	13,819
5.0	$-1.435(10)^6$	$4.425(10)^5$	17,219
10.0	$-1.178(10)^6$	$5.564(10)^5$	20,498
15.0	$-9.255(10)^5$	$6.482(10)^5$	23,310
20.0	$-6.788(10)^5$	$7.181(10)^5$	25,525
25.0	$-4.398(10)^5$	$7.669(10)^5$	27,098
30.0	$-2.103(10)^5$	$7.952(10)^5$	28,021
35.0	$7.860(10)^3$	$8.039(10)^5$	28,309
40.0	$2.131(10)^5$	$7.942(10)^5$	27,987
45.0	$4.038(10)^5$	$7.671(10)^5$	27,093
50.0	$5.786(10)^5$	$7.242(10)^5$	25,671
55.0	$7.361(10)^5$	$6.667(10)^5$	23,775
60.0	$8.751(10)^5$	$5.962(10)^5$	21,466
65.0	$9.945(10)^5$	$5.145(10)^5$	18,817
70.0	$1.094(10)^6$	$4.232(10)^5$	15,917
75.0	$1.171(10)^6$	$3.243(10)^5$	12,892
80.0	$1.227(10)^6$	$2.194(10)^5$	9,952
85.0	$1.261(10)^6$	$1.107(10)^5$	7,531
90.0	$1.272(10)^6$	0.0000	6,502

[1] The Angle is measured from the centerline of the trunnion.

2.6.8 Corner Drop

The Universal Transport Cask is composed of materials other than fiberboard or wood, and the weight of the package exceeds 220 lb (100 kg). Therefore, according to 10 CFR 71.71(c)(8), this test is not applicable to the Universal Transport Cask.

2.6.9 Compression

According to 10 CFR 71.71(c)(9), this test is not applicable to the Universal Transport Cask because the package weight is greater than 11,000 lb (5,000 kg).

2.6.10 Penetration

According to 10 CFR 71.71(c)(10), a penetration test involving a 13-lb (6-kg) penetration cylinder dropped from a height of 1 m is required for evaluation of packages during normal conditions of transport. However, Regulatory Guide 7.8 states that "the penetration test of 71.71 is not considered by the NRC staff to have structural significance for large shipping casks (except for unprotected valves and rupture disks) and will not be considered as a general requirement." Because the Universal Transport Cask has no unprotected valves or rupture disks that could be affected by normal conditions of transport, a penetration test is not performed.

2.6.11 Fabrication Stresses

The process of manufacturing the Universal Transport Cask can introduce thermal stresses in the inner and outer shells as a result of pouring molten lead between them. These thermal stresses are evaluated in this section to provide assurance that the manufacturing process does not adversely affect the normal operation of the cask or its ability to survive an accident. According to Regulatory Position 7 of Regulatory Guide 7.6, any residual stresses in the containment vessel shell resulting from inelastic strain associated with the secondary local bending stresses, which are due to the lead pour thermal gradient, must be considered in the total stress range for normal and accident load conditions. Residual stresses in the containment vessel and the outer shell induced by shrinkage of the lead shielding after the lead pouring operation are relieved early in the life of the cask because of the low creep strength of lead.

For the lead pour process, the initial temperature of the cask shells is controlled between 550°F and 650°F, and the lead temperature before pouring is between 698°F and 790°F. The cask is initially heated, at a rate not to exceed 90°F/hour, by using heaters inside the inner shell and heating rings around the outside of the outer shell. Heat-up is time-controlled consistent with uniform increases in shell temperatures. The heating procedures ensure that the cask surface temperature does not exceed 800°F during the molten lead pouring process. The shell temperatures are measured by thermocouples attached to the shell surfaces. A portable thermometer is also used to measure temperature at any location. To minimize the time that the cask is at elevated temperatures, cask heating begins only after all preparations have been completed.

The lead is poured after the cask reaches the specified temperatures. Molten lead is poured continuously through a filling tube with its open end maintained under the lead surface. The pouring time is kept as short as possible. During pouring, the interior heaters and exterior heating rings are continuously energized.

The cooling process consists of sequentially turning the exterior heating rings and interior heaters off, starting from the lowest point, and of spraying the cask with water from the outside. A layer of molten lead is maintained until the upper surface starts to solidify. This process allows the molten lead to fill the open space below it created by the lead shrinkage as it cools. The basic requirements and procedures for the Universal Transport Cask lead pour operations are described in Section 8.3.3.

2.6.11.1 Lead Pour

2.6.11.1.1 Cask Shell Geometry

At 70°F, the Type 304 stainless steel shell geometry is:

Inner Shell

Inside Diameter (d_{i-70})	= 67.61 in.
Outside Diameter (d_{o-70})	= 71.61 in.
Shell Thickness (t_i)	= 2 in.

Outer Shell

Inside Diameter (D_{i-70})	= 77.11 in.
Outside Diameter (D_{o-70})	= 82.61 in.
Shell Thickness (T_{o-70})	= 2.75 in.

2.6.11.1.2 Stresses Resulting from Lead Pour

The hydrostatic pressure produced by the column of lead is:

$$q = \rho h = 73.8 \text{ psi}$$

where $\rho = 0.41 \text{ lb/in}^3$ (lead density)

$h = 180$ in (maximum height of lead column)

For this analysis, it is assumed that the lead at a maximum temperature of 790°F, and the shell initially at 650°F, reach an equilibrium temperature of 750°F. At 750°F, key shell geometric dimensions are:

$$d_{o\text{-}750} = d_{o\text{-}70}(1+\alpha\ \Delta T) = 72.09 \text{ in.}$$

$$D_{i\text{-}750} = D_{i\text{-}70}(1+\alpha\ \Delta T) = 77.62 \text{ in.}$$

$$t_{i\text{-}750} = t_{i-70}(1+\alpha\ \Delta T) = 2.01 \text{ in.}$$

where α = 9.76 x 10^{-6} in/in/°F at 750°F (stainless steel)

ΔT = 750 - 70 = 680°F.

The hydrostatic pressure of the molten lead subjects the inner shell to an external hydrostatic pressure, and the outer shell to an internal hydrostatic pressure. The hydrostatic pressure will vary from a maximum of 73.8 psi at the bottom of the inner shell to 0 psi at the top of the lead cylinder.

Using Reference [28] Table 29, Case 6, the deformation at the bottom of the inner shell, y_B, is found to be -1.955×10^{-3} in.

The maximum circumferential membrane stress in the inner shell is:

$$S_{\theta_{max}} = \frac{y_B E}{R} = -1323 \text{ psi}$$

where $E = 24.4 \times 10^6$ psi at 750°F

$R = 72.09/2 = 36.045$ in.

This stress will exist only as long as the lead is molten and will produce no plastic deformation of the inner shell. When the lead solidifies and begins to cool, it will shrink and exert a uniform external pressure on the inner shell because lead's coefficient of expansion is larger than that of stainless steel.

2.6.11.2 Cooldown

2.6.11.2.1 Hoop (Circumferential) Stresses

Lead decreases in volume during solidification. As the lower lead region solidifies, the molten lead above fills the shrinkage void between the solidifying lead and the inner and outer shells.

Using the coefficients of expansion for stainless steel and lead, the outer diameter of the steel shell and the inner diameter of the lead cylinder (assuming it is free to shrink) can be determined at 620°F (the melting point of lead) and at 70°F (normal conditions). Because the lead has a higher coefficient of expansion than stainless steel, a shrinkage force will develop between the steel shell outer surface and the lead inner surface. At 620°F, the outside diameter of the inner shell, and the inside diameter of the lead as it begins to solidify is:

$$d_{oshell620} = d_{oshell70}(1 + \alpha\ \Delta T) = 71.61(1 + 9.56 \times 10^{-6}(620 - 70)) = 71.98 \text{ in.}$$

where $d_{oshell70} = 71.61$ in.

$\alpha_{shell} = 9.56 \times 10^{-6}$ in./in./ °F (at 620°F)

If the lead were cooled without restraint to 70°F, the inner diameter of the lead cylinder would shrink to:

$$d_{ilead\,70} = d_{ilead\,620}(1 - \alpha\ \Delta T) = 71.98(1 - 20.2 \times 10^{-6}(620 - 70)) = 71.18 \text{ in.}$$

where

$d_{ilead620} = d_{oshell620} = 71.98$ in.

$\alpha_{lead} = 20.2 \times 10^{-6}$ in./in./°F

The interference between the lead cylinder and the inner shell is (71.61-71.18)/2 = 0.215 in. To fully accommodate this interference, the lead must be deformed 0.215 in.

For δ = 0.215 in., the maximum circumferential stress, $S_{\theta max}$, in the inner shell is:

$$S_{\theta max} = \frac{\delta\,(E)}{R} = 13.8 \text{ psi}$$

where $R = 71.18/2 = 35.6$ in.

$E = E_{lead70} = 2.28 \times 10^3$ psi

From Reference [28], Table 29, Case 12, the radial deformation of the inner shell under a uniform external radial pressure of 13.8 psi is determined for values of x, the distance from the open end of the inner shell, at 0.15 ft increments and the results are tabulated in Table 2.6.11.2-1. Examination of the data in Table 2.6.11.2-1 shows that the maximum radial deformation and circumferential stress, S_θ, occur at x = 13.65 ft.

The maximum circumferential membrane stress in the inner shell is:

$$S_{\theta_{max}} = \frac{yE}{R} = -255.3 \text{ psi}$$

where y = the radial deformation, -3.299×10^{-4} in.

$E = 28.3\times10^{6}$ psi

$R = 71.61/2 = 35.805$ in.

Axial Stresses

Axial stresses also develop in the lead shell and inner shell during fabrication as a result of the unequal shrinkage of the lead and steel shells. Assuming that the lead bonds to the inner shell during the cooldown process after completion of lead pouring, the strain in the lead, when cooled to 70°F, is:

$$M_{lead} = (\alpha_{lead} - \alpha_{shell})\Delta T = 0.0060 \text{ in/in.}$$

where $\alpha_{lead} = 20.2 \times 10^{-6}$ in/in/°F

$\alpha_{shell} = 9.56 \times 10^{-6}$ in/in/°F

$\Delta T = 620 - 70 = 550$°F

$$S_{lead} = \varepsilon E = 0.006 \times 2.28\times10^{6} = 13{,}680 \text{ psi}$$

The calculated stress is above the yield point of lead (ranging from 20 psi at 620°F to 640 psi at 70°F). The axial load placed on the steel inner shell by shrinkage of the lead is therefore limited by the yield strength of lead. The maximum load is:

$$P_{lead} = 640 \times (38.56^2 - 35.805^2)\pi = 411{,}930 \text{ lb.}$$

The corresponding compression stress in the inner shell to maintain equilibrium is:

$$S_{shell} = \frac{P}{A} = \frac{-411{,}930}{\pi\left((35.805)^2 - (33.805)^2\right)} = -942 \text{ psi}$$

This value is conservative because the yield strength of lead is very low at elevated temperatures (505 psi at 200°F; 380 psi at 300°F), therefore, the creep rate is high. Also, complete bonding of

the lead to the stainless steel inner shell is not expected to occur. Because it is based on the yield strength of lead at 70°F, this case bounds all others to be considered for axial loading.

2.6.11.2.2 Effects of Temperature Differential During Cooldown

The preceding analyses assume that the inner and outer shells and the lead are always at the same temperature at any time during the cooldown process. This assumption may not be true under actual conditions. However, because of the high thermal conductivity of the stainless steel and the lead, and because of the time-controlled cooldown process, the temperature differential between any two of the above shells is kept to a minimum. To determine the effect of temperature differential on the stresses in the shells, a temperature differential of 100°F is used.

If the inner shell is cooler than the lead, the interference between them as well as the corresponding interface pressure and hoop stresses are less than for the case of equal temperatures. Hence, the preceding analysis is conservative.

If the inner shell is hotter than the lead shell, an analysis is required. Assume the temperature of the inner shell to be 170°F and that of the lead to be 70°F. The inner radius of the stress-free lead shell at 70°F is 35.59 in.; the outer radius of the inner shell at 170°F is:

$$r_o = 35.805\,[1 + (8.54 \times 10^{-6})(100)] = 35.836 \text{ in.}$$

The interference between the inner shell and the lead is 35.836 - 35.59 = 0.246 in. To fully accommodate this interference, the lead must undergo a deformation of 0.246 in.

For $\delta = 0.246$ in., $S = \dfrac{\delta(E)}{R} = 15.6$ psi

where $R = 71.18/2$ in. $= 35.59$ in.

$E = 2.28\times10^{3}$ psi (at 70°F)

Using the same method as in the previous section, the radial deformation of the inner shell at x = 13.65 ft., the point of maximum deflection, is found to be -3.293×10^{-4} in.

The maximum circumferential membrane stress in the inner shell is:

$$S_{\theta_{max}} = \frac{yE}{R} = \frac{-3.293\times10^{-4}\left(27.8\times10^{6}\right)}{35.836} = -255.5 \text{ psi}$$

The axial stress in the inner shell also increases when the inner shell is 100°F hotter than the lead shell. As shown previously, the axial load on the inner shell is limited by the yield strength of the lead. Therefore, the previously computed axial load is the bounding case for this analysis.

Temperature differentials between the inner and outer shells are of no consequence, because the axial restraint between them is welded in place after cooldown, when the cask is at a uniform ambient temperature. Welding of the outer shell and the bottom inner forging to the bottom outer forging after cooldown is, therefore, a necessary fabrication step.

2.6.11.3 Lead Creep

As discussed in Section 2.6.11, cooling of the lead shell and inner shell introduces acceptably low hoop and axial stresses in the inner shell. Because lead demonstrates a significant creep rate at both room and elevated temperatures, these small stresses will be relieved early in the life of the cask, and will be further relieved during the thermal test of the cask.

Table 2.6.11.2-1 Stress Analysis Results for Uniform Pressure Loading of Inner Shell Due to Lead Pouring

X (ft)	Hoop stress, σ_2 (psi)	Radial Deflection, y (in.)
0.00	-247.1	-0.00031
0.15	-247.1	-0.00031
0.30	-247.1	-0.00031
0.45	-247.1	-0.00031
0.60	-247.1	-0.00031
0.75	-247.1	-0.00031
0.90	-247.1	-0.00031
1.05	-247.1	-0.00031
1.20	-247.1	-0.00031
1.35	-247.1	-0.00031
1.50	-247.1	-0.00031
1.65	-247.1	-0.00031
1.80	-247.1	-0.00031
1.95	-247.1	-0.00031
2.10	-247.1	-0.00031
2.25	-247.1	-0.00031
2.40	-247.1	-0.00031
2.55	-247.1	-0.00031
2.70	-247.1	-0.00031
2.85	-247.1	-0.00031
3.00	-247.1	-0.00031
3.15	-247.1	-0.00031
3.30	-247.1	-0.00031
3.45	-247.1	-0.00031
3.60	-247.1	-0.00031
3.75	-247.1	-0.00031
3.90	-247.1	-0.00031
4.05	-247.1	-0.00031
4.20	-247.1	-0.00031
4.35	-247.1	-0.00031
4.50	-247.1	-0.00031
4.65	-247.1	-0.00031
4.80	-247.1	-0.00031

Table 2.6.11.2-1 Stress Analysis Results for Uniform Pressure Loading of Inner Shell Due to Lead Pouring (Continued)

X (ft)	Hoop stress, σ_2 (psi)	Radial Deflection, y (in.)
4.95	-247.1	-0.00031
5.10	-247.1	-0.00031
5.25	-247.1	-0.00031
5.40	-247.1	-0.00031
5.55	-247.1	-0.00031
5.70	-247.1	-0.00031
5.85	-247.1	-0.00031
6.00	-247.1	-0.00031
6.15	-247.1	-0.00031
6.30	-247.1	-0.00031
6.45	-247.1	-0.00031
6.60	-247.1	-0.00031
6.75	-247.1	-0.00031
6.90	-247.1	-0.00031
7.05	-247.1	-0.00031
7.20	-247.1	-0.00031
7.35	-247.1	-0.00031
7.50	-247.1	-0.00031
7.65	-247.1	-0.00031
7.80	-247.1	-0.00031
7.95	-247.1	-0.00031
8.10	-247.1	-0.00031
8.25	-247.1	-0.00031
8.40	-247.1	-0.00031
8.55	-247.1	-0.00031
8.70	-247.1	-0.00031
8.85	-247.1	-0.00031
9.00	-247.1	-0.00031
9.15	-247.1	-0.00031
9.30	-247.1	-0.00031
9.45	-247.1	-0.00031
9.60	-247.1	-0.00031
9.75	-247.1	-0.00031

Table 2.6.11.2-1 Stress Analysis Results for Uniform Pressure Loading of Inner Shell Due to Lead Pouring (Continued)

X (ft)	Hoop stress, σ_2 (psi)	Radial Deflection, y (in.)
9.90	-247.1	-0.00031
10.05	-247.1	-0.00031
10.20	-247.1	-0.00031
10.35	-247.1	-0.00031
10.50	-247.1	-0.00031
10.65	-247.1	-0.00031
10.80	-247.1	-0.00031
10.95	-246.9	-0.00031
11.10	-246.9	-0.00031
11.25	-246.9	-0.00031
11.40	-246.9	-0.00031
11.55	-246.9	-0.00031
11.70	-246.7	-0.00031
11.85	-246.7	-0.00031
12.00	-246.7	-0.00031
12.15	-246.7	-0.00031
12.30	-246.9	-0.00031
12.45	-247.1	-0.00031
12.60	-247.6	-0.00031
12.75	-248.2	-0.00031
12.90	-249.1	-0.00032
13.05	-250.4	-0.00032
13.20	-251.7	-0.00032
13.35	-253.2	-0.00032
13.50	-254.5	-0.00032
13.65	-255.3	-0.00032
13.80	-255.1	-0.00032
13.95	-253.2	-0.00032
14.10	-248.6	-0.00031
14.25	-240.7	-0.0003
14.40	-227.9	-0.00029
14.55	-209.9	-0.00027
14.70	-185.9	-0.00024
14.85	-156.5	-0.0002
15.00	-123.5	-0.00016

2.6.12 PWR Transportable Storage Canister Analysis - Normal Conditions of Transport

In this section, the Transportable Storage Canister assembly containing PWR fuel is evaluated for the normal conditions of transport. The principal components of the canister assembly are the canister, the fuel basket assembly, the shield lid, and the structural lid. The canister and the canister shell, bottom plate, and lids are shown in Figures 2.6.12-1 and 2.6.12-2.

Spacers are used to properly locate the canisters containing Class 1 and 2 PWR fuel in the cask cavity. The analysis of the spacers is presented in Section 2.6.16. The geometries and materials of construction of the canister, baskets, and spacers are described in Section 1.2.1.2.

2.6.12.1 Analysis Description

The Transportable Storage Canister contains and confines the spent fuel in the fuel basket. The canister is the defined confinement boundary for its contents during transport and storage operations, but the canister is not considered to provide containment during transport operation; the Universal Transport Cask provides the containment boundary for transport. The canister in the transfer cask serves as the handling component for its basket and contents during loading, closure, and transfer from the pool to storage or to the transport vehicle.

Three canisters of varying lengths are designed to accommodate the three classes of PWR fuel. The design parameters of the canisters are provided in Table 1.2-3. For this analysis, the canister is modeled with the heaviest fuel (Class 2).

The structural design criteria for the canister is from the ASME Code Section III, Subsection NB. Consistent with this criterion, the structural components of the canister are shown to satisfy the allowable stress limits presented in Tables 2.1.2-2 and 2.1.2-3 as applicable. The allowable stresses used in this analysis are based on a temperature of 380°F for all locations in the canister, unless otherwise indicated. These allowables are conservative for all sections in the canister with the exception of Sections 5 and 6 (see Figure 2.6.12.3-1 for section locations).

For the canister structural lid weld (Section 13, Figure 2.6.12.3-1), base metal properties are used to define the allowable stress limits since the weld filler rod tensile properties are greater than the base metal. Also, the allowable stress is multiplied by a stress reduction factor of 0.8 per ISG-4 [49].

Figure 2.6.12-1 PWR Transportable Storage Canister

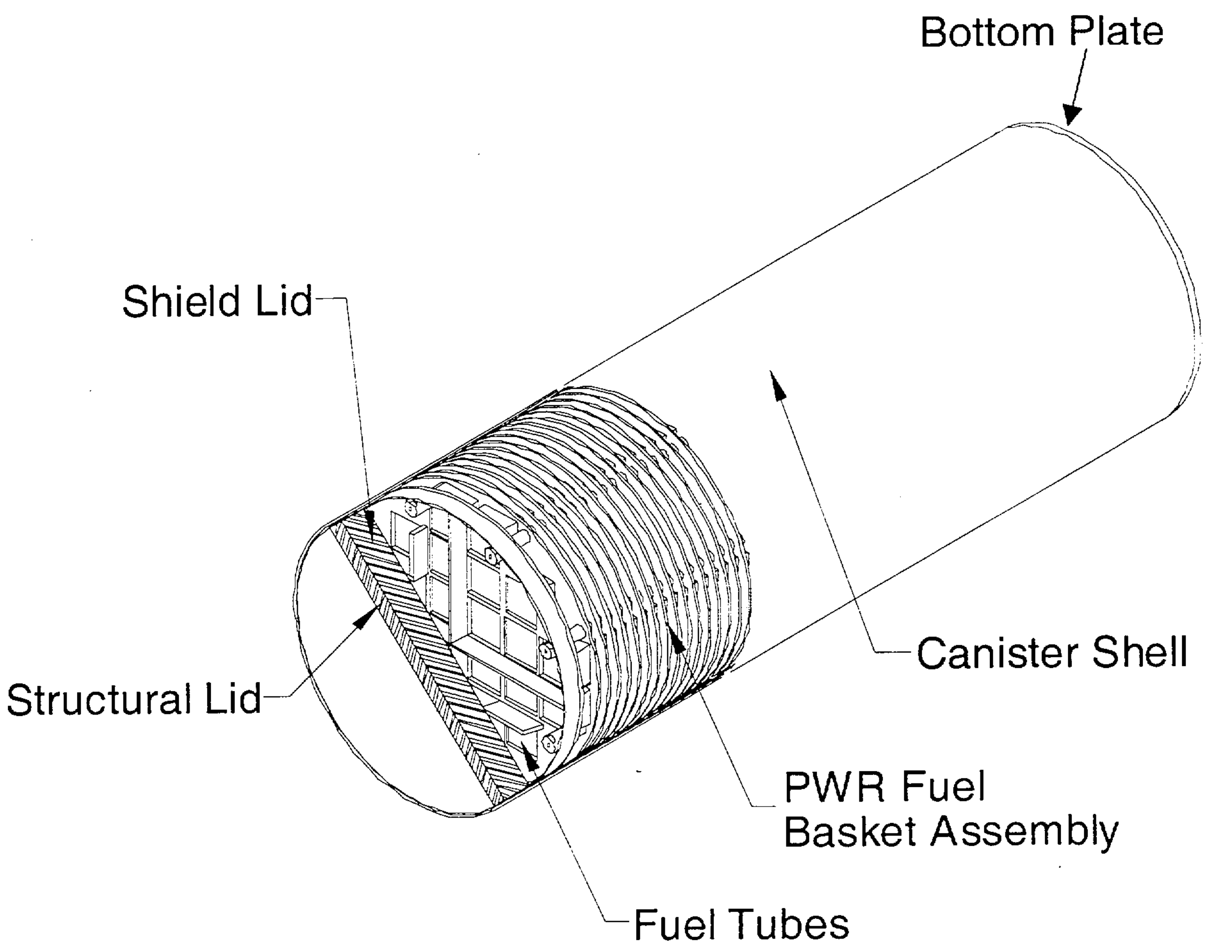

Figure 2.6.12-2 PWR Transportable Storage Canister Shell and Lids

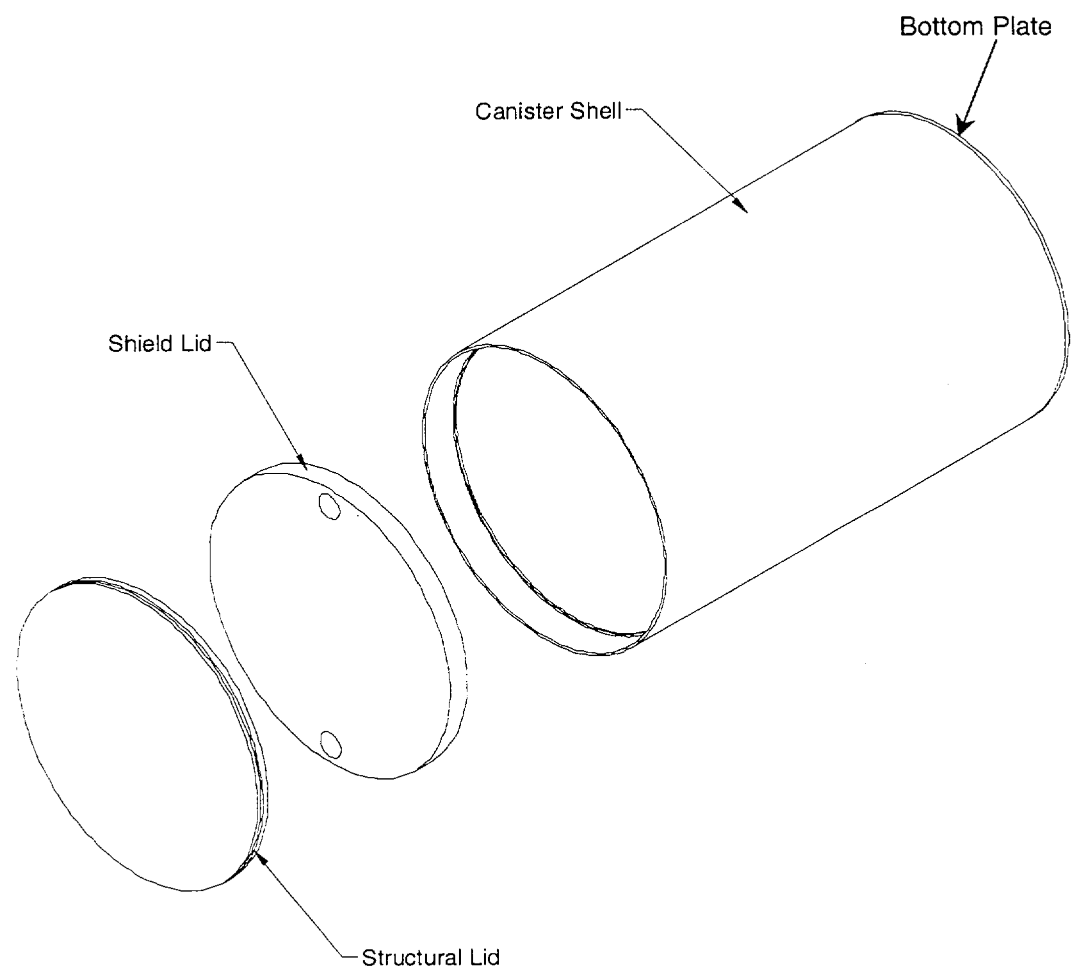

The maximum temperature in the canister shell central region is 408°F as determined in the thermal analysis presented in Section 3.4.2. This increase in temperature reduces the allowable S_m for Type 304L stainless steel from 16.0 ksi to 15.7 ksi. A review of the margins of safety for all cases evaluated indicates that the minimum margin for Sections 5 or 6 is 4.3 for the side-drop with pressure (Table 2.6.12.6-3). Using the allowable stress based on a temperature of 408°F reduces this minimum margin of safety to 4.23. Because this change in margin of safety is small, the increased peak temperature in the center of the canister has a negligible impact on the presented minimum margins.

The canister is analyzed by using the ANSYS [32] finite element computer program for the 1-ft free-drop condition in the top and bottom end, side, and top and bottom corner impact orientations. In addition, the effects of normal operating internal pressure and thermal stresses resulting from exposure of the cask to the hot (100°F ambient and solar insolance) and cold (-40°F ambient) normal conditions are evaluated. The worst-case stresses from these analyses are presented in Section 2.6.12.4.

2.6.12.2 Finite Element Model Description - PWR Canister

To evaluate the PWR Transportable Storage Canister for normal conditions of transport, ANSYS is used to construct and analyze a finite element model of the canister and its contents. The contents modeled consist of the fuel basket support disks and weldments. The fuel assemblies, fuel tubes, aluminum heat transfer disks, tie-rods, and related hardware are not explicitly modeled but rather are accounted for by applying pressure loads to the support disk slots as appropriate.

The finite element model of the canister is constructed by using ANSYS solid (SOLID45) elements. The model represents a one-half (180°) section of the canister and fuel basket. The basket support disks are modeled with three-dimensional shell (SHELL63) elements. The model uses gap-spring elements to simulate contact between adjacent components. Interaction between the basket and canister is accomplished by using three-dimensional gap elements (CONTAC52) along the periphery of the support disks. Contact between the canister and the cask inner shell is also modeled by using CONTAC52 gap elements. Contact between the canister structural lid and shield lid is modeled by using COMBIN40 combination elements in the axial degree of freedom. Simulation of the spacer ring is accomplished by using a ring of COMBIN40 spring

gap elements connecting the shield lid and the canister in the axial direction at the lid lower outside radius. In addition, CONTAC52 elements are used to model interaction between the structural lid and canister shell and the shield lid and canister shell just below the respective lid weld joints. The size of the CONTAC52 gaps are determined from the nominal dimensions of contacting components. The COMBIN40 elements used between the structural and shield lids and for the spacer ring are assigned small gap sizes of $1(10)^{-8}$ in. All gap-spring elements are assigned a stiffness of $1(10^{8})$ lb/in. Table 2.6.12.2-1 lists the element types assigned to specific gaps of the model. Table 2.6.12.2-2 lists the material properties used for the model.

Boundary conditions are applied to enforce symmetry at the cut boundary of the model. All nodes on the cask shell side of the canister-to-cask gap elements are fixed in all degrees of freedom. In addition, the axial and in-plane rotational degrees of freedom of the basket nodes are fixed.

Figure 2.6.12.2-1 is a plot of the entire canister finite element model including the support disks. An isolated view of the canister shield and structural lids portion of the model is presented in Figure 2.6.12.2-2, and an enlarged view of the model in the structural lid and shield lid weld regions is shown in Figure 2.6.12.2-3. The canister bottom plate portion of the model is shown in Figure 2.6.12.2-4.

The loading for the normal operating condition is based on 1-ft drops in conjunction with the internal pressure loading (to the canister). Drop orientations considered are the top and bottom end, side, and top and bottom corner-drops. In the end-drop orientation, the fuel contents load is transferred to the canister end and directly to the transport cask end through the cavity spacer. This corresponds to a compressive stress in the canister ends that is present in the finite element model. The canister shell is designed to be flush with the top surface of the structural lid with the worse case tolerance stack-up. This ensures that the content weight will be transferred through the lids to the transport cask during a top end or top corner drop condition. For the side-drop condition, the loads from the canister contents weight are transferred through the support disks into the canister wall, which is backed by the cask inner shell. Because the canister wall and the inner shell have different radii, a gap exists between the two surfaces. This gap results in the load passing only through regions in which the canister shell deflects to contact the inner shell. This load pattern is reflected in the side-drop analysis. For the corner-drop orientation, both the end-and side-load reactions with the cask inner shell are present.

The modeled contents weight includes 37,080 lb for all fuel assemblies (24 Class 1 PWR fuel assemblies), the fuel tube weight (3,417 lb), the aluminum heat transfer disk weight (1,946 lb), the disk spacer weight (1,879 lb), and the tie rod and nut and washer weights (783 + 94 lb). The weight of the support disks and weldments is accounted for by their being physically modeled. The PWR Class 1 configuration results in the largest load per support disk. The modeled canister length is 173.75 inches.

For the side and corner-drops, the weights of the fuel assemblies (W_{fuel}), aluminum heat transfer disks ($W_{ht\ disks}$), fuel tubes (W_{tubes}), tie rods (W_{rods}), nuts/washers (W_{nuts}), and spacers ($W_{spacers}$) are included in the model by applying a pressure load (F_{slot}) to the slot openings of the modeled support/weldment disks. This pressure load is calculated according to the following equation:

$$F_{slot} = \frac{W_{fuel} + W_{ht\ disks} + W_{tubes} + W_{rods} + W_{nuts} + W_{spacers}}{N_{slots} \times w_{slot} \times N_{disks}} \times g$$

where:

N_{slots} = number of slot openings in each support/weldment disk,
w_{slot} = width of each slot opening in each support/weldment disk,
N_{disks} = number of support/weldment disks, and
g = the associated g-loading for the drop height of interest.

For basket orientations other than 0°, the components of this resulting pressure load are applied to two faces of the slot opening. Additionally, for the corner-drops, the component resulting from accounting for the drop angle is used as the pressure load on the disk slot openings. For the PWR canister drop analyses, with 24 slot openings, a slot opening width of 9.272 inches, and a total of 34 support/weldment disks (32 support disks and 2 weldment disks), the resulting base pressure load used is:

$$F_{slot} = \frac{37{,}080 + 1{,}946 + 3{,}417 + 783 + 94 + 1{,}879}{24 \times 9.272 \times 34} \times g = 5.974 \times g$$

For the end drops, a uniform pressure representing the total weight of the fuel and fuel basket (52,369 lb) is applied to the canister shield lid (for top end-drop) or canister bottom plate (for

bottom end-drop). For the corner-drops, the component of this uniform pressure resulting from accounting for the drop angle is applied to the appropriate elements.

Changes were made to the fuel and fuel basket weight calculations after the finite element analyses were performed. These changes resulted in a total fuel and fuel basket weight of 52,565 lb. The total weight of the fuel and fuel basket analyzed in the PWR canister models is 52,369 lb. The revised calculations result in an increase in fuel and fuel basket weight of less than 1%; therefore, the modeled configuration will provide adequate stress results. Additionally, the length of the PWR Class 1 canister length was increased from 173.75 in. to 175.05 in. This is an increase of less than 1% and would also not sufficiently affect the results presented from these analyses.

The operational conditions also contain loads developed from the temperature distribution in the canister. These are included in the canister model analyses. The thermal analyses are described in Section 3.4.

The canister is analyzed for basket orientations of 0° and 45°. The angles describe the orientation of the basket elements with respect to the symmetry plane of the model. A value of 0° orients the ligaments in the basket elements parallel and perpendicular to the symmetry plane; a value of 45° orients the basket ligaments at +/- 45° from the symmetry plane. To accurately predict the canister response to impact, both orientations are run for the side, top-over-center-of-gravity, and bottom-over-center-of-gravity drop orientations. Top-end and bottom-end drops with varying basket orientations are not required since the basket disks are not included in these runs (their presence is accounted for by using applied pressure loads to the inner surface of the top or bottom).

Figure 2.6.12.2-1 PWR Canister Assembly Finite Element Model

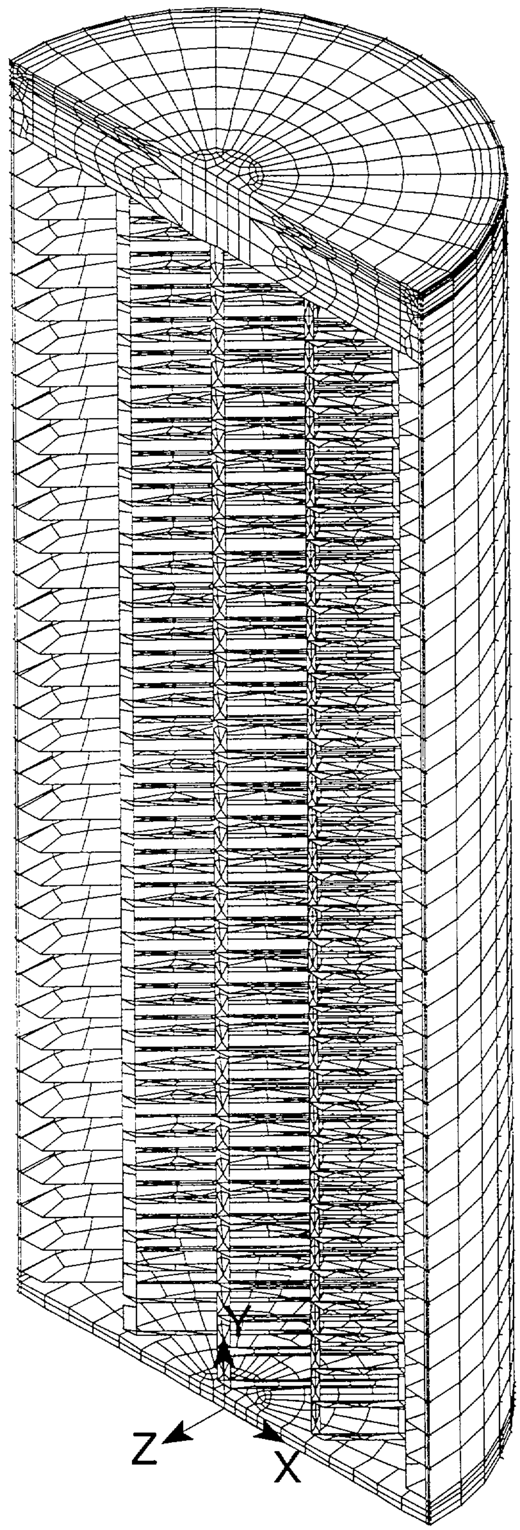

Figure 2.6.12.2-2 Canister Structural and Shield Lid Finite Element Mesh

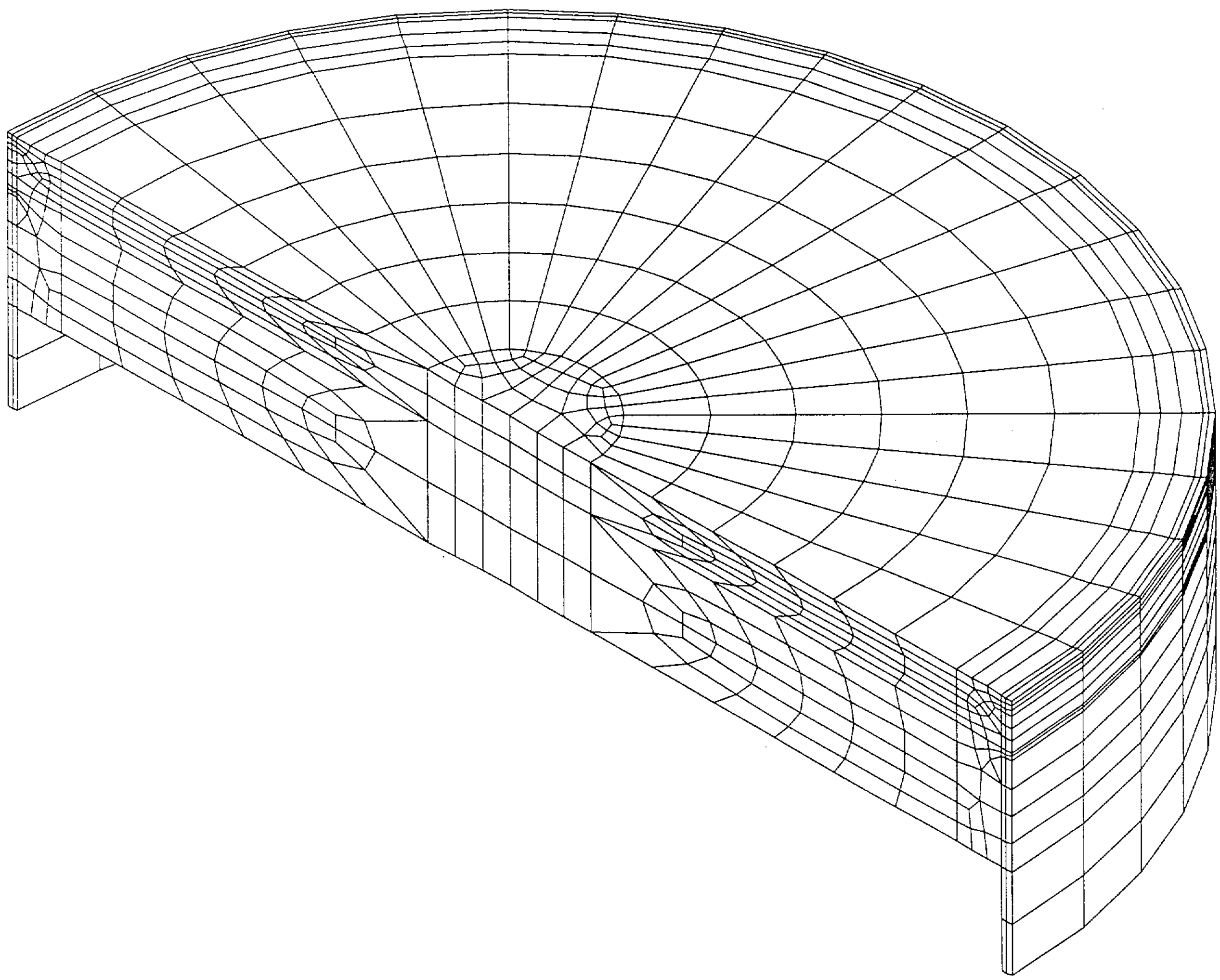

Figure 2.6.12.2-3 Structural and Shield Lid Weld Regions Finite Element Mesh

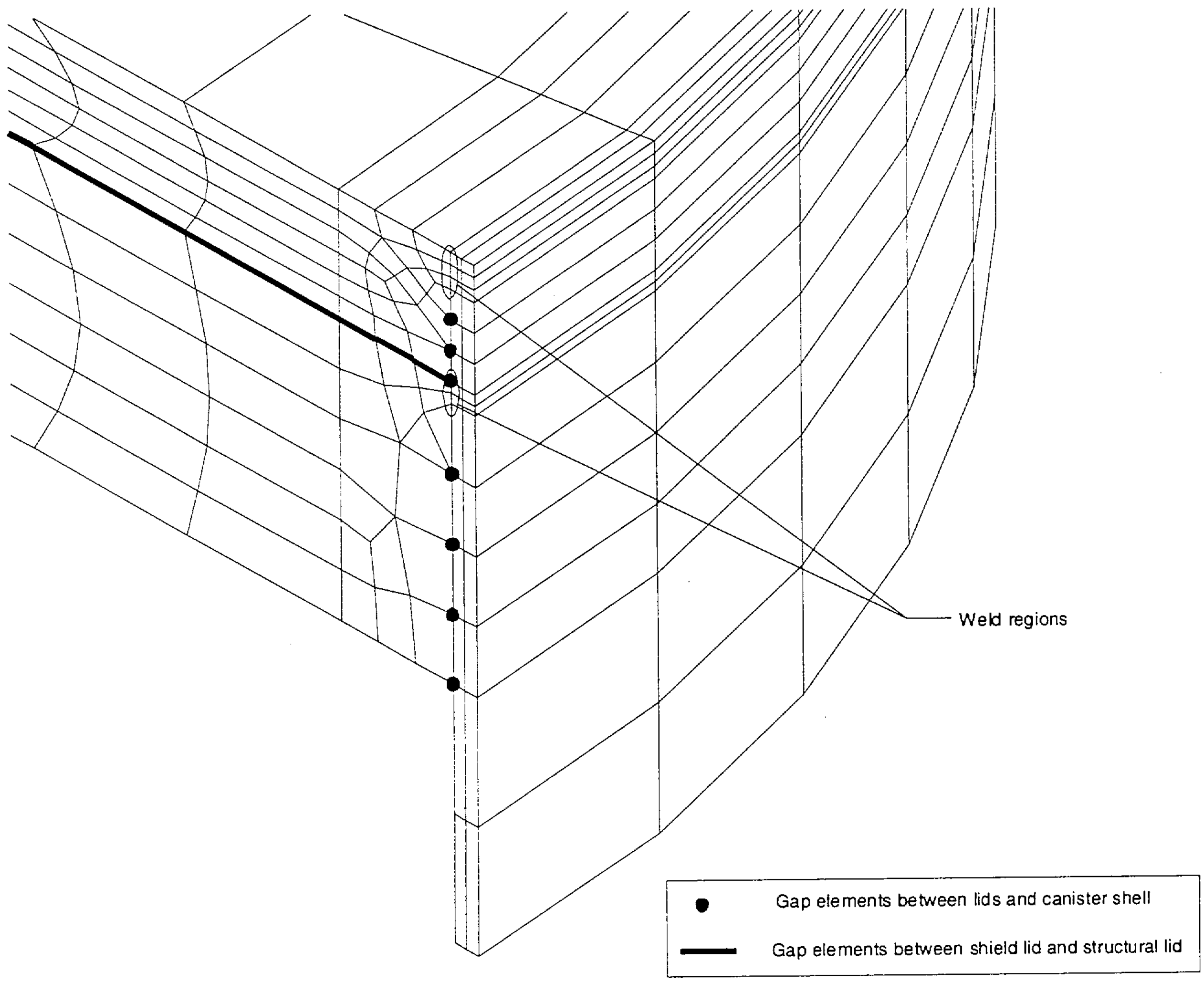

Figure 2.6.12.2-4 Canister Bottom Plate Finite Element Mesh

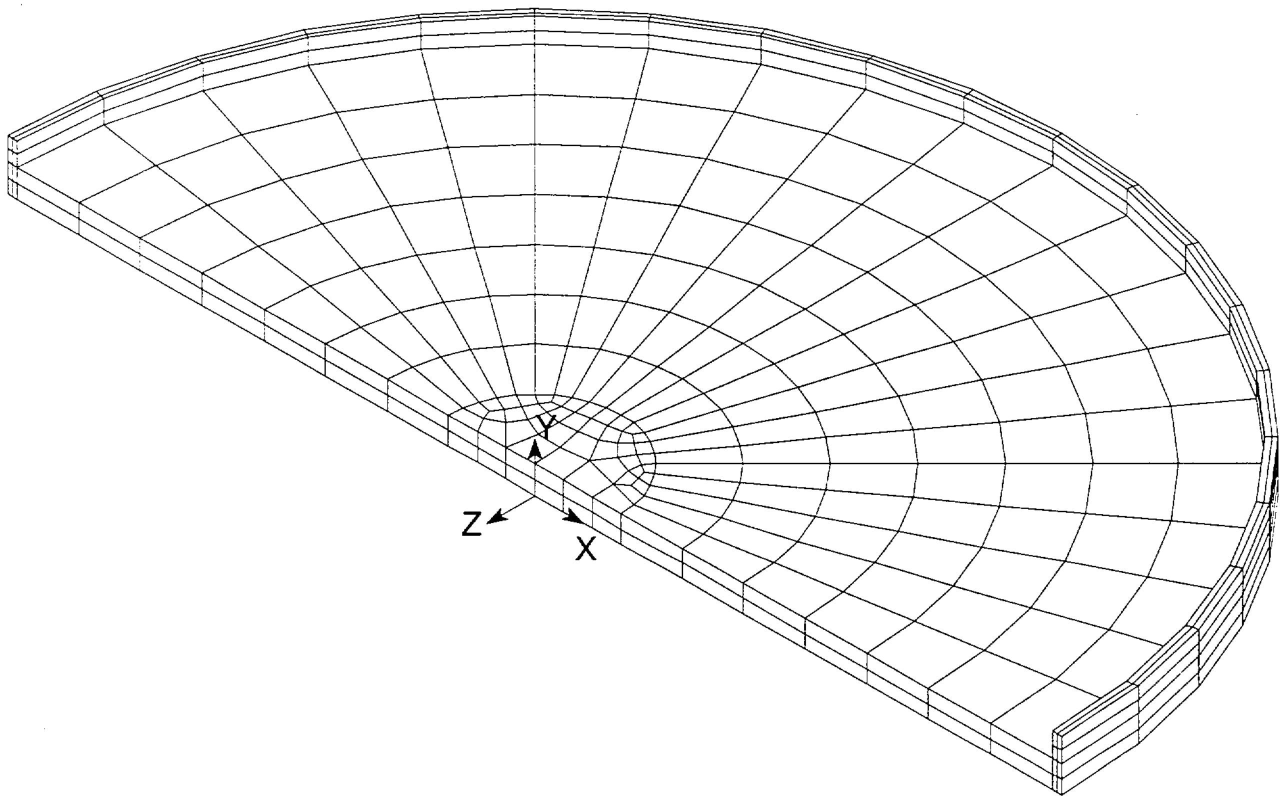

Table 2.6.12.2-1 Gap and Element Type Definition - Canister Model

Component
Axial Gaps from Canister Bottom Plate to Cask Shell (CONTAC52)
Radial Gaps from Canister Side to Cask Shell (CONTAC52)
Axial Gaps from Structural Lid Top to Cask Shell (CONTAC52)
Axial Gaps Between Structural and Shield Lid (COMBIN40)
Radial Gaps Between Shield Lid and Canister Inner Surface (CONTAC40)
Radial Gaps Between Shield Lid and Canister Inner Radius (CONTAC52)
Axial Gaps Between Shield Lid and Canister Wall to Simulate Spacer Ring (COMBIN40)
Radial Gaps Between Basket and Canister Inner Surface (CONTAC52)

Table 2.6.12.2-2 Material Definition - Canister Model

Component	Material
Canister Shell and Structural Lid	304L Stainless Steel; ASME SA240
Top and Bottom Weldments	304 Stainless Steel; ASME SA240
Shield Lid	304 Stainless Steel; ASME SA240
Support disk	17-4 PH, ASME SA693 Type 630 Stainless Steel

2.6.12.3 Thermal Expansion and Thermal Stresses Evaluation of Canister for PWR Fuel

A thermal stress evaluation performed by using ANSYS determines the differential thermal expansion and the associated thermal stresses that result from a heat load of 20 kW. In assessing the thermal stresses, the following three extreme conditions are possible:

Condition	Ambient Temperature	Solar Insolance Applied to Cask Surface	20 kW Fuel Load
1	100°F	Yes	Yes
2	-40°F	No	Yes
3	-40°F	No	No

The temperatures employed in the thermal stress analysis are obtained by applying temperatures at 36 key locations on the canister shell and ends as thermal boundary conditions to the thermal equivalent model of the structural canister model. These temperatures are taken from the thermal evaluation described in Section 3.4. The structural finite element model described in Section 2.6.12.2 is used in this analysis. The equivalent thermal model is obtained by changing the structural element (SOLID45, which has three global displacements for degrees of freedom) to a SOLID70, which has temperature degrees of freedom at the individual nodes. The temperature-dependent thermal conductivity for the canister material is employed in the thermal conduction analysis. The temperatures generated in this analysis are used in the thermal stress analysis to evaluate the properties at temperature, as well as the stresses resulting from thermal expansion. Using this method, two separate cases: (Conditions 1 and 2) are evaluated: a hot case (100°F ambient with solar heat load and maximum decay heat) and a cold case (-40°F ambient and maximum decay heat). Condition 3 is not evaluated because the entire assembly would be at -40°F for the conditions described.

According to the ASME Code, Section III, Subsection NB, the allowable stress criteria are based on the evaluation of linearized stresses across critical cross sections through the canister wall. For the evaluation of the thermal stresses, the criteria for the stresses is based on peak stresses. The stress values taken from the analyses are the nodal stresses at the surface. The sections used in this evaluation are shown in Figure 2.6.12.3-1. Sections are evaluated every 9° around the circumference for each of the locations shown. The thermal stresses reported in Tables

2.6.12.3-1 and 2.6.12.3-2 correspond to the maximum stresses for any circumferential section, for each of the locations shown in Figure 2.6.12.3-1.

For Condition 1 or 2, the canister is hotter than the cask body and will undergo more thermal expansion than the cask body. To conservatively determine the minimum gap between the canister and the cask body resulting from thermal expansion, only expansion of the canister is considered. The canister is considered to be at 408°F (maximum shell temperature for thermal heat condition) and the cask inner shell temperature is assumed to be 70°F. Using the outer diameter of the canister of 67.06 in. and the coefficient of expansion for Type 304L stainless steel of 9.19 $(10)^{-6}$ at 400°F, the canister inner shell gap is reduced by (9.19 $(10)^{-6}$)(67.06 in.)(329°F) = 0.203 in. Because the nominal diametrical canister-inner shell gap is 67.61-67.06 = 0.55 in., the canister shell does not bind with the inner shell as a result of thermal expansion.

The maximum canister shell temperature is 408°F. This temperature is conservative to use for the axial expansion since a temperature gradient exists along the length of the canisters (i.e., the canister is cooler on the ends). The thermal expansion coefficient of Type 304L stainless steel at 400°F is 9.19 $(10)^{-6}$ in/in-°F. The longest canister configuration is PWR Class 3 with a length of 191.95 in. The increase in length of the canister is then

$$l = l_0 \, \alpha \, \Delta T$$

$$\Delta l = 191.95 \, (9.19 \, (10)^{-6} \text{ in/in-°F}) \, (399 - 70) = 0.58 \text{ in.}$$

The canister length increases to 191.95 + 0.58 = 192.53 in.

The minimum cask shell temperature is conservatively assumed to be 150°F (the peak inner shell temperature is 367.7°F; the upper forging minimum temperature is 237.5°F). The thermal expansion coefficient of Type 304 stainless steel at 70°F is conservatively used since the expansion coefficient increases with temperature 8.46 $(10)^{-6}$ in/in-°F. The cask cavity nominal length is 192.5 in. The increase in length of the cask cavity is then

$$\Delta l = 192.5 \, (8.46 \, (10)^{-6} \text{ in/in-°F}) \, (150 - 70) = 0.13 \text{ in.}$$

The cask cavity length increases to 192.5 + 0.13 = 192.63 in. The resulting axial gap is 192.63 - 192.53 = 0.1 inch. Therefore, the canister and cask will expand axially and not bind during normal transport conditions.

Figure 2.6.12.3-1 Identification of Sections for Evaluating Linearized Stresses in Canister

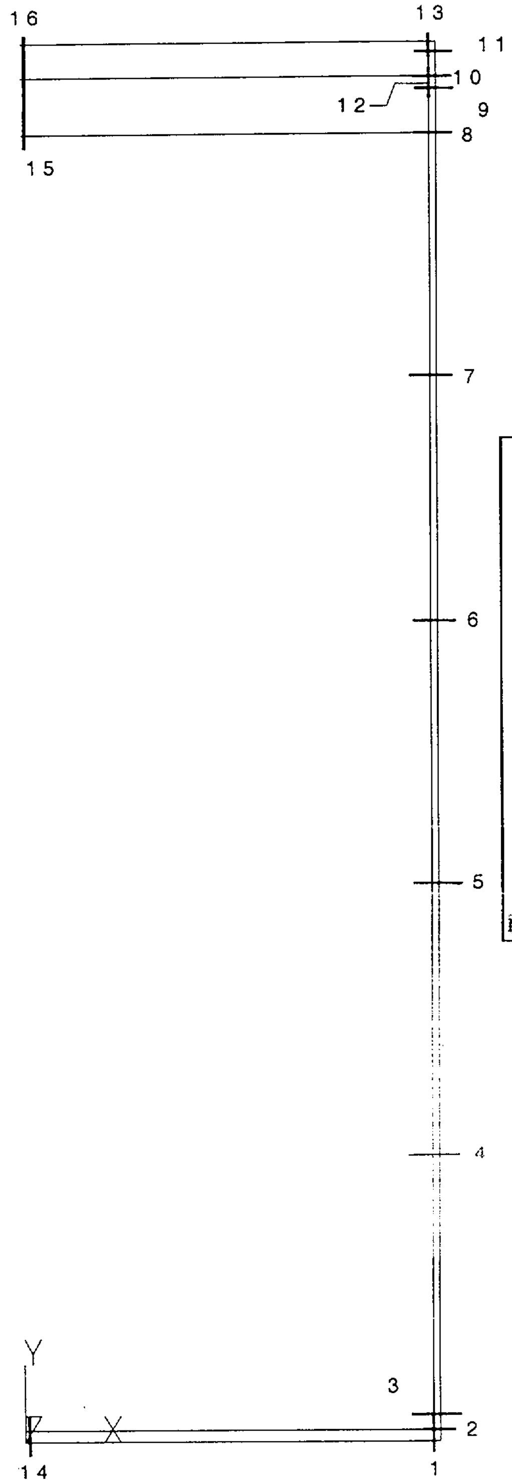

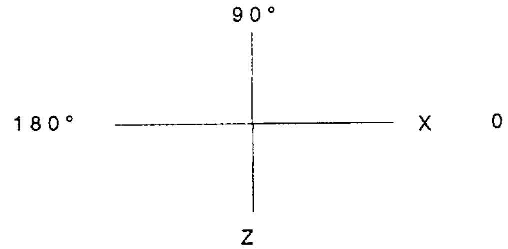

Top View of Axis

Section Coordinates at Z = 0

Axial Section	Node 1 x	Node 1 y	Node 2 x	Node 2 y
1	32.905	0.0	32.905	1.75
2	32.905	1.75	33.53	1.75
3	32.905	2.25	33.53	2.25
4	32.905	34.15	33.53	34.15
5	32.905	66.55	33.53	66.55
6	32.905	98.95	33.53	98.95
7	32.905	131.35	33.53	131.35
8	32.905	163.75	33.53	163.75
9	32.905	170.25	33.53	170.25
10	32.905	170.75	33.53	170.75
11	32.905	172.87	33.53	172.87
12	32.905	170.25	32.905	170.75
13	32.905	172.87	32.905	173.75
14	0.1	0.0	0.1	1.75
15	0.1	163.75	0.1	170.73
16	0.1	170.75	0.1	173.75

Note: Dimensions in inches.

Table 2.6.12.3-1 PWR Canister Linearized Q Stresses - Thermal Only (Hot 1)

Section Location	Angle of Peak Stress Location	Q Stresses (ksi)						SI (ksi)		
		Sx	Sy	Sz	Sxy	Syz	Sxz			
1	180	0.2	0.1	2.1	-0.1	0	-0.1	2.2		
2	9	-0.3	-1.2	0.7	-0.1	0	0.2	1.9		
3	9	-0.1	-1.1	0.9	-0.1	0	0.2	1.9		
4	0	0	-0.2	0.1	0	0	0	0.3		
5	0	0	-0.8	0.7	0	-0.2	0	1.5		
6	0	0	-0.6	0.3	0	0.1	0	0.9		
7	0	0	-0.6	0.1	0	0	0	0.6		
8	90	1	1.6	0	0	0	0	1.6		
9	162	0.1	-1.6	-0.5	-0.1	0	0.2	1.7		
10	90	0.3	1.7	-0.2	-0.2	0	0	1.9		
11	81	-0.5	-1.4	0.2	-0.1	-0.1	-0.1	1.6		
12	162	-0.3	0.6	-0.1	-0.1	0.1	-0.2	1.1		
13	81	-0.4	0.1	-0.7	0	-0.1	0	0.8		
14	0	-8.1	-1.4	-7.9	0.8	0.8	0.5	7.3		
15	180	0.4	0	-0.1	-0.8	0	1.7	3.8		
16	180	-0.2	0	0.1	-0.7	0	-1.2	2.7		

Table 2.6.12.3-2 Linearized Stresses - Thermal Only (Cold 2)

Section Location	Angle of peak stress location	Q Stresses (ksi)						SI (ksi)		
		Sx	Sy	Sz	Sxy	Syz	Sxz			
1	180	0.2	0.1	2.4	-0.1	0	-0.2	2.4		
2	9	-0.3	-1.2	0.9	-0.1	0	0.2	2.1		
3	9	-0.1	-1.1	1	-0.1	0	0.2	2.1		
4	0	0	-0.3	0.1	0	0	0	0.4		
5	0	0	-0.9	0.8	0	-0.2	0	1.7		
6	0	0	-0.7	0.4	0	0.1	0	1.1		
7	0	0	-0.7	0.1	0	0	0	0.8		
8	90	1.1	1.8	0	0	0	0	1.8		
9	162	0.1	-1.6	-0.5	-0.1	0	0.2	1.7		
10	90	0.4	2	-0.2	-0.2	0	0	2.2		
11	81	-0.6	-1.5	0.2	-0.1	-0.1	-0.1	1.8		
12	162	-0.3	0.6	-0.1	-0.1	0.2	-0.2	1.1		
13	81	-0.5	0.1	-0.8	0	-0.1	0	0.9		
14	0	-9.1	-1.7	-8.8	0.7	0.9	0.5	8		
15	180	0.4	0	-0.1	-0.7	0	1.5	3.4		
16	180	-0.2	0	0.1	-0.6	0	-1	2.4		

2.6.12.4 Stress Evaluation of PWR Canister for 1-Foot End-Drop Load Condition

A structural analysis performed by using ANSYS evaluates the effect of a 1-ft end-drop impact for both the bottom and top-end orientations of the PWR canister. The ASME Code, Section III, Subsection NB requires that stresses arising from operational loads be assessed on the basis of the primary loads. The primary loads for the 1-ft drop result from the deceleration of the canister and its contents and the 25-psig pressure load internal to the canister. The applied deceleration is 20 *g* for both orientations. The inertial load of the canister is addressed by the deceleration factor applied to the canister density. The weight of the contents is represented by a pressure load on the inner end surface of the canister. Displacement constraints are applied to the plane of symmetry and the gap elements attached at the canister end to represent the top or bottom of the transport cask.

To determine the effect of the 25-psig pressure load, the top-end and bottom-end orientations with and without the pressure load are analyzed.

The locations of the linearized stresses are shown in Figure 2.6.12.3-1. The summary for P_m and $P_m + P_b$ stresses due to the internal pressure of 25 psig are summarized in Table 2.6.12.4-2 and 2.6.12.4-3, respectively. Results from the end-drops are summarized in Tables 2.6.12.4-4 through 2.6.12.4-7 for the conditions that produce the minimum margin of safety. Table 2.6.12.4-1 provides a summary of critical section stresses for the top and bottom end-drop conditions. The margins of safety in these tables are calculated as:

MS = (allowable stress/SI) -1.

Table 2.6.12.4-1 PWR Canister Critical Sections for the Pressure Only and 1-Foot End-Drop Load Condition

Condition	Stress	Critical Section	Table	Minimum Margin of Safety
Pressure (only)	P_m	2	2.6.12.4-2	+ 3.32
Pressure (only)	$P_m + P_b$	3	2.6.12.4-3	+ 0.71
Top-End Drop Inertia	P_m	2	2.6.12.4-4	+ 4.04
Top-End Drop Inertia	$P_m + P_b$	3	2.6.12.4-5	+ 1.1
Bottom-End Drop + Pressure	P_m	4	2.6.12.4-6	+ 4.33
Bottom-End Drop + Pressure	$P_m + P_b$	2	2.6.12.4-7	+ 5.71

Table 2.6.12.4-2 PWR Canister P_m Stresses - Internal Pressure

Section Location	Angle of Peak Stress Location	P_m Stresses (ksi)						SI (ksi)	Allowable Stress (ksi)	Margin of Safety
		Sx	Sy	Sz	Sxy	Syz	Sxz			
1	0	0.2	2.4	1	-0.3	0	0.1	2.4	16	5.75
2	0	1.6	-1.6	-2	-0.3	0	-0.2	3.7	16	3.32
3	0	0.3	0	-2.7	0.3	0	-0.2	3.3	16	3.83
4	0	0	0.6	1.3	0	0	0.1	1.3	16	10.98
5	0	0	0.6	1.3	0	0	0.1	1.3	16	11.02
6	0	0	0.6	1.3	0	0	0.1	1.3	16	11.02
7	0	0	0.6	1.3	0	0	0.1	1.3	16	11.02
8	0	0	0.6	0.7	0	0	0.1	0.7	16	22.64
9	180	0	0.5	0.3	-0.1	0	0	0.5	16	33.63
10	180	-0.3	0.3	0.2	0.1	0	0	0.6	16	25.71
11	0	0.3	-0.1	0.2	0	0	0	0.4	16	37.08
12	0	-0.1	-0.4	0	-0.1	0	0	0.5	16	33.99
13	9	0	0.3	0.2	0	0	0	0.3	12.8*	41.67
14	90	0.2	-0.2	0.2	-0.1	0.2	0	0.6	16	23.81
15	90	0	0	0	0	0	0	0	16	1025.99
16	0	0	0	0	0	0	0	0	16	365.18

* Allowable stress includes a stress reduction factor for weld: 0.8 x allowable stress.

Note: All of the allowable stress values presented in this table are based on SA240, Type 304L stainless steel at a temperature of 380°F unless otherwise stated. Localized peak temperatures in the central portion of the canister shell reach 408°F—resulting in slightly lower allowable stress values and subsequently slightly lower margins of safety for sections 5 and 6 than those presented in the table. However, this difference is negligible as discussed in Section 2.6.12.1.

Table 2.6.12.4-3 PWR Canister $P_m + P_b$ Stresses - Internal Pressure

Section Location	Angle of Peak Stress Location	$P_m + P_b$ Stresses (ksi) Sx	Sy	Sz	Sxy	Syz	Sxz	SI (ksi)	Allowable Stress (ksi)	Margin of Safety
1	0	1.9	5.9	0.2	0	0	-0.1	5.7	24	3.24
2	0	0.8	-11.2	-5.1	-0.8	0	-0.4	12.2	24	0.97
3	0	0.7	-13.3	-6.5	0.1	0	-0.5	14	24	0.71
4	0	0	0.6	1.3	0	0	0.1	1.4	24	16.74
5	0	0	0.7	1.3	0	0	0.1	1.4	24	16.73
6	0	0	0.7	1.3	0	0	0.1	1.4	24	16.73
7	0	0	0.6	1.3	0	0	0.1	1.4	24	16.73
8	180	0	0.7	0.7	0	0	-0.1	0.7	24	31.59
9	180	0.1	0.9	0.5	-0.1	0	0	0.9	24	26.24
10	180	-0.1	1.4	0.6	0	0	-0.1	1.5	24	14.58
11	0	0.2	-1	-0.1	0.1	0	0	1.2	24	19.74
12	0	-0.4	-0.8	-0.1	-0.2	0	0	0.7	24	34.13
13	180	-0.4	0	0	-0.1	0	0	0.4	19.2*	47.00
14	90	7.6	-0.2	7.6	-0.1	0.2	0	7.8	24	2.06
15	90	-0.6	0	-0.6	0	0	0	0.6	24	40.86
16	81	0.3	0	0.3	0	0	0	0.3	24	74.05

* Allowable stress includes a stress reduction factor for weld: 0.8 x allowable stress.

Note: All of the allowable stress values presented in this table are based on SA240, Type 304L stainless steel at a temperature of 380°F unless otherwise stated. Localized peak temperatures in the central portion of the canister shell reach 408°F—resulting in slightly lower allowable stress values and subsequently slightly lower margins of safety for sections 5 and 6 than those presented in the table. However, this difference is negligible as discussed in Section 2.6.12.1.

Table 2.6.12.4-4 PWR Canister P_m Stresses - 1-Foot Top End Drop

Section Location	Angle of Peak Stress Location	P_m Stresses (ksi)						SI (ksi)	Allowable Stress (ksi)	Margin of Safety
		Sx	Sy	Sz	Sxy	Syz	Sxz			
1	0	-0.1	-2	-0.7	0.3	0	0	1.9	16	7.31
2	0	-1.3	1.2	1.8	0.3	0	0.2	3.2	16	4.04
3	0	-0.3	0	2.5	-0.2	0	0.2	3	16	4.38
4	144	0	-0.7	0	0	0	0	0.7	16	20.58
5	153	0	-0.9	0	0	0	0	0.9	16	16.18
6	162	0	-1.1	0	0	0	0	1.1	16	13.28
7	180	0	-1.3	0	0	0	0	1.3	16	11.21
8	180	0	-1.2	0	0	0	0	1.3	16	11.57
9	180	0	-0.9	-0.2	0	0	0	1	16	15.82
10	144	-0.1	-0.9	-0.1	0	0	0.1	0.9	16	17.09
11	135	-0.1	-0.9	-0.1	0	0	0.1	0.9	16	17.3
12	144	0	-0.7	-0.1	0	0	0	0.7	16	21.43
13	180	0	-0.7	-0.1	0	0	0	0.7	12.8*	17.29
14	90	-0.2	0	-0.2	0.1	-0.1	0	0.4	16	44.06
15	144	0	-0.3	0	0	0	0	0.4	16	44.54
16	0	0	-0.4	0	0	0	0	0.4	16	40.07

* Allowable stress includes a stress reduction factor for weld: 0.8 x allowable stress.

Note: All of the allowable stress values presented in this table are based on SA240, Type 304L stainless steel at a temperature of 380°F unless otherwise stated. Localized peak temperatures in the central portion of the canister shell reach 408°F—resulting in slightly lower allowable stress values and subsequently slightly lower margins of safety for sections 5 and 6 than those presented in the table. However, this difference is negligible as discussed in Section 2.6.12.1.

Table 2.6.12.4-5 PWR Canister $P_m + P_b$ Stresses - 1-Foot Top End Drop

Section Location	Angle of Peak Stress Location	$P_m + P_b$ Stresses (ksi)						SI (ksi)	Allowable Stress (ksi)	Margin of Safety
		Sx	Sy	Sz	Sxy	Syz	Sxz			
1	0	-1.4	-4.7	0.1	0	0	0.1	4.8	24	3.99
2	0	-0.6	9	4.3	0.7	0	0.4	9.8	24	1.45
3	0	-0.5	10.8	5.6	0	0	0.5	11.4	24	1.1
4	162	0	-0.8	0	0	0	0	0.8	24	30.8
5	162	0	-0.9	0	0	0	0	0.9	24	24.77
6	144	0	-1.1	0	0	0	0	1.1	24	20.42
7	171	0	-1.3	0	0	0	0	1.3	24	17.3
8	180	0.1	-1.2	0	-0.1	0	0	1.3	24	17.37
9	45	-0.1	-1.1	-0.1	0	0	-0.1	1.1	24	21.59
10	180	0	-1	-0.2	0	0	0	1	24	22.45
11	135	-0.1	-1	-0.1	0	0	0.1	1	24	23.42
12	180	0	-0.7	-0.1	-0.1	0	0	0.7	24	31.5
13	180	0	-0.8	-0.1	0	0	0	0.7	19.2*	26.43
14	90	-6.8	-0.1	-6.8	0.1	-0.1	0	6.7	24	2.57
15	81	0.1	-0.3	0.1	0	0	0	0.4	24	55.49
16	0	0	-0.4	0	0	0	0	0.4	24	59.08

* Allowable stress includes a stress reduction factor for weld: 0.8 x allowable stress.

Note: All of the allowable stress values presented in this table are based on SA240, Type 304L stainless steel at a temperature of 380°F unless otherwise stated. Localized peak temperatures in the central portion of the canister shell reach 408°F—resulting in slightly lower allowable stress values and subsequently slightly lower margins of safety for sections 5 and 6 than those presented in the table. However, this difference is negligible as discussed in Section 2.6.12.1.

Table 2.6.12.4-6 PWR Canister P_m Stresses - 1-Foot Bottom End Drop, Internal Pressure

Section Location	Angle of Peak Stress Location	P_m Stresses (ksi)						SI (ksi)	Allowable Stress (ksi)	Margin of Safety
		Sx	Sy	Sz	Sxy	Syz	Sxz			
1	180	0	-0.6	0	0.1	0	0	0.6	16	24.4
2	180	0.3	-1.9	-0.3	0.1	0	0	2.2	16	6.24
3	180	0.1	-1.9	-0.3	-0.1	0	0	2	16	7.08
4	180	0	-1.7	1.3	0	0	-0.1	3	16	4.33
5	180	0	-1.5	1.3	0	0	-0.1	2.8	16	4.69
6	180	0	-1.3	1.3	0	0	-0.1	2.6	16	5.11
7	180	0	-1.1	1.3	0	0	-0.1	2.4	16	5.58
8	180	0	-0.7	0.7	0	0	-0.1	1.4	16	10.31
9	18	-0.1	-0.5	-0.4	-0.1	0	-0.1	0.4	16	36.52
10	180	0.4	-0.3	-0.2	-0.1	0	0	0.7	16	21.21
11	0	-0.5	0.1	-0.2	0	0	0	0.6	16	27.29
12	99	-0.1	0.5	0.1	0	-0.1	0	0.6	16	27.09
13	0	0	-0.5	-0.3	0	0	0	0.4	12.8*	31.00
14	0	0.1	-0.4	0.1	0	0	0	0.4	16	34.57
15	108	0	0	0	0	0	0	0.1	16	302.05
16	0	0	0	0	0	0	0	0.1	16	286.36

* Allowable stress includes a stress reduction factor for weld: 0.8 x allowable stress.

Note: All of the allowable stress values presented in this table are based on SA240, Type 304L stainless steel at a temperature of 380°F unless otherwise stated. Localized peak temperatures in the central portion of the canister shell reach 408°F—resulting in slightly lower allowable stress values and subsequently slightly lower margins of safety for sections 5 and 6 than those presented in the table. However, this difference is negligible as discussed in Section 2.6.12.1.

Table 2.6.12.4-7 PWR Canister $P_m + P_b$ Stresses - 1 Foot Bottom End Drop, Internal Pressure

Section Location	Angle of Peak Stress Location	$P_m + P_b$ Stresses (ksi)						SI (ksi)	Allowable Stress (ksi)	Margin of Safety
		Sx	Sy	Sz	Sxy	Syz	Sxz			
1	180	0.2	-0.4	0.1	0.1	0	0	0.7	24	34.19
2	180	0.2	-3.4	-0.7	0.1	0	0.1	3.6	24	5.71
3	180	0.1	-3.3	-0.6	-0.1	0	0	3.3	24	6.16
4	0	0	-1.7	1.3	0	0	0.1	3	24	6.95
5	0	0	-1.5	1.3	0	0	0.1	2.8	24	7.5
6	0	0	-1.3	1.3	0	0	0.1	2.6	24	8.11
7	0	0	-1.1	1.3	0	0	0.1	2.4	24	8.82
8	27	0.2	-0.9	0.5	0	0	0.2	1.5	24	14.94
9	108	-0.5	-1.1	-0.1	0	0.1	0.1	1.1	24	21.15
10	99	-0.7	-1.6	0.1	0	0	0.1	1.8	24	12.44
11	0	-0.2	1.3	0.2	-0.1	0	0	1.5	24	14.78
12	99	0.2	0.9	0.5	0	-0.2	0.1	0.8	24	29.14
13	0	0.5	0	0	-0.1	0	0	0.5	19.2*	37.40
14	0	0.1	-0.4	0.1	0	0	0	0.5	24	49.26
15	90	0.8	0	0.8	0	0	0	0.8	24	28.07
16	0	-0.4	0	-0.4	0	0	0	0.4	24	56.39

* Allowable stress includes a stress reduction factor for weld: 0.8 x allowable stress.

Note: All of the allowable stress values presented in this table are based on SA240, Type 304L stainless steel at a temperature of 380°F unless otherwise stated. Localized peak temperatures in the central portion of the canister shell reach 408°F—resulting in slightly lower allowable stress values and subsequently slightly lower margins of safety for sections 5 and 6 than those presented in the table. However, this difference is negligible as discussed in Section 2.6.12.1.

2.6.12.5 Stress Evaluation of PWR Canister for Combined Thermal and 1-Foot End Drop Load Condition

The thermal stress loads described in Section 2.6.12.3 are applied in conjunction with the primary loads in Section 2.6.12.4 to produce a combined thermal stress plus end-impact loading. The stress evaluation is performed according to the ASME Code, Section III, Subsection NB. The most critical sections are listed in Table 2.6.12.5-1. The stresses reported in this table correspond to the nodal stress at the surface. The minimum margin of safety is +2.44 when 3 S_m is used as the stress criterion. Tables 2.6.12.5-2 through 2.6.12.5-5 tabulate the peak stresses for both the hot and cold conditions for both the top-and bottom-end-drop cases for the conditions that result in the minimum margin of safety. For both top and bottom orientations, the minimum margins occur without the addition of pressure. The margins of safety are calculated as:

MS = (allowable stress/SI) -1.

Table 2.6.12.5-1 PWR Canister Critical Sections for the Combined 1-Foot End Drop and Thermal Load Condition

Condition	Stress	Critical Section	Table	Minimum Margin of Safety
Top-End Drop + Thermal (cold)	P + Q	14	2.6.12.5-2	+ 2.44
Top-End Drop + Thermal (hot)	P + Q	3	2.6.12.5-3	+ 2.6
Bottom-End Drop + Thermal (cold)	P + Q	14	2.6.12.5-4	+ 7.47
Bottom-End Drop + Thermal (hot)	P + Q	14	2.6.12.5-5	+ 8.44

Table 2.6.12.5-2 PWR Canister $P_m + P_b + Q$ Stresses - 1-Foot Top End Drop, Thermal Cold

Section Location	Angle of Peak Stress Location	$P_m + P_b + Q$ Stresses (ksi)						SI (ksi)	Allowable Stress (ksi)	Margin of Safety
		Sx	Sy	Sz	Sxy	Syz	Sxz			
1	90	1.3	-5.8	-1.8	0	0	0	7.2	47.9	5.67
2	45	3.4	10.6	3.4	0.4	-0.6	3.5	10.8	47.9	3.46
3	9	-0.1	-10.9	0.8	-0.6	0	0.2	11.8	47.9	3.08
4	0	0	-1.2	0	0	0	0	1.2	47.9	37.94
5	0	0	-2.1	0.6	0	-0.2	0	2.8	47.9	16.12
6	0	0	-2.3	0.2	0	0	0	2.5	47.9	18.39
7	0	0	-2.6	0	0	0	0	2.6	47.9	17.46
8	9	-0.2	-3.4	-0.3	0	0.1	0	3.3	47.9	13.67
9	162	0.1	-3.1	-0.7	-0.2	-0.1	0.3	3.3	47.9	13.63
10	0	-0.1	-2	-0.5	0.1	0	0	1.8	47.9	25.05
11	171	0	-3.3	-0.8	0	0	0.1	3.3	47.9	13.51
12	0	0.4	-0.9	0	0.2	0	0	1.3	47.9	35.99
13	0	0.2	-1	-0.1	0	0	0	1.2	**38.32***	**30.93**
14	0	-15.7	-1.8	-15.4	0.1	-1	0.1	14	47.9	2.44
15	81	0.1	-0.3	0.1	0	0	0	0.4	47.9	116.3
16	0	0.1	-0.5	0.1	0	0	0	0.6	47.9	85.61

* Allowable stress includes a stress reduction factor for weld: 0.8 x allowable stress.

Note: All of the allowable stress values presented in this table are based on SA240, Type 304L stainless steel at a temperature of 380°F unless otherwise stated. Localized peak temperatures in the central portion of the canister shell reach 408°F—resulting in slightly lower allowable stress values and subsequently slightly lower margins of safety for sections 5 and 6 than those presented in the table. However, this difference is negligible as discussed in Section 2.6.12.1.

Table 2.6.12.5-3 PWR Canister $P_m + P_b + Q$ Stresses-1-Foot Top End Drop, Thermal Heat

Section Location	Angle of Peak Stress Location	$P_m + P_b + Q$ Stresses (ksi)						SI (ksi)	Allowable Stress (ksi)	Margin of Safety
		Sx	Sy	Sz	Sxy	Syz	Sxz			
1	90	1.2	-5.9	-1.8	0	0	0	7.1	47.9	5.77
2	45	3.3	10.5	3.3	0.4	-0.6	3.5	10.8	47.9	3.44
3	9	-0.1	-11	0.7	-0.6	0.1	0.1	11.8	47.9	3.08
4	0	0	-1.1	0	0	0	0	1.2	47.9	40.01
5	0	0	-2	0.5	0	-0.2	0	2.5	47.9	17.84
6	0	0	-2.1	0.2	0	0	0	2.3	47.9	20.04
7	0	0	-2.4	0	0	0	0	2.4	47.9	19.03
8	9	-0.2	-3.2	-0.3	0	0.1	0	3	47.9	14.85
9	162	0.1	-3	-0.7	-0.1	-0.1	0.3	3.2	47.9	14.01
10	162	-0.3	-2	-0.5	-0.2	-0.1	0.1	1.8	47.9	26.36
11	171	0	-3	-0.7	0	0	0.1	3	47.9	14.76
12	0	0.3	-0.9	-0.1	0.2	0	0	1.2	47.9	37.66
13	0	0.2	-0.9	-0.1	0	0	0	1.1	38.32*	33.84
14	0	-14.8	-1.6	-14.6	0.1	-0.9	0	13.3	47.9	2.6
15	81	0.1	-0.3	0.1	0	0	0	0.4	47.9	116.41
16	0	0.1	-0.5	0.1	0	0	0	0.5	47.9	87.74

* Allowable stress includes a stress reduction factor for weld: 0.8 x allowable stress.

Note: All of the allowable stress values presented in this table are based on SA240, Type 304L stainless steel at a temperature of 380°F unless otherwise stated. Localized peak temperatures in the central portion of the canister shell reach 408°F—resulting in slightly lower allowable stress values and subsequently slightly lower margins of safety for sections 5 and 6 than those presented in the table. However, this difference is negligible as discussed in Section 2.6.12.1.

Table 2.6.12.5-4 PWR Canister $P_m + P_b + Q$ Stresses -1-Foot Bottom End Drop, Thermal Cold

Section Location	Angle of Peak Stress Location	$P_m + P_b + Q$ Stresses (ksi)						SI (ksi)	Allowable Stress (ksi)	Margin of Safety
		Sx	Sy	Sz	Sxy	Syz	Sxz			
1	9	0.1	-2.1	1.2	-0.3	0.1	0.2	3.4	47.9	13.23
2	9	-0.3	-4.5	0.3	-0.1	0.1	0.1	4.8	47.9	9.04
3	9	-0.1	-4	0.6	0	0.1	0.1	4.6	47.9	9.38
4	0	0	-3.2	0	0	0	0	3.2	47.9	14.02
5	0	0	-3.5	0.6	0	-0.2	0	4.1	47.9	10.6
6	0	0	-3	0.2	0	0.1	0	3.2	47.9	13.91
7	0	0	-2.6	0	0	0	0	2.7	47.9	17.02
8	9	-0.2	-2.7	-0.2	0	0.2	0	2.6	47.9	17.55
9	162	-0.2	-3.3	-1.4	0.1	0.1	0.4	3.3	47.9	13.69
10	0	0.4	-3.9	-1.5	0	0.1	-0.1	4.3	47.9	10.22
11	0	-0.5	2.7	0.7	-0.1	0.1	0.1	3.2	47.9	13.86
12	18	1.1	1.7	0.3	0.4	0.1	-0.1	1.6	47.9	28.65
13	0	-1.4	-2	-1	0.3	0	0	1.2	38.32*	30.93
14	0	-11.2	-5.5	-10.9	0	0.1	0.1	5.7	47.9	7.47
15	81	1.7	0	1.4	0	0	0	1.7	47.9	27.66
16	72	-0.7	0	-0.6	0	0	0	0.7	47.9	68.32

* Allowable stress includes a stress reduction factor for weld: 0.8 x allowable stress.

Note: All of the allowable stress values presented in this table are based on SA240, Type 304L stainless steel at a temperature of 380°F unless otherwise stated. Localized peak temperatures in the central portion of the canister shell reach 408°F—resulting in slightly lower allowable stress values and subsequently slightly lower margins of safety for sections 5 and 6 than those presented in the table. However, this difference is negligible as discussed in Section 2.6.12.1.

Table 2.6.12.5-5 PWR Canister $P_m + P_b + Q$ Stresses - 1-Foot Bottom End Drop, Thermal Heat

Section Location	Angle of Peak Stress Location	$P_m + P_b + Q$ Stresses (ksi)						SI (ksi)	Allowable Stress (ksi)	Margin of Safety
		Sx	Sy	Sz	Sxy	Syz	Sxz			
1	9	0.1	-1.9	1.1	-0.3	0.1	0.2	3.1	47.9	14.36
2	9	-0.3	-4.5	0.1	-0.1	0.1	0.1	4.6	47.9	9.45
3	9	-0.1	-4	0.4	0	0.1	0.1	4.4	47.9	9.79
4	0	0	-3.1	0	0	0	0	3.1	47.9	14.64
5	0	0	-3.3	0.6	0	-0.2	0	3.9	47.9	11.41
6	0	0	-2.8	0.2	0	0.1	0	3	47.9	14.76
7	0	0	-2.5	0	0	0	0	2.5	47.9	17.96
8	9	-0.2	-2.6	-0.2	0	0.2	0	2.4	47.9	18.74
9	162	-0.2	-3.2	-1.3	0.1	0.1	0.4	3.1	47.9	14.46
10	162	0	-3.8	-1.4	-0.1	0.1	0.5	4	47.9	10.93
11	9	-0.5	2.5	0.5	-0.1	0.1	0.1	3.1	47.9	14.68
12	162	0.6	1.9	0.2	-0.4	0	0.1	1.8	47.9	25.24
13	0	1	-0.2	0.2	-0.1	0	-0.1	1.2	38.32*	30.93
14	0	-10	-4.9	-9.7	0	0.1	0	5.1	47.9	8.44
15	72	1.7	0	1.4	0	0	0	1.6	47.9	28.14
16	72	-0.7	-0.1	-0.6	0	0	0	0.7	47.9	68.12

* Allowable stress includes a stress reduction factor for weld: 0.8 x allowable stress.

Note: All of the allowable stress values presented in this table are based on SA240, Type 304L stainless steel at a temperature of 380°F unless otherwise stated. Localized peak temperatures in the central portion of the canister shell reach 408°F—resulting in slightly lower allowable stress values and subsequently slightly lower margins of safety for sections 5 and 6 than those presented in the table. However, this difference is negligible as discussed in Section 2.6.12.1.

2.6.12.6 Stress Evaluation of PWR Canister for 1-Foot Side Drop Load Condition

The stresses in the PWR canister that result from a 1-ft side-drop are determined by using ANSYS. In the local regions of the lids and bottom plate, the loads are transmitted through the canister shell into the cask body inner shell. Outside of the lid and bottom plate regions, stress develops in the canister shell as a result of the basket loading the canister wall. The difference in the radii of the basket, canister, and cask body implies that the contact angle between the components is dependent on the loading. For this reason, the finite element model described in Section 2.6.12.2 contains a half model of the basket. Gap elements between the basket and the canister allow the interface to be dependent on the loading. The interface between the canister and the cask body inner shell is also represented by gap elements.

The load resulting from the contents is applied to the basket by means of pressure acting in the plane of the disks. The weight is assumed to act over the effective width of 9.272 in., in which the disk is 0.5 in. thick. This weight is distributed over the 32 support disks plus two end weldments. A deceleration factor of 20 *g* applied to the weights provides the loading for the basket assembly. In addition to the contents load, a 25-psig pressure is applied to the inner surface of the canister.

Analyses of the canister are performed for basket orientations of 0° and 45°. The angles describe the orientation of the basket elements with respect to the symmetry plane of the model. A value of 0° orients the ligaments in the basket elements parallel and perpendicular to the symmetry plane, a value of 45°orients the basket ligaments at +/- 45° from the symmetry plane. To assess the impact of the basket orientation on the canister response during impact, both basket orientations are run for the side-impact loading.

The methodology used to evaluate the stresses for the side-drop are similar to that used for the end-drop (Section 2.6.12.4) with following exceptions. Sections 9, 10, and 11 at the 0° circumferential position (see Figure 2.6.12.3-1) are not included in the evaluation. These regions are characterized as a bearing stress since they result from the canister shell bearing against the cask inner shell. Section 2.6.12.11 provides an assessment of the canister shell bearing stresses. Sections 9, 10, and 11 at all other angular locations are included in the evaluation. Also, Sections 12 and 13 at 0° are treated as local membrane stresses. According to the ASME Code Section III, Paragraph NB-3213.10, a stressed region may be considered local if the distance over which the membrane stress intensity exceeds 1.1 S_m does not extend more than 1.0 times the

square root of RT in the meridional direction, where R is the minimum midsurface radius of curvature and T is the minimum thickness in the region considered. For Section 13, the minimum thickness is that of the canister shell (0.625 in.) and the midsurface radius of the shell is 33.2175 in. The resulting distance is 4.56 in. A section located 4.56 in. from Section 13 in the meridional direction results in a membrane stress intensity of 6.7 ksi, which is below S_m. This section conservatively encompasses Section 12 since it is located 1.56 in. from this section. The stresses at adjacent circumferential sections (i.e., at 9°) for Sections 12 and 13 are also included in the tables for comparison. The critical section stresses are reported in Table 2.6.12.6-1 for the P_m and $P_m + P_b$ stresses.

Results are calculated for 1-ft side-drop with internal pressure both the 0° and 45° basket orientations. Tables 2.6.12.6-2 and 2.6.12.6-3 present the worst-case margins for the side-drop which occurs with the conditions noted. The minimum margin occurs for membrane without pressure and with pressure for membrane plus bending. The minimum margin of safety for the PWR canister in the side-drop is +0.02, which occurs at Section 12 in Table 2.6.12.3-1. The margins of safety are calculated as:

$$MS = (\text{allowable stress}/SI) - 1.$$

Table 2.6.12.6-1 PWR Canister Critical Sections for the 1-Foot Side Drop Load Condition

Condition	**Stress**	**Critical Section**	**Table**	**Minimum Factor of Safety**
Side Drop	Pm	1	2.6.12.6-2	+ 0.07
Side Drop + Pressure	$P_m + P_b$	12	2.6.12.6-3	+ 0.02